GEORGIA INSTITUTE OF TECHNOLOGY — OFFICE OF CONTRACT ADMINISTRATION

# PROJECT ADMINISTRATION DATA SHEET

[x] ORIGINAL [ ] REVISION NO. ____

Project No. E-19-607 GTRI/~~GIT~~ DATE 10/20/82

Project Director: Dr. Jack Winnick School/~~Lab~~ ChE

Sponsor: Gas Research Institute CD

Chicago, IL 60631

Type Agreement: Grant No. 5082-260-0652

Award Period: From 8/1/82 To ~~7/31/84~~ (Performance) 11/30/84 (Reports)

Sponsor Amount: Total Estimated: $ 140,688 12-31-84 Funded: $ 140,688

Cost Sharing Amount: $ na Cost Sharing No: na

Title: Hydrogen Sulfide Removal from Hot Gas and Concentration to Sulfur Using Electrochemistry

## ADMINISTRATIVE DATA

OCA Contact Linda H. Bowman x4820

1) Sponsor Technical Contact:

Dr. John L. Cox
Manager, Organic Chemistry
GRI
8600 West Bryn Mawr Ave.
Chicago, IL 60631

(312) 399-8100

2) Sponsor Admin/Contractual Matters:

Ms. Christine M. Kucharz
Contract Administrator
GRI
8600 West Bryn Mawr Ave.
Chicago, IL 60631

(312) 399-8100

Defense Priority Rating: none

Military Security Classification: none

(or) Company/Industrial Proprietary: ____

## RESTRICTIONS

See Attached na Supplemental Information Sheet for Additional Requirements.

Travel: Foreign travel must have prior approval – Contact OCA in each case. Domestic travel requires sponsor approval where total will exceed greater of $500 or 125% of approved proposal budget category.

Equipment: Title vests with GRI in excess of $500; except Hewlett Packard Flame Photometric Detector vests with GIT.

## COMMENTS:

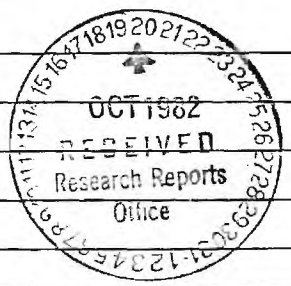


## COPIES TO:

| | | |
|---|---|---|
| Research Administrative Network | Research Security Services | Research Communications (2) |
| Research Property Management | ~~Reports Coordinator (OCA)~~ | Project File |
| Accounting | GTRI | Other ____ |
| Procurement/EES Supply Services | Library | Other ____ |

OCA 4:781 (Rev 982)

EORGIA INSTITUTE OF TECHNOLOGY OFFICE OF CONTRACT ADMINISTRATION

SPONSORED PROJECT TERMINATION/CLOSEOUT SHEET

Date April 1, 1986

oject No. E-19-607 School ~~XXXX~~ Ch.E.

ludes Subproject No.(s)

ject Director(s) Dr. Jack Winnick GTRI / ~~XXX~~

nsor Gas Research Institute

e Hydrogen Sulfide Removal from Hot Gas and Concentration to Sulfur Using Electrochemistry.

ctive Completion Date: 12/31/84 (Performance) 4/30/85 (Reports)

nt/Contract Closeout Actions Remaining:

- [ ] None
- [ ] Final Invoice or Final Fiscal Report – Already submitted.
- [ ] Closing Documents
- [X] Final Report of Inventions Sent memo to L&SD.
- [X] Govt. Property Inventory & Related Certificate
- [ ] Classified Material Certificate
- [ ] Other

nues Project No. Continued by Project No.

ES TO:

t Director
ch Administrative Network
ch Property Management
nting
ement/EES Supply Services
ch Security Services
s Coordinator (OCA)
ervices

Library
GTRI
Research Communications (2)
Project File
Other Heyser, Jones, Embry

OCA 60:1028

E-19-607

Attachment D

# ENVIRONMENTAL CONTROL OF GAS APPLIANCES

ANNUAL REPORT
(August 1983-August 1984)

Prepared by

Jack Winnick

Georgia Institute of Technology
School of Chemical Engineering
Atlanta, Georgia 30332-0100

For

GAS RESEARCH INSTITUTE
Grant 5082-260-0652

GRI Project Manager
John L. Cox
Organic Chemistry

January 1985

Attachment A

# GRI DISCLAIMER

LEGAL NOTICE This report was prepared by Georgia Institute of Technology as an account of work sponsored by the Gas Research Institute (GRI). Neither GRI, members of GRI, nor any person acting on behalf of either:

a. Makes any warranty or representation, express or implied, with respect to the accuracy, completeness, or usefullness of the information contained in this report, or that the use of any apparatus, method, or process disclosed in this report may not infringe privately owned rights; or

b. Assumes any liability with respect to the use of, or for damages resulting from the use of, any information, apparatus, method, or process disclosed in this report.

Attachment E

101

| RT DOCUMENTATION PAGE | 1. REPORT NO. | 2. | 3. Recipient's Accession No. GRI-84/0201 |
|---|---|---|---|
| e and Subtitle | Hydrogen Sulfide Removal From Hot Gas And Concentration To Sulfur Using Electrochemistry | | 5. Report Date January 1985 |
| | | | 6. |
| hor(s) | Jack Winnick | | 8. Performing Organization Rept. No. |
| forming Organization Name and Address | Georgia Institute of Technology<br>Department of Chemical Engineering<br>Atlanta, Georgia 30332-0100 | | 10. Project/Task/Work Unit No.<br>11. Contract(C) or Grant(G) No.<br>(C)<br>(G) 5082-260-0652 |
| onsoring Organization Name and Address | Gas Research Institute<br>8600 West Bryn Mawr Avenue<br>Chicago, Illinois 60631 | | 13. Type of Report & Period Covered Annual Report Aug. 1983-Aug. 1984<br>14. |

pplementary Notes

stract (Limit: 200 words)

The virtual omnipresence of sulfur in fossil fuels raises concern regarding the in-ased use of coal for high temperature fuel utilization and conversion processes. A ical raw gas composition from burning Illinois #6 coal (3.9% sulfur) in an air-blown ifier is 19.6% CO, 8.1% $CO_2$, 10% $H_2$, 3.4% $H_2O$, 3% $CH_4$, 0.6% $H_2S$ with the balance being rts. This gas has several potential uses. Of most interest is its conversion to high-SNG which requires passage over a methanation catalyst at 300-400°C. The methanation alysts, however, are sensitive to even small (5ppm) concentrations of $H_2S$. Thus, in absence of a very effective high-temperature sulfur clean-up process, the gas must be ed to the temperatures of operation of commercially available processes (e.g.,Selexol ectisol). The use of high-temperature clean-up is estimated to allow savings of up % of the energy value of the gas[1].

Since a high-temperature sulfur removal process is desirable several have undergone ination. Most are based on reaction of a metal oxide with the $H_2S$, with subsequent neration to the fresh sorbent and a concentrated stream of $H_2S$. This $H_2S$ is then to a Claus Plant to be oxidized to elemental sulfur (and water). Difficulties of us kinds have not permitted any of these processes from as yet reaching commercializa-

[1]Grainger, L. and J. Gibson, "Coal Utilization", New York: Wiley, 1981' Wen, C.Y. .S. Yee, "Coal Conversion Technology", London: Addison-Wesley, 1979.

nent Analysis a. Descriptors

tifiers/Open-Ended Terms

TI Field/Group

| ty Statement | 19. Security Class (This Report) | 21. No. of Pages 76 |
|---|---|---|
| | 20. Security Class (This Page) | 22. Price |

18) See Instructions on Reverse

OPTIONAL FORM 272 (4-77)
(Formerly NTIS-35)
Department of Commerce

| | |
|---|---|
| Title | Hydrogen Sulfide Removal From Hot Gas and Concentration to Sulfur Using Electrochemistry |
| Contractor | Georgia Institute of Technology |
| Principal Investigator | J. Winnick |
| Time Span | August 1983 - August 1984<br>Annual Report |

**Major Achievements**

The technical feasibility of the electrochemical removal of $H_2S$ from gaseous fuels at high temperatures (650-900°C) has been demonstrated by laboratory scale tests for a limited range of process parameters. It was found that the intrinsic chemical kinetics exceed the rate controlling, mass transfer, processes. The mechanism for the electrochemical reduction of $H_2S$ and oxidation of $S^{-2}$ was found to be the same as that observed at lower temperatures in sulfur batteries. The effect of $CO_2$ and $H_2O$ in the gaseous mixture was to convert part of the electrolyte ($K_2S$-$Na_2S$) to carbonate. A high level of electrolyte carbonation can be tolerated since only a small concentration of $S^{-2}$ is required to transfer the electrolysis current. Furthermore, the pressence of carbonate in the electrolyte enhanced the $H_2S$ removal efficiency.

**Description of Work Completed**

A high temperature (650-700°C) electrochemical cell was constructed and used to study the removal of $H_2S$ from gaseous fuel streams by electrolysis. The $H_2S$ removal entails the reduction of the $H_2S$ in the gaseous mixture at the cathode, transport of sulfide ions across the electrolyte to the anode where they are oxidized to elemental sulfur and released by vaporization. Electroanalytical techniques were employed to investigate the chemical and electrochemical steps involved in the process over a limited range of gas compositions and experimental parameters.

**Recommendations**

The technical feasibility should be studied of operating an electrolysis cell for the removal of $H_2S$ at lower temperatures (300-500°C). This should entail the search for suitable electrolytes and electrode materials, a study of their compatibility with the electrolysis concept, and removal efficiencies (voltage, rate, current efficiency) as a function of temperature, gas composition and pressure.

Project Implications

Acid gas ($H_2S$ and $CO_2$) removal from natural and substitute natural gas is generally required to produce a fuel gas suitable for commercial use. The cost and efficiency of existing processes for acid gas removal, which can be considerable, translates into higher costs of methane to consumers. Acid gas removal can constitute as much as 10-15% of the cost of substitute natural gas.

An efficient, cost-effective process for the high temperature (300-700°C) removal of acid gases would fit particularly well into coal gasification processes where the gas issuing from the gasifier can be processed to remove the $H_2S$ without having to first cool it to the low temperature required for conventional $H_2S$ removal technology. This investigation is developing fundamental information on an electrochemical technique that appears to have the potential of providing such an option. The effort is directed toward providing fundamental information on the electrochemical $H_2S$ removal that is needed to assess its technical and economic viability. While results to date are encouraging, a broader data base is required to make a technical and economic study of its viability. Further studies will be undertaken with specific focus on identifying the lower temperature limits for electrochemical removal of $H_2S$.

John L. Cox, Manager
Organic Chemistry
Basic Research

TABLE OF CONTENTS

## SUMMARY

The virtual omnipresence of sulfur in fossil fuels raises concern regarding the increased use of coal for high temperature fuel utilization and conversion processes. A typical raw gas composition from burning Illinois #6 coal (3.9% sulfur) in an air-blown gasifier is 19.6% CO, 8.1% $CO_2$, 10% $H_2$, 3.4% $H_2O$, 3% $CH_4$, 0.6% $H_2S$ with the balance being inerts. This gas has several potential uses. Of most interest is its conversion to high-BTU SNG which requires passage over a methanation catalyst at 300-400$^oC$. The methanation catalysts, however, are sensitive to even small ( 5ppm) concentrations of $H_2S$. Thus, in the absence of a very effective high-temperature sulfur clean-up process, the gas must be cooled to the temperatures of operation of commercially available processes (e.g., Selexol or Rectisol). The use of high-temperature clean-up is estimated to allow savings of up to 7% of the energy value of the gas[1].

Since a high-temperature sulfur removal process is desirable several have undergone examination. Most are based on reaction of a metal oxide with the $H_2S$, with subsequent regeneration to the fresh sorbent and a concentrated stream of $H_2S$. This $H_2S$ is then sent to a Claus Plant to be oxidized to elemental sulfur (and water). Difficulties of various kinds have not permitted any of these processes from as yet reaching commercialization.

(1) Grainger, L. and J. Gibson, "Coal Utilization", New York: Wiley, 1981; Wen, C.Y. and E.S. Yee, "Coal Conversion Technology", London: Addison-Wesley, 1979.

Recently, an electrochemical membrane cell was shown to have distinct promise[2]. In addition to providing high-temperature $H_2S$ removal, the sulfide is electrochemically oxidized directly to elemental sulfur. Further, the hydrogen (in the $H_2S$) is added to the coal gas. Thus, to the advantage in energy savings of high-temperature clean-up is added the elimination of the need for a Claus plant.

In spite of the perceived promise of electrochemical $H_2S$ removal, many questions of fundamental nature remain unanswered. To understand more fully the chemistry and electrochemistry involved, an experiment using free-electrolyte (no ceramic membrane) was devised. The electrolyte consisted of a binary mixture of $Na_2S$ and $K_2S$. An operating temperature of 1000 K was used for all runs. Cyclic voltammetric experiments were conducted to examine the effect of variable gas composition on the electrochemical electrode reactions. In addition, gas chromatography was used to monitor the effect of applied current on $H_2S$ removal.

The qualitative cyclic voltammetric experiments corresponded well with the results reported in the literature. The most probable mechanism for this system assumes that the active species is a low concentration of polysulfide dissolved in sulfide. It is proposed that there are two reactions each transferring one electron at voltages very close together occurring within one cyclic voltammogram peak. The exchange current is also assumed to be dependent upon the polysulfide level in the electrolyte.

The $H_2S$ removal experiments proved that electrochemistry is a viable desulfurization method. For an applied current of 100 mA, the ratio of the removal current to the limiting current was approximately 10% with a process

[2]Lim, H.S. and J. Winnick, J. Electrochem. Soc., 131, 562 (1984).

gas containing 0.26% $H_2S$ and approximately 20% for a process gas containing 0.42% $H_2S$. It must be understood that this electrochemical cell was designed to study kinetics and mechanism of $H_2S$ removal rather than to operate at 100% efficiency. An actual commercial cell would hold the electrolyte in an inert matrix and would experience a much higher reliable efficiency.

The effect of the presence of $CO_2$ upon the removal of $H_2S$ from a process gas stream is very important because this experiment better represents the industrial case. The ratio of the removal current to the limiting current was 88% for the process gas containing $CO_2$ at the point of maximum sulfide removal. As expected with the $Na_2S/K_2S$ electrolyte, less than 4 mole % of the original sulfide was converted to carbonate with the passage of process gas which contained $CO_2$.

# NOMENCLATURE

| | |
|---|---|
| $a$ | Activity of a phase |
| $A$ | Active electrode area ($cm^2$) |
| $C_o$ | Concentration of the active species (mole/cc) |
| $C_{dl}$ | Double-layer capacitance (mF) |
| C/R | Potential from counter to refernce electrode (V) |
| $D_o$ | Diffusivity of the active species ($cm^2$/sec) |
| $e^-$ | An electron |
| $E$ | Potential (V) |
| $E_p$ | Peak potential (V) |
| $F$ | Gas flow rate (cc/min) |
| $F$ | Faraday's constant (96500 coul/eq) |
| GC | Gas chromatograph |
| $\Delta G^o$ | Standard state free energy |
| $i_l$ | Limiting current (mA) |
| $i_p$ | Peak current (A) |
| $i_r$ | Removal current (mA) |
| $i_s$ | Stoichiometric current (mA) |
| $I_{APP}$ | Applied current (mA) |
| $j$ | Current density |
| $k_g$ | Mass transfer coefficient |
| $n$ | Number of electrons exchanged |
| $n_a$ | Number of electrons involved in rate determining step |

| | |
|---|---|
| $N_{max}$ | Maximum flux |
| OX | Oxidized species |
| OD | Outside diameter (inches) |
| P | Pressure (PSIA) |
| Q | Number of coulombs passed |
| R | Universal gas constant (1.987 cal/mol K) |
| RED | Reduced species |
| $R_e$ | Reynolds number |
| $R_s$ | Solution resistance ($\Omega$) |
| $S_c$ | Schmidt number |
| t | Time (sec) |
| T | Temperature (K) |
| w/C | Potential from working to counter electrode (mV) |
| w/R | Potential from working to reference electrode (V) |

Subscripts

| | |
|---|---|
| a | Anodic |
| c | Cathodic |

Superscripts

| | |
|---|---|
| s | At the electrode surface |
| * | In the bulk phase |

Greek Letters

| | |
|---|---|
| $\alpha$ | Transfer coefficient |
| $\Delta$ | Denotes a change of any variable |
| $\eta$ | Overpotential |
| $\nu$ | Cyclic voltammetric sweep rate (mV/sec) |
| $\phi$ | Inner potential |
| $\Psi$ | Surface potential |
| $\psi$ | Outer potential |

# CHAPTER I

## INTRODUCTION

Today's society is placing ever-increasing demands on the fuel industry. Market projections predict that the long term supply of existing energy sources will continue to be a practical concern. Environmentalists are concerned about the rapid dissipation of relatively clean fuels. We are being forced to turn to less conventional methods of energy production. These methods must involve both the application of new technology and the introduction of unconventional fuels.

As the nation's energy requirements increase, it is believed that the United States will turn to coal to supply a greater portion of the national energy requirements [1]. One of the problems delaying the greater use of coal now is its sulfur content. When the coal is burned in a conventional manner, the sulfur is converted to sulfur dioxide. Removal of the sulfur dioxide from the combustion gases is costly and often produces a large volume of waste material that must be disposed of. Concern over acid rain will require more thorough removal of certain atmospheric polluting by-products of coal utilization.

An alternate to direct combustion of the coal is coal gasification. Coal gasification is likely to be a major factor in the increased use of high-sulfur coals [2,3]. In coal combustion processes the sulfur in the coal is converted to sulfur dioxide, while in coal gasification the sulfur is converted to hydrogen sulfide.

The removal of hydrogen sulfide from gas is easier than the removal of sulfur dioxide. However, commercial hydrogen sulfide removal technology requires that the gas stream be at or near the ambient temperature. In

addition, removal of the hydrogen sulfide accounts for a significant percentage of the cost of a coal gasification plant. The overall coal gasification process would become more competitive if cost effective technology could be developed for $H_2S$ from hot fuel gas.

## Hydrogen Sulfide Removal Process

Wet scrubbing processes are presently used to remove the $H_2S$ from coal gasification product streams. These processes require cooling the syngas and normally suffer economically because of this and the use of a Claus plant (see Figure 1). Two such processes are the Selexol and Rectisol processes. Both require the contacting of a syngas stream with a scrubbing liquid with resultant pressure drops on the order of 10-20 inches of $H_2O$.

The Selexol process, licensed by Allied Chemical, is the most widely used and employs a high molecular weight polymer (dimethyl ether of polyethylene glycol) to wash the syngas of $H_2S$, COS, $CO_2$ and various mercaptans. This enriched solvent is flashed to a lower pressure, after which the flash gas containing $CO_2$, CO, and $H_2$ goes to a boiler. The solvent stream leaving the flash drum goes to a stripping column, where the $H_2S$, COS, and remaining $CO_2$ are removed and sent to a Claus plant [4]. The Selexol process is used with the Texaco gasification process which has successfully been operated with any type of coal except semi-anthracite [5].

The Rectisol process is similar to the Selexol process. It has been used with a Lurgi gasifier [6]. Refrigeration is required since the Rectisol solvent (methanol) is much more volatile than the Selexol solvent.

Aside from the fact that both the Selexol and Rectisol processes are low-temperature processes, another disadvantage is that the product gas enriched in $H_2S$ must be further treated in a Claus plant. Developed in the

1880's, the Claus process consists of oxidizing the $H_2S$, either catalytically or thermally, to form elemental sulfur. Over 50% of the sulfur produced in 1970 was produced by the Claus process [7]. However, the process is designed to treat gases congaining 20% or more $H_2S$, and is therefore only a sulfur recovery process.

In the context of a high Btu gasification process shown in Figure 1, a high-temperature desulfurization process would be advantageous since it would eliminate the need for cooling of the syngas which is associated with irreversible heat exchange and energy loss.

## Electrochemical Desulfurization

Lim [8] demonstrated on a laboratory scale that a scheme for electrochemically removing $H_2S$ at high temperatures performs quite well. Figure 2 conceptually shows the cell used. Process gas containing $H_2S$ leaves a coal gasifier and flows past the working electrode of an electrochemical cell, where it is reduced:

$$H_2S + 2e^- \rightarrow H_2 + S^{2-} \qquad (1)$$

The $S^{2-}$ ions produced migrated through the electrolyte to the counter electrode. If a $N_2$ stream flows past the counter electrode sulfide ions are oxidized according to the reaction:

$$S^{2-} \rightarrow 1/2\ S_2 + 2e^- \qquad (2)$$

Alternately, a $H_2$ stream may flow past the counter electrode in which case the following reaction occurs:

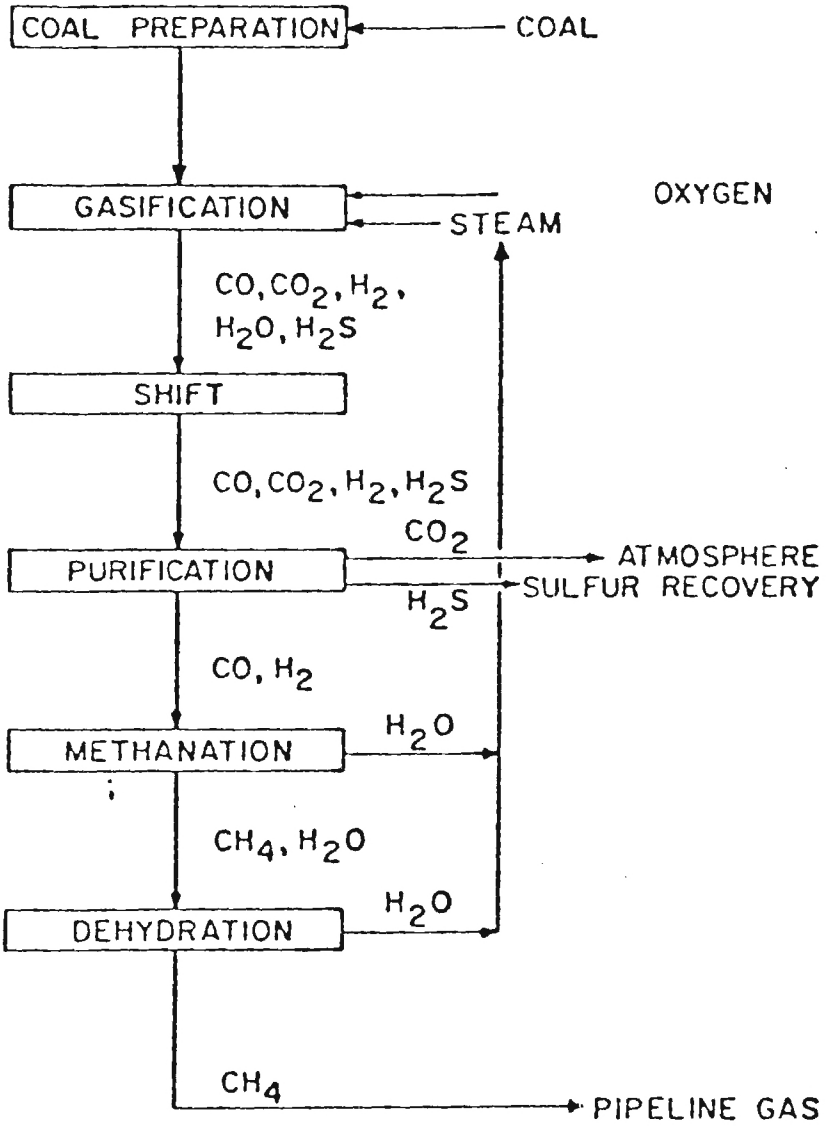


Figure 1. General high Btu gasification process scheme.

$$H_2 + S^{2-} \rightarrow H_2S + 2e^- \qquad (3)$$

The current required is calculated directly from the rate of $H_2S$ to be removed, at two Faradays per mole. the power demand follows from knowledge of the potential needed to drive the separation.

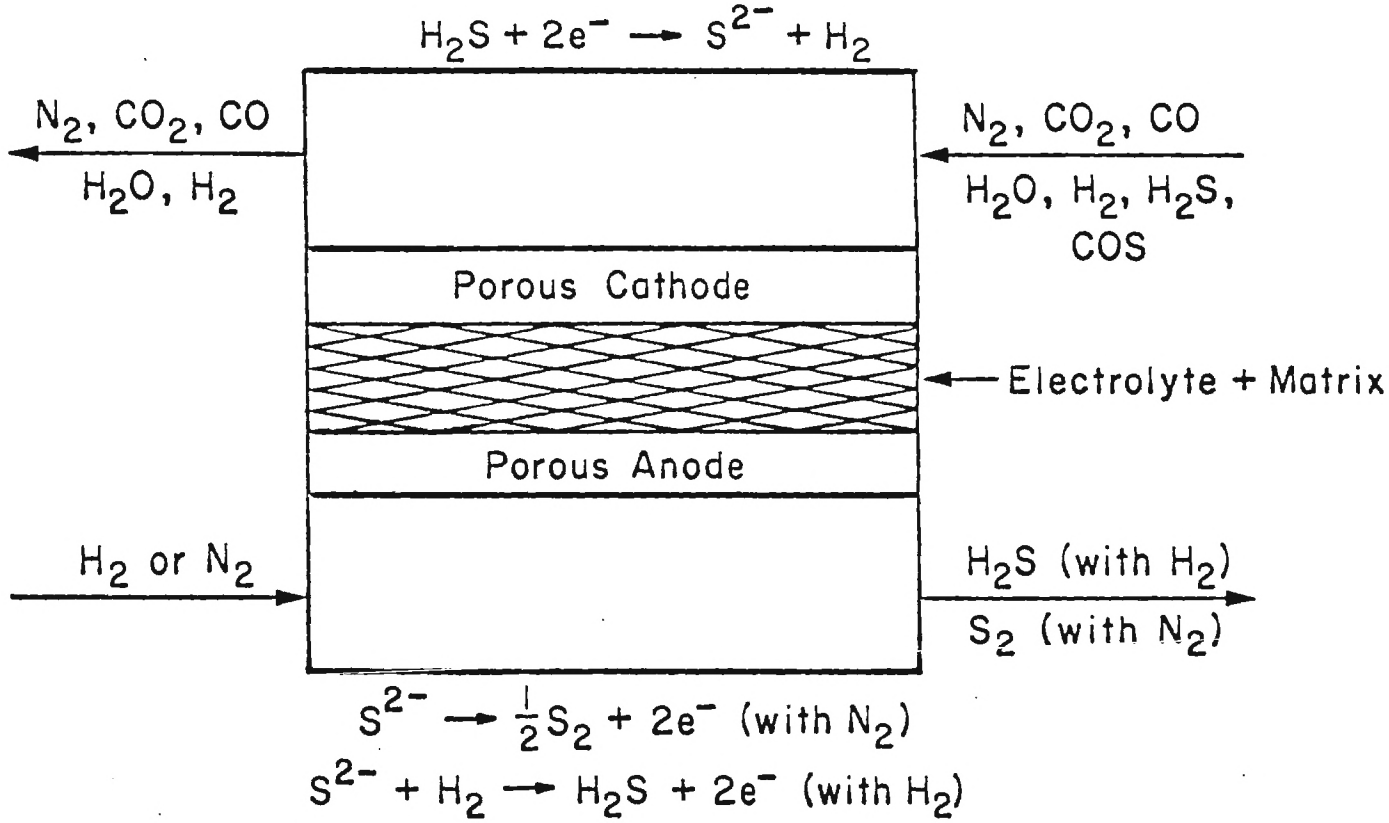


Electrochemical Desulfurization Cell

Figure 2. Gas Flow in an Electrochemical Desulfurization Cell

The equilibrium potential can be calculated from the Gibbs free energy of the overall reactions and the activities of the gas components in the electrochemical anodic and cathodic reactions through the Nernst equation. If $N_2$ is supplied to the counter electrode, the potential, E, refers to the combined cathode and anode reaction:

$$H_2S + H_2 + 1/2\ S_2 \qquad (4)$$

The equilibrium potential becomes

$$E = E_o - \frac{RT}{nF}\ \ell n\ \left[\frac{(a_{H_2})_{CA}\ (a_{S_2})^{1/2}_{AN}}{(a_{H_2S})_{CA}}\right] \qquad (5)$$

where:

$$-nFE_o = \Delta G^o_{H_2S}$$

$$(a_{H_2})_{CA} = P \cdot (C_{H_2})_{CA}$$

$$(a_{H_2S})_{CA} = P \cdot (C_{H_2S})_{CA}$$

$$(a_{S_2})_{AN} = P \cdot (C_{S_2})_{AN}$$

Equation (5) shows the small equilibrium potential required for this separation. For example, with a gasifier operating at 20 atmospheres at 1000 K this potential is only 0.67 volts for an exit stream of 10 ppm $H_2S$ in a fuel gas of 10% $H_2$, with an anode product of pure sulfur vapor (at 20 atm):

$$E = E_o - \frac{RT}{2F} \ln \frac{(0.1 \times 20)(20)^{1/2}}{(10 \times 10^{-6} \times 20)}$$

$$\text{with } E_o = -0.21 \text{ v}$$

Reduction of the exit $H_2S$ to 1 ppm requires only an additional 0.1 v. Lower temperature or pressure operation lowers the equilibrium voltage.

This is an extreme example. In practice, the sulfur vapor would be purged from the anode chamber, lowering its activity markedly. Further, an operational device would be constructed in stages so that only the final stage would encounter this low $H_2S$ partial pressure. At this final stage very little $H_2S$ is transferred, thus the current required at the higher voltages is very low. The main current demand will be at the most upstream stage where the $H_2S$ pressure is about 1% of the total pressure. Here the equilibrium potential will be less than 0.2 v.

The actual potential required depends on kinetic considerations. Thus, it is important to find the parameters which are influential in determining these driving forces.

## Purpose of Research

Before scale-up of the process demonstrated by Lim can be realized, the associated reaction kinetics and fundamental design parameters must be established. The objective of this investigation is to further determine the feasibility of using an electrochemical cell to remove $H_2S$ from hot coal gas. Cyclic voltammetric experiments will be conducted to examine the effect of variable gas compositions on the electrochemical electrode reactions along with determining the associated reaction mechanisms. In addition, gas chromatography will be used on all entering and exit gas streams to monitor the effect of applied current on $H_2S$ removal. Special emphasis will be placed on the removal experiments using a process gas containing $H_2S$ and $CO_2$ since this gas better represents the product stream from a coal gasifier.

# CHAPTER II

# THEORY

## Basic Electrochemistry

In the chemical reactions known as redox, the fundamental step is the exchange of one or more electrons between two species, 1 and 2:

$$OX_1 + ne^- \rightarrow RED_1 \quad (6)$$

$$RED_2 \rightarrow OX_2 + ne^- \quad (7)$$

$$OX_1 + RED_2 \rightarrow OX_2 + RED_1 \quad (8)$$

where OX and RED represent the oxidized and reduced forms, respectively. Frequently, this fundamental process is complicated by other chemical changes, but the basic process is simply the transfer of electrons from species 1 to 2.

The importance of a redox reaction lies in the fact that the transfer of electrons from reductant to oxidant can be made to take place at a pair of electrodes connected through external circuitry. The reductant transfers one or more electrons to the counter electrode. To maintain overall electrical balance, an equal number of electrons

must leave the counter electrode and pass through the external wiring. Simultaneously, the working electrode yields a like number of electrons to the oxidant. This constitutes a complete electrical circuit, and the extent of the redox process can be monitored or controlled by electronic operations on the external portion of the circuit. It is this ability to control the extent and direction of a reaction by electrical means that constitutes the unique importance of electrochemistry.

Analytical electrochemistry is concerned with small currents (seldom greater than a few milliamperes) at low voltages (up to perhaps 2 volts). This is precisely the magnitude easily handled by modern integrated-circuit electronics, allowing the vast body of electronic techniques of measurement and control to be utilized directly. In electrochemical experiments, most of the change in potential occurs within several angstroms of the electrode-electrolyte interface [9]. The consequence of this occurrence is that tremendous electric fields exist in the vicinity of the electrode. Such high electric fields enable electrochemical reactions to occur at a much faster rate than corresponding chemical reactions since the activation energy barrier can be easily crossed.

If the cell is left without an external controlling instrument, it will exhibit a difference of potential, E,

between its electrodes, indicating the tendency of the electrons to circulate outside the cell. This potential, in turn, is a measure of the free energy, $\Delta G$, of the reaction:

$$E = - \Delta G/nF \qquad (9)$$

where the negative sign indicates that $\Delta G$ is negative for a spontaneous reaction. In equation (9), the factor n is the number of electrons exchanged, and F is the Faraday constant. Equation (9) is strictly valid only if there is no current passing through the cell. This is because the passage of current causes not only changes of concentration, but also voltage drops and heat effects. Fortunately, with the very small currents needed by modern measuring devices, the error is usually negligible, and one can measure E, and thus $\Delta G$, with great accuracy.

For electric current to pass through the cell, redox processes must occur at both electrodes, to the extent of one mole for each nF coulombs. It can thus be written:

$$\text{Number of moles reacted} = Q/nF = (1/nF) \int I \, dt \qquad (10)$$

where Q is the number of coulombs passed, which in turn, is equal to the time-integral of the current, I.

## Galvanostatic Measurements

If the current passing through an electrochemical cell is specified, the extent of the total redox process is completely determined at each moment. The only condition required of the chemical species is that there is enough of it present at the electrode to be oxidized or reduced at the rate required by the current. In order to obtain meaningful analytical measurements, one of the electrodes should be of constant potential without changing from experiment to experiment. This electrode is called the reference electrode and because of its invariance, any change in the cell potential must be due to the condition of the working electrode. For these measurements, it is desirable to utilize a cell containing three electrodes, so connected that the reference electrode cannot pass any appreciable current. The remaining electrode is designated as the counter electrode, and the reactions taking place in its vicinity are generally of little interest.

### Open-Circuit Voltage Measurements

One always measures differences of potentials rather than the separate values for the two electrodes. The existence of such absolute potentials has preoccupied

chemists for a long time, and it appears that it is not possible to measure the potential of a single electrode [10]. Moreover, one cannot even measure the difference of potential between two dissimilar chemical phases. The only measurable quantity is the difference of potential between two portions of chemically identical material.

The electrical potential of a phase can be defined as the work necessary to bring a unit charge from a great distance to the interior of the phase. The charge must not alter the potential of the phase by its presence and must not enter into any chemical interaction. The potential so defined is called the inner, or Galvani, potential, $\phi$, and is not a measurable quantity.

It is possible to define a very similar quantity, the outer, or Volta, potential, $\Psi$, which is accessible to measurement. This concept can be derived from the model of the Galvani potential by removing the condition that the charge must actually penetrate the phase [9]. It is now only required to approach it very closely. The difference between $\phi$ and $\Psi$ is known as the surface potential, $\chi$. Of the three, only the outer potential $\psi$ is measurable, although the inner potential $\phi$ has a clearer thermodynamic significance. Even though inner potentials cannot be measured directly, some combinations of them are accessible through experimentation.

Voltage Measurements with Finite Current

In the previous discussion, the current passing through the cell was considered to be very small. In contrast, if appreciable current is allowed to pass, the following types of alterations in the voltage may occur:

1. An ohmic drop, usually referred to as an IR-drop caused by the transport of electricity through the solution and various conductors.
2. Concentration overpotential, $\eta_c$, a shift in potential caused by changes in the concentrations of OX and RED in the immediate vicinity of the electrodes. The redox process causes an increase in the concentration of one species and a corresponding decrease of the other. This change is partially offset by diffusion or stirring but the concentrations at the electrode surface $C^s_{ox}$ and $C^s_{RED}$, will still be different from those in the bulk of the solution, $C^*_{OX}$ and $C^*_{RED}$. This causes a shift in the potential as calculated by the Nernst equation to the new potential, $E^s$:

$$E^s = E^* + \eta_c = E^* + \frac{0.0592}{n} \log \left(\frac{C^s_{OX} \cdot C^*_{RED}}{C^*_{RED} \cdot C^*_{OX}}\right) \qquad (11)$$

where $E^*$ is the potential exhibited when the surface concentrations are equal to the bulk values. Note that $E^S$ is an equilibirum quantity in a sense.

3. Charge-transfer overpotential, $\eta_T$, which is the excess voltage necessary to accelerate the redox reaction to the desired rate. It is a kinetic rather than a thermodynamic quantity.

In light of the above, the total voltage, E, of a cell that uses a reference electrode can be written as follows:

$$E_{CELL} = E_{WORKING} - E_{REF} = \left(E^o + \frac{0.0592}{n} \log \frac{C^*_{OX}}{C^*_{RED}} + \eta_c + \eta_T + IR\right) - E_{REF} \qquad (12)$$

## Electrochemical Kinetics

Electrode kinetics is part of that branch of kinetics in which chemical reactions are stoichiometrically linked to electrons through Faraday's laws, and thus the rates of these processes are directly linked to the passage of current. When the electrode kinetics being referred to include only those of the actual electrode process in which the form of charge movement changes between ionic conduction

and electronic conduction, they are called charge-transfer kinetics.

Polarization

It is an experimental fact that when a net current flows through the interphase region around an electrode, the potential of that electrode will be changed. If the potential of an electrode through which zero net current if flowing is written as E(O), the difference between the actual potential of the electrode, E, and E(O) is called the polarization of the electrode:

$$\eta = E - E(O) \qquad (13)$$

Polarization is a function of the current density, j, and generally increases with increasing current density.

Transfer Coefficient

The effect of overpotential on the two reactions directions is a complicating factor that has not yet been considered. If the overpotential is positive, it would accelerate the movement of charge in the direction so as to increase anodic current. It would also decelerate the movement of charge in the direction of the cathodic current. Thus, the effects are twofold: an increase in anodic current and a decrease in cathodic current. These two effects need not be equal. Their difference will depend

on the symmetry of the electrochemical activation energy barrier that exists in the electrode interphase region (the compact double layer). The possibility of asymmetry is taken into consideration by introduction of the transfer coefficient $\alpha$. The transfer coefficient is that fraction of the overpotential that goes to increase the anodic current. Since $0 < \alpha < 1$, the fraction $(1 - \alpha)$ must therefore be the fraction of the overpotential that goes to decrease the cathodic current. The transfer coefficient $\alpha$ normally does not change significantly with potential over small potential ranges, and is frequently taken equal to 0.5. The assumption is then that the activation energy surface is symmetric.

Measured values of transfer coefficients in aqueous solution generally range from 0.2 to 0.8.

Reversible and Irreversible Reactions

The terms reversible and irreversible are commonly used in kinetics. The acceptable meaning of an irreversible reaction is that the rate of the forward reaction is so much greater than that of the backward reaction that the backward reaction can be neglected. If the rate of the forward reaction is equal to or less than the rate of the backward reaction, then the reaction is reversible. Unfortunately, the rates of charge-transfer reactions are potential dependent. Thus, the meaning of reversible and irreversible

depends upon the current demanded and the overpotential thereby produced. Great care must be used when applying these terms to a system.

## Cyclic Voltammetry

Rapid voltage scan techniques in which the direction of voltage scan is reversed are called cyclic techniques. In these techniques, a ramp is applied over the full voltage scan range and then reversed so that a descending range returns, almost invariably to the original potential. The scan rate in the forward and reverse direction is normally the same, so that the excitation waveform is actually an isosceles triangle. Cyclic voltammetry is that voltammetric technique in which the current that flows in a system is measured as a function of time and in which the excitation signal is a triangular potential (see Figure 3). Cyclic voltammetry can be used in single-cycle or multicycle modes, depending upon the electrode, the reaction in question, and the information sought. Multicycle techniques have not been used for quantitative measurements because the theory is not that far developed. They are, however, useful diagnostic tools when complex mechanisms are involved. The theoretical equations for cyclic voltammetry have been developed by Nicholson and Shain [11,12,13], and by Piekarski and Adams [14].

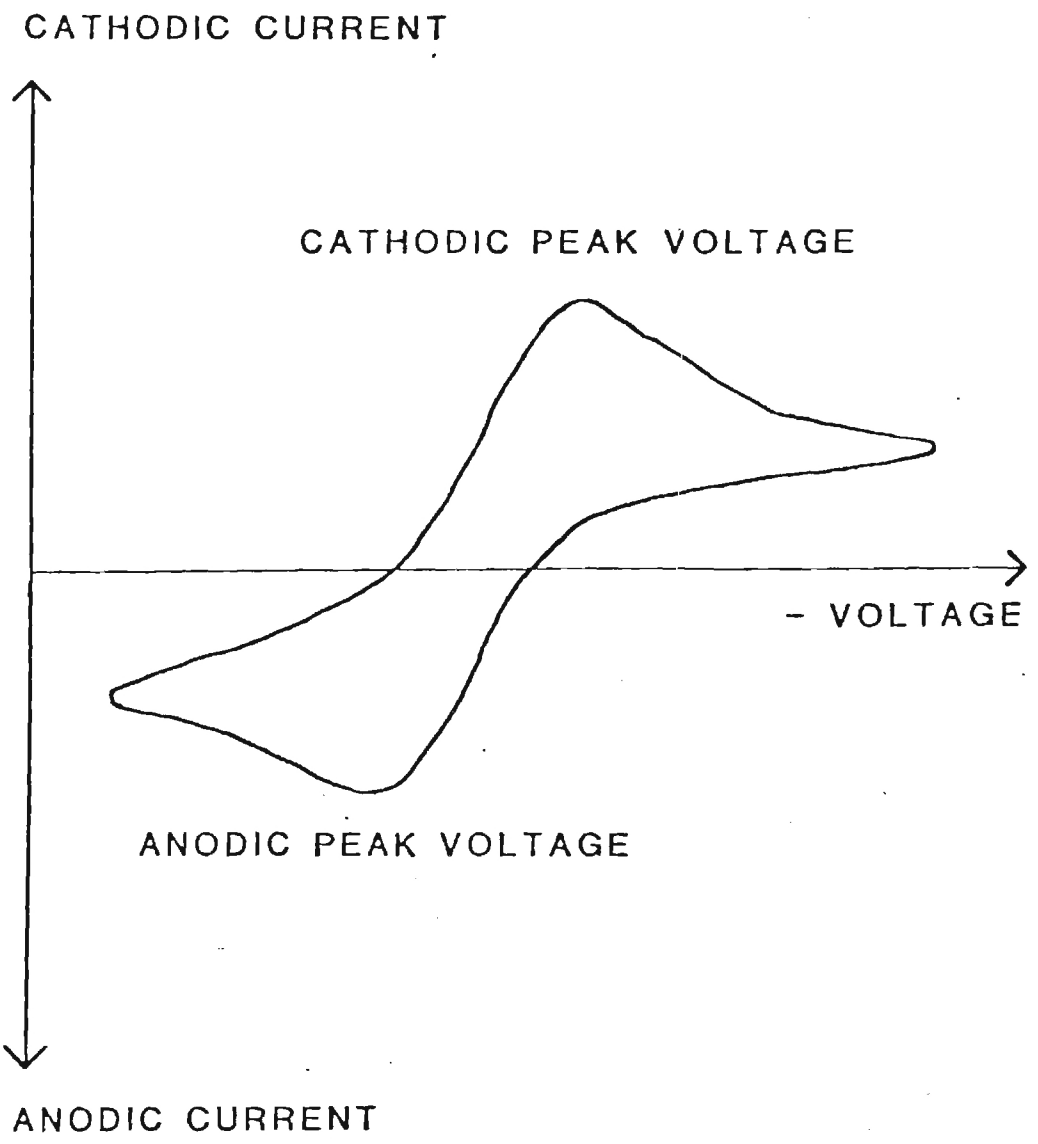


Figure 3. Cyclic Voltammogram

It is usual to plot the cyclic voltammogram on an X-Y potentiometric recorder. The measured parameters in cyclic voltammetry are the anodic and cathodic peak potentials $E_{p,c}$ and $E_{p,a}$; the anodic and cathodic peak currents $I_{p,c}$ and $I_{p,a}$; and the half-peak potentials, which are the potentials $E_{p/2,c}$ and $E_{p/2,a}$ at which the cathodic and anodic currents reach half of their peak values. The independent variables are the voltage scan rate and the range of potential over which the scan is made.

# CHAPTER III

## INSTRUMENTATION AND EQUIPMENT

### Furnace

The electrochemical reaction occurs in a 12.5 inch high furnace which is constructed of 4 inch schedule 80 #310 SS and is located in a fume hood (see Figure 4). The upper 4 inches of the furnace is cooled by a baffled water jacket. A 1 liter alumina crucible (Coors CN-1000) fits inside the furnace to protect the #310 SS from any spilled electrolyte. Several layers of refractory brick and of a kaolin-based wool insulate the furnace to assure an accurately controlled operating temperature.

The top of the furnace is sealed by a 5 inch diameter Pyrex disc. Four holes are drilled in the disc through which a 1/4 inch OD $Al_2O_3$ tube, a 5/16 inch OD mullite tube, and two 3/4 inch OD $Al_2O_3$ tubes are passed. The 1/4 inch OD $Al_2O_3$ tube is closed at the bottom and serves as a thermocouple protection tube. The mullite tube is also closed at the bottom and houses the reference electrode. Each 3/4 inch OD outer $Al_2O_3$ tube encases a 3/8 inch OD

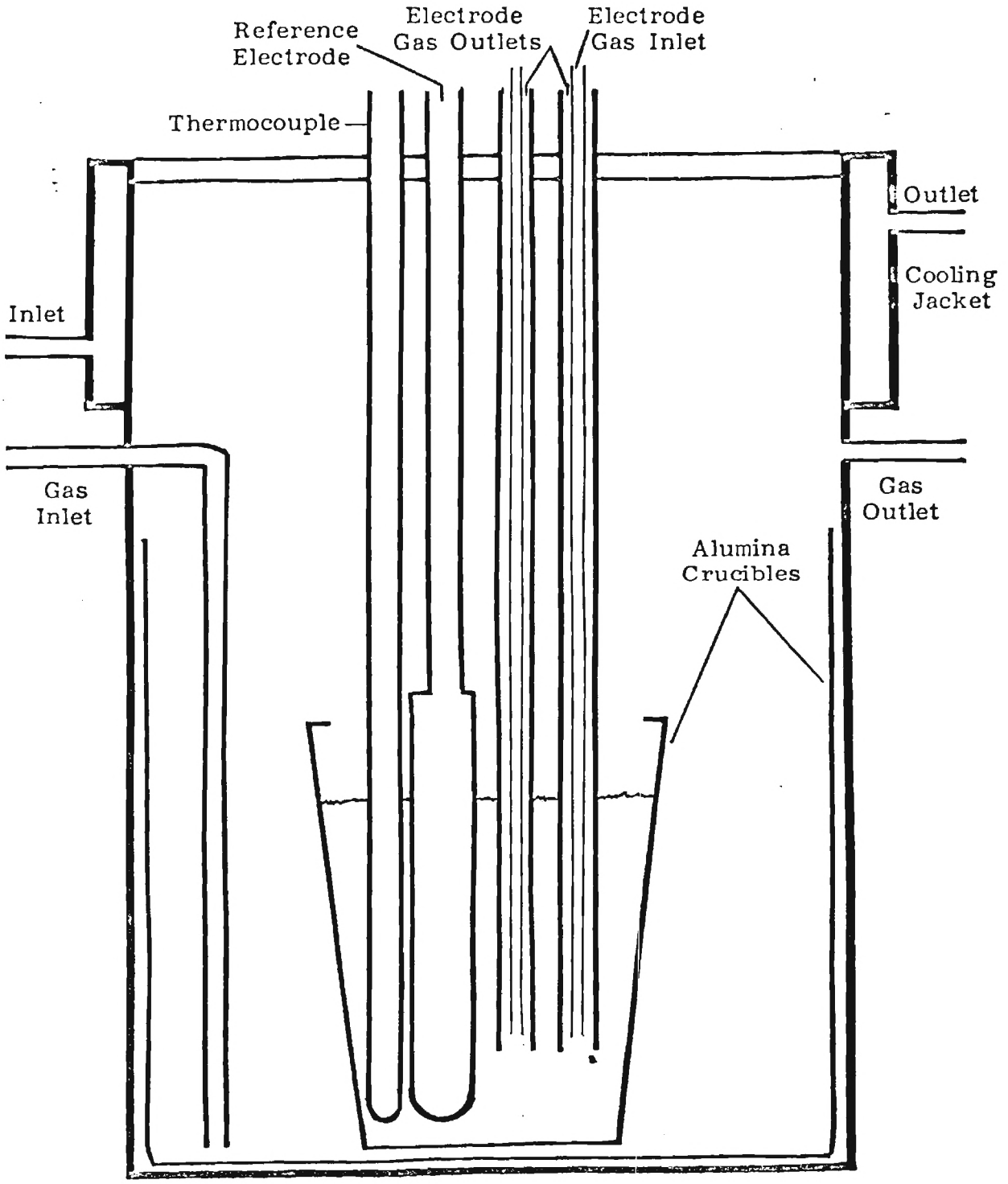


Figure 4. Reaction Furnace

inner $Al_2O_3$ tube which contains a 1/8 inch thick grade HLM graphite electrode (Great Lakes Carbon Coporation). This configuration is more fully explained in the next section.

The 99.8% $Al_2O_3$ tubes (Coors grade AD-998) are immersed in a 100 ml conical $Al_2O_3$ crucible which serves as the reaction vessel containing the electrolyte. A strip of Grafoil (Union Carbide) is wrapped around the reaction vessel to detect the unwanted presence of air in the furnace. One hundred percent silicon sealant is used at the top of the furnace to create an air tight seal between the tubes and the Pyrex disc.

A #316 SS gas inlet tube is located 5 inches from the top of the furnace. A #316 SS gas outlet tube is at the same height on the opposite side of the furnace. The inlet tube delivers a constant purge stream of $H_2$ to the furnace while the outlet tube directs the gas flow to the fume hood. Airtight operation was assured by the use of O-ring seals above and below the Pyrex plate.

Tygon tubing is used for all gas connections outside the furnace. The tubing is not affected by any gas except COS which is present in trace amounts:

$$H_2S + CO_2 \rightarrow COS + H_2O \qquad (14)$$

When COS flows through Tygon, the tubing turns amber but is not otherwise altered. Rotameters (Airco 752) used to measure the gas flow were fabricated from stainless steel to prevent corrosion.

Reference, Working and Counter Electrodes

The reference electrolyte is a mixture of 10 wt. % $Ag_2SO_4$ in a ternary alkali-sulfate eutectic (79 m % $Li_2SO_4$, 12 m % $K_2SO_4$, 9 m % $Na_2SO_4$). The electrolyte and a silver wire is added to the $Na^+$ conducting mullite tube to complete the electrode. The top of the mullite tube was sealed around the Ag lead with silicon sealant [15, 16].

The working/counter electrode configuration consists of a 1/8 inch diameter graphite rod encased in a 3/8 inch OD $Al_2O_3$ gas inlet tube which is mounted in a 3/4 inch OD $Al_2O_3$ gas outlet tube. The graphite rod is positioned such that the rod terminates flush with the bottom of the inner $Al_2O_3$ tube. This assured that the electrode gas which flowed downward through the annular region between the $Al_2O_3$ tube and the graphite rod makes good contact with the electrode-electrolyte interface. The smaller inner $Al_2O_3$ tube is terminated 7/8 inches from the bottom of the larger outer $Al_2O_3$ tube. The entering gas will react and then exit up through the outlet tube rather than bubble through the electrolyte into the reaction crucible (see Figure 5).

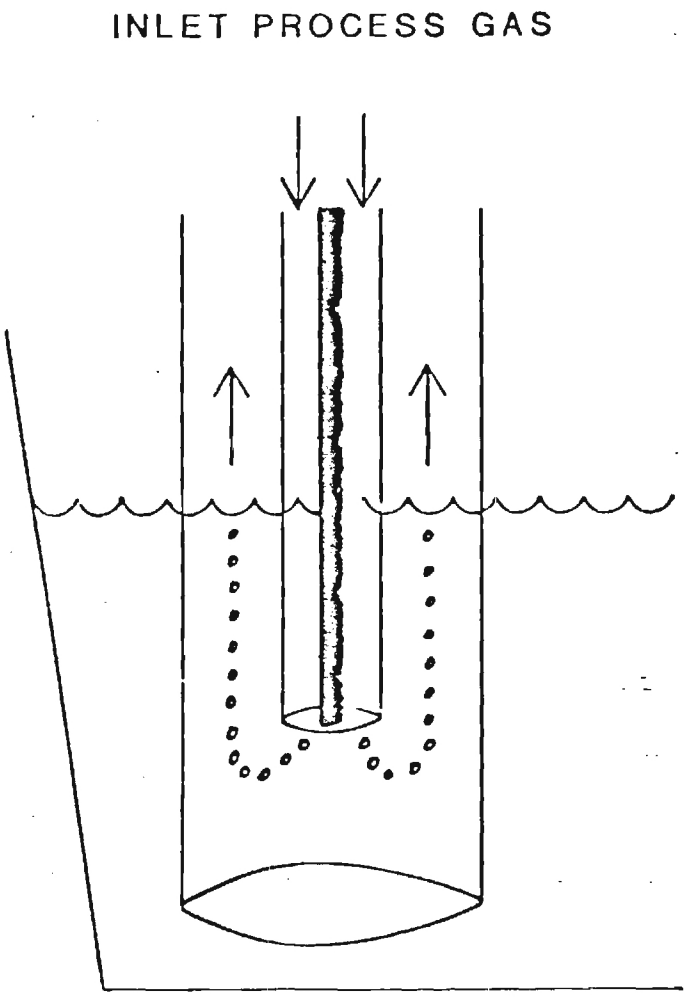


Figure 5. Gas Flow Inside the Furnace

This follows the principle that a gas will always take the path of least resistance or lowest pressure drop.

The graphite rods are 12 inches long and it was necessary to use gold wire leads from the rods to the outside of the furnace. The gold lead was threaded through the Tygon connection and sealed with silicone on one end. At the other end, it was threaded through a 0.5 mm diameter hole in the electrode.

A hole was drilled through the 1 inch OD section of Tygon, which was connected to the outlet $Al_2O_3$ tube, so that the inlet $Al_2O_3$ tube could be installed at its proper position. Rubber septum stoppers were installed into the side arm of plastic tees to create sampling ports for gas syringe samples. These sampling ports were placed into the Tygon tubing at convenient locations so that the inlet/outlet streams could be analyzed (see Figure 6). All connections were made airtight with silicone sealant.

## Electrical Instrumentation

Two Hewlett-Packard 5840A gas chromatographs (GC) were used to analyze the composition of the various gas streams. The GC is a digital processor based instrument operated from a terminal. The terminal is connected to the main frame module which houses the injection port, column oven, detectors, gas flow systems and the electronics. One

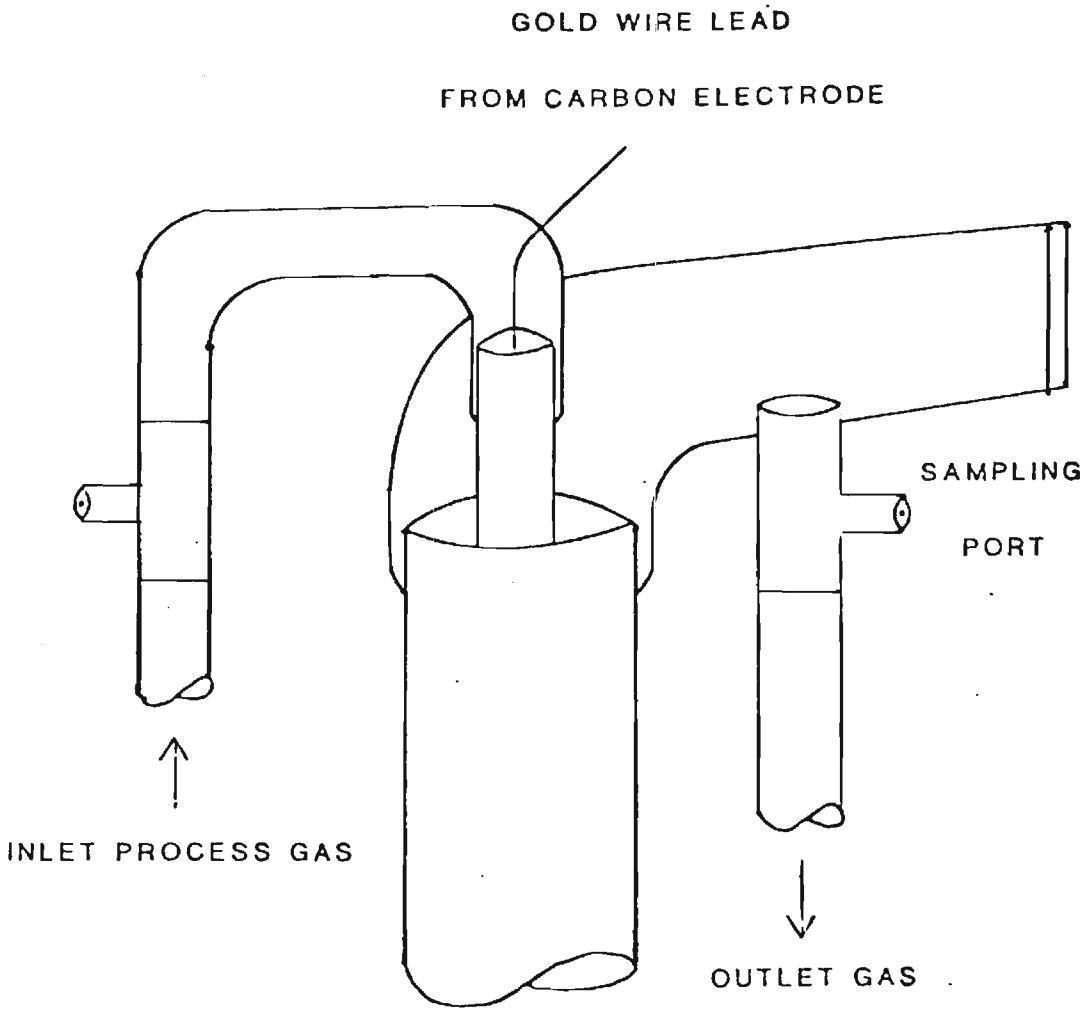


Figure 6. Gas Flow Into the Furnace

GC is fitted with a Thermal Conductivity Detector (TCD) to analyze for $CO_2$ composition, while the other is equipped with a Flame Photometric Detector (FPD) to examine for sulfur levels.

A 30 amp variable auto transformer (Standard Electrical Products Company) was used to power two semi-cylindrical heating elements (Lindberg) capable of 1473 K operation. The thermocouple protection tube houses a Type K (Chromel-Alumel) thermocouple which was connected to a voltmeter (Simpson 460 Series 5) so that the furnace temperature could be constantly monitored. A 3050 RMP fan (Redmond) was used to assist the baffled water jacket in keeping the top of the furnace cool.

A potentiostat-galvanostat (Princeton Applied Research Model 371) powered the electrochemical experiments. Current and voltage monitors integral to the Model 371 allowed observation of these parameters by a storage oscilloscope (Tektronix 5111A with 5A19N Differential Amplifier and 5B10N Time Base/Amplifier). A function generator (Hewlett-Packard 3310B) provided sinusoidal inputs or step inputs as needed, while an X-Y recorder (Hewlett-Packard 7015B) documented certain cell responses.

# CHAPTER IV

## EXPERIMENTAL PROCEDURE

### Electrolyte Preparation

A 60 mole % $K_2S$ and 40 mole % $Na_2S$ mixture of electrolyte was used as suggested by White [17]. Sufficient quantities of the alkali sulfide constituents had to be initially purified since the most pure source of $K_2S$ commercially available is only 44% pure (Alfa Chemical) while commercially available $Na_2S$ is 99% pure (Alfa Chemical). The method of purification involved heating each alkali sulfide separately, up to 1270 K in 75 ml porcelain crucibles in a $H_2$ atmosphere. The hydrates and excess polysulfides are reduced as these conditions are maintained for at least 24 hours.

Once a sufficient quantity of the alkali sulfides was purified, weighed amounts of $K_2S$ and $Na_2S$ were placed in a 250 ml $Al_2O_3$ crucible. This resulting mixture was heated beyond its melting point and left at an elevated temperature for some time to assure a homogeneous mixture. After cooling, the mixture was crushed into small chunks with a clean hammer and loaded into a Bluer Mill to grind the electrolyte into a fine powder. The electrolyte was then

stored in a container and placed in a dessicator for further use.

GC Preparation

The GC requires a minimum amount of routine maintenance to guarantee reproducible results. The initial maintenance procedure was followed as specified by the operations manual. To check the accuracy of the two detectors, several gases with varying compositions of $H_2S$, $CO_2$, CO, $H_2$ and $N_2$ were sampled until reproducible peaks were obtained. So as to operate within the dynamic range of the detectors, a 50 µl syringe was always used for FPD analyses while a 500 µl syringe was constantly used when sampling with the TCD. A FPD calibration curve was constructed by sampling the standardized 1.5% $H_2S$ gas bottle with different µl syringes and recording the resulting peaks. Then, the peak area was plotted versus the amount injected to obtain a curve which blanketed the range within which sample results were expected (see Figure 7).

Cell Preparation

To begin an experimental run, the Pyrex plate, with its associated four tubes sealed into place, was positioned on a stand outside the furnace. The 100 ml $Al_2O_3$ reaction crucible was placed at an appropriate height below the plate and the electrolyte powder was firmly packed into the

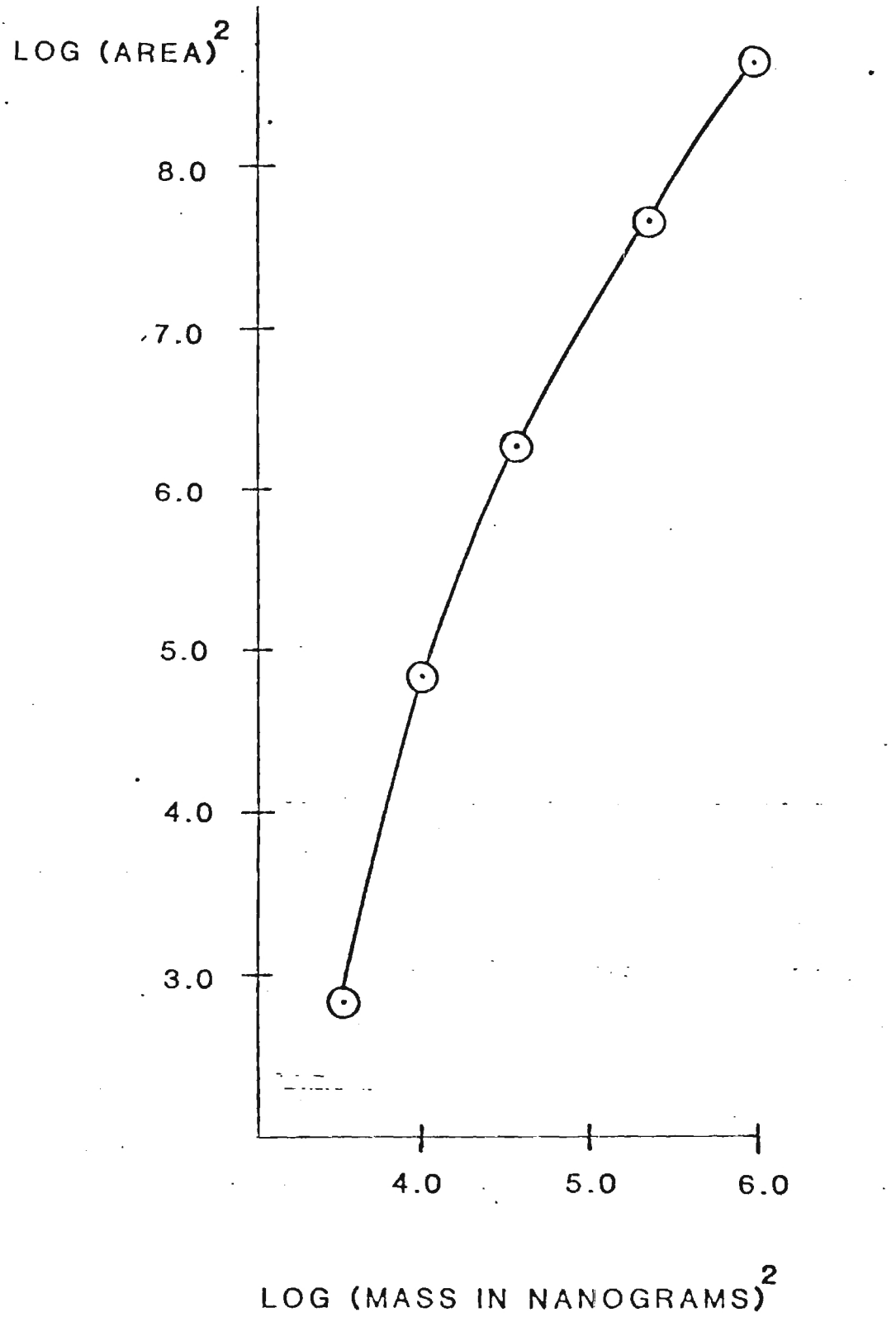


Figure 7. FPD Calibration Curve

crucible between the inner walls and tubes. The whole assembly was carefully lowered into the furnace and the furnace was sealed. After the proper gas connections were made, the furnace was purged with $H_2$ and the furnace was slowly heated.

During the heating process, the melting point of the electrolyte was observed visually and by an AC-impedance method. The AC-impedance method involved application of a sinusoidal voltage across the series combination of the cell and a resistor of known value. AC voltages across the cell and across the resistor were measured. As the melting point of the electrolyte was approached, the voltage across the cell decreased rapidly and suddenly, indicating that the electrolyte was becoming ionically conductive.

After the melting point was noted, the cell was heated to an operating temperature of 1000 K. Gas flow to the electrodes was checked visually by observing the reaction crucible for bubbling. If vigorous bubbling was not evident, the furnace was cooled to room temperature and more electrolyte was added. In general, a sufficient quantity of electrolyte was added by the second or third attempt to insure proper cell performance.

Solution Resistance and Double-layer Capacitance

The solution resistance, $R_s$, and the double-layer capacitance, $C_{dl}$, are important parameters of the

electrolyte. After the particular gas flow to the electrodes had stabilized and the system had reached thermal equilibrium, $R_s$ and $C_{dl}$ could be determined. The current interruption technique [18] is the standard measurement technique for solution resistance. After a steady-state current was established in the cell, the current was shut off, and the voltage response was recorded on an oscilloscope. The instantaneous voltage drop is equal to the IR drop and the value of $R_s$ could be calculated. To determine $C_{dl}$, a current step, $I_{APP}$, was applied to the cell using the galvanostat and the voltage response was recorded as an oscilloscope trace. The value of the double-layer capacitance was calculated from the following equation:

$$C_{dl} = \frac{I_{APP}}{(dE/dt)_{t=0}} \qquad (15)$$

As an aid to accurately determine the slope, a Polaroid picture of the oscilloscopic trace was taken using an Oscilloscope Camera (Tektronix C-5C).

Cyclic Voltammetry Experiments

Cyclic voltammetry made it possible to investigate the electrode reaction kinetics of the cell. The flow rate of the gas bubbled to the working electrode was allowed to stabilize. Voltages between the working/counter electrodes, the working/reference electrodes and the counter/reference

electrodes were observed. These values were recorded as W/C, W/R, and C/R respectively. An equilibrium state was assumed when W/C, W/R, and C/R showed no trend to change over a five minute period. As the electrolyte became saturated with the particular process gas, the electrical instrumentation was prepared for the cyclic voltammetry experiment.

The potentiostat/galvanostat was set to the potentiostatic mode and the appropriate connections were made to the cell. A voltmeter was then placed into the system to read W/R. The potentiostat was set to the applied voltage which made W/R = 0. This was done so that all voltage sweeps would begin at the equilibrium potential of the cell and then exhibit the cathodic/anodic overpotentials.

The function generator was connected to the potentiostat so that the voltage would sweep in the negative direction first and then sweep in the positive direction. A multimeter was connected to the function generator to read the voltage output level. The phase button on the function generator was adjusted until the voltages swept negatively and positively by the same amount after the manual trigger button was depressed. The X-Y recorder was placed into the system to document the resulting current response when the voltage was swept. By trial and error, the output level of

Table 1. Open-Circuit Voltages

| Process Gas | Counter Electrode Gas | Working Electrode Gas | Actual $CO_2$(%) | W/C (mV) | W/R (V) | C/R (V) |
|---|---|---|---|---|---|---|
| 1 | None | $H_2$ | 0 | -10.8 | -1.898 | -1.888 |
| 2 | None | 0.26% $H_2S$ | 0 | -17.0 | -1.911 | -1.895 |
| 3 | None | 0.42% $H_2S$ | 0 | +25.0 | -1.830 | -1.857 |
| 4 | None | 0.47% $H_2S$ | 5.8 | +68.8 | -1.928 | -1.991 |

the function generator was manipulated until both the cathodic and anodic peaks could be clearly distinguished on the X-Y recorder. So that each sweep would start at a current of i = 0, the DC offset of the function generator was adjusted until the current monitor on the potentiostat read zero. With the help of a stopwatch, the sweeprate of the function generator was determined in mV/sec when the range bottom was set at its slowest value of 0.0001.

The following process gases* were used in the cyclic voltammetry experiments on different days:

1) 1.5% $H_2S$ ---50% $H_2$----BALANCE $N_2$

2) 0.3% $H_2S$----50% $H_2$----BALANCE $N_2$

3) 0.65% $H_2S$---8% $CO_2$----25% CO ---20% $H_2$----BALANCE $N_2$

Sweep rates of 250, 500, 750, 1000, 1250, 1500, 1750 and 2000 mV/sec were used for each of the three gases so that the effect of different compositions could be studied. The range and fine tuning range buttons of the function generator were adjusted to achieve the desired sweeprates. Once it was assured that the electrolyte was saturated with the particular process gas, the gas to the electrode was shut off and the excess pressure between the gas lines and the electrolyte (due to a pressure drop associated with gas bubbling through the electrolyte) was released. The power was applied to the cell and a cyclic voltammogram was run at

*Water-gas-shift equilibrium brought gas no. 3 to simulated coal-gas composition. This is detailed later.

the given sweeprate. After the sweep, the power was turned off and the gas was turned back on to the electrode. The system was allowed to return to equilibrium (approximately 30 minutes) before the next sweeprate was run. When all the sweeprates had been run with the particular gas of the day, the function generator was reconnected to the potentiostat so that it would sweep in the positive direction first before sweeping negatively. The above procedure was also used for this set of runs.

Removal Experiments

In several of the experimental runs, it was necessary to dilute a standardized $H_2S$ containing gas with $H_2$ to produce a gas stream of a lower $H_2S$ concentration. Measurement of concentration of this diluted stream was accomplished by an accurate measurement of the flow rates of the two unmixed streams. For this a bubblemeter was employed. A bubblemeter is a volumetric device which allows one to measure the time for a given volume of gas to be displaced. All rotameters were calibrated by setting the needle valves over a wide range of scale readings and then directing the gas flows through the bubblemeter to determine the flowrate at each particular rotameter scale reading. Excellent reproducibility was achieved, and the desired $H_2S$ concentration could be obtained in the diluted stream.

The valves on the working/counter electrode outlet sampling lines were closed during initial heat-up to keep the purge gas from exiting through the sample lines. A small $H_2$ stream was passed through both electrode inlet tubes to keep the electrolyte from blocking the inlet tubes as it became molten. To assure that the outlet sampling lines were working properly, the inlet flow to each electrode was individually interrupted and the flow through the respective sampling line was observed.

All removal experiments were run with diluted $H_2S$ gas stream bubbling through the working electrode with no gas flow at the counter electrode. Both the inlet and outlet streams of the working electrode were daily sampled at open circuit with a 50 µl syringe. This was done to get a clear understanding of the background sulfur emitted from the electrolyte when no current was applied. The W/C, W/R and C/R open circuit voltages were daily and continuously recorded to observe the equilibrium potential of the cell.

To test for the removal of the sulfur species from the outlet gas stream, currents of ±10, ±25, ±50 and ±100 mA were applied to the cell. The inlet and outlet streams of the working electrode were sampled on the FPD so that the effect of removal could be noted by comparing the open circuit outlet samples versus the applied current outlet samples. After sufficient data had been collected with the

diluted $H_2S$ gas, a new process gas was introduced to the working electrode which contained 0.65% $H_2S$, 8% $CO_2$, 25% CO, 20% $H_2$ and a balance of $N_2$. To examine the combined effects of $CO_2$ and $H_2S$ on the cell, open circuit samples were taken of the inlet/outlet working electrode streams on both the TCD and FPD, respectively. Again, open circuit voltages were recorded and then inlet/outlet samples were taken on both the TCD and FPD when currents of ±10, ±25,±50, and ±100 mA were applied.

# CHAPTER V

# EXPERIMENTAL RESULTS

## Open-Circuit Voltages

A multimeter was employed to measure the open circuit voltages (OCV) of the cell. These voltages were recorded while no current was flowing through the electrolyte and they do not include any type of overpotential or IR drop. Therefore, the open-circuit voltage should only include Nernstian effects. Table 1 reports values of the working to counter, working to reference and counter to refernce voltages for the four different gas flow conditions reported in this work. Each gas containing $H_2S$ was run for approximately a week and the reported values are an average of the voltages observed during that time period.

## Resistance, Capacitance, Electrode Area and Limiting Currents

Values of the solution resistance, $R_s$, were constant for different applied currents during a particular day. The average value of $R_s$ was 1.0 Ω. Determination of the double-layer capacitance $C_D$, was dependent upon taking the slope of a tangent to a curve and was therefore somewhat subject to interpretation. An average value of $C_D$ was 750 mF. Of

more interest is the apparent double-layer capacitance per unit electrode area. Using a value for the electrode area of 2.5 $cm^2$, as observed by White [17], an average value for this parameter was 296 $mF/cm^2$.

When the limiting current flows, $i_l$, the electrode process is occurring at the maximum rate possible for the given set of mass transfer conditions. The $i_l$ is dependent upon parameters which can be calculated for this experiment such as Reynolds number, Schmidt number, mass-transfer coefficient and the maximum flux. The calculated limiting currents for this experiment are listed in Table 2.

$$k_g L/D_o = (0.65)\ Re^{1/2}\ Sc^{1/3} \qquad (16)$$

$$N_{max} = k_g A\ (C_{inlet} - C_{surface}) \qquad (17)$$

$$i_l\ (coul/sec) = (N_{max}\ mole/sec)\ (96500\ coul/eq)\ (2\ eq/mole) \qquad (18)$$

Table 2. Limiting Currents

| Process Gas Composition, Percent | | | | | | $i_\ell$, mA |
|---|---|---|---|---|---|---|
| $H_2S$ | $CO_2$ | CO | $H_2$ | $H_2O$ | $N_2$ | |
| 0.26 | 0 | 0 | 50 | 0 | rem. | 25.1a |
| 0.42 | 0 | 0 | 50 | 0 | rem. | 42.6 |
| 0.47 | 5.8 | 27.2 | 17.8 | 2.2 | rem. | 27.6 |

## Cyclic Voltammetry

Figures 8 through 10 show the current-potential profiles obtained for this system. All profiles begin from the equilibrium rest potential and then sweep the voltage in the cathodic direction before reversing and sweeping the voltage in the anodic direction. The peak currents, $i_p$, and the actual peak voltages, $E_p$, obtained at their respective sweeprates are recorded in Tables 3 through 5 for different gases. Note that the actual peak voltages have been corrected by the following equation:

$$E_p \text{ (actual)} = E_p \text{ (from scan)} + i_p R_s \qquad (19)$$

## Stoichiometric Current and Removal Current

The current is a basic measure of the rate of an electrochemical reaction. The stoichiometric current, $i_s$, and the removal current, $i_r$, were calculated for this experiment by using the following equations:

$$\begin{aligned} i \text{ (mA)} = \; & \text{(96500 coul/eq) (2 eq/mole)} \\ & \cdot \text{ (F cc gas/min) (C cc } H_2S\text{/100 cc gas)} \\ & \cdot \text{ (mole } H_2S\text{/24000 cc } H_2S\text{) (min/60 sec)} \\ & \cdot \text{ (Amp/(coul/sec)) (1000 mA/amp)} \end{aligned} \qquad (20)$$

$$i_s \text{ (mA)} = 1.34 \ FC_s \qquad . \ (21)$$

$$i_r \text{ (mA)} = 1.34 \ FC_r$$

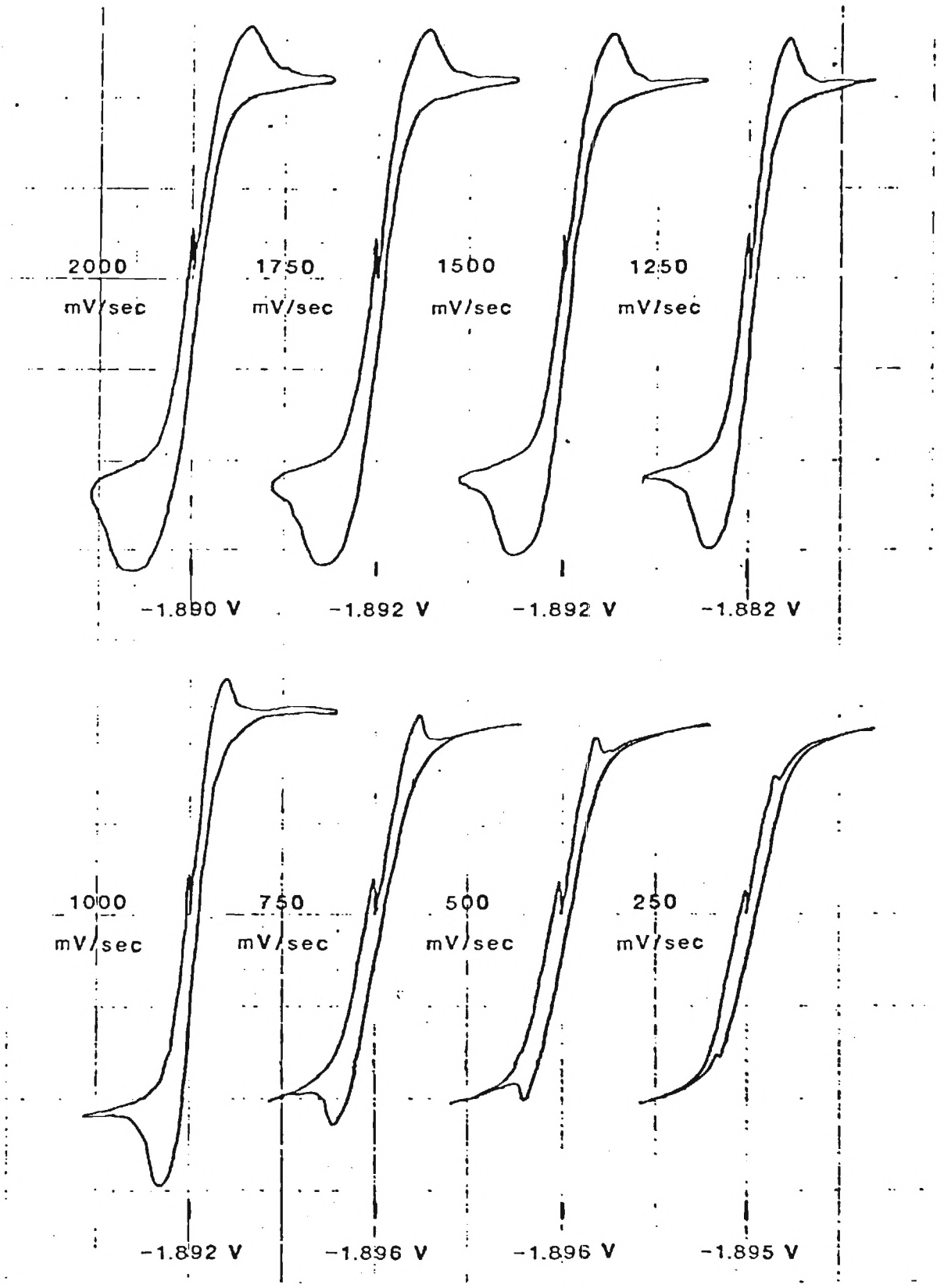


Figure 8. Cyclic Voltammograms for Process Gas Containing 0.3% $H_2S$

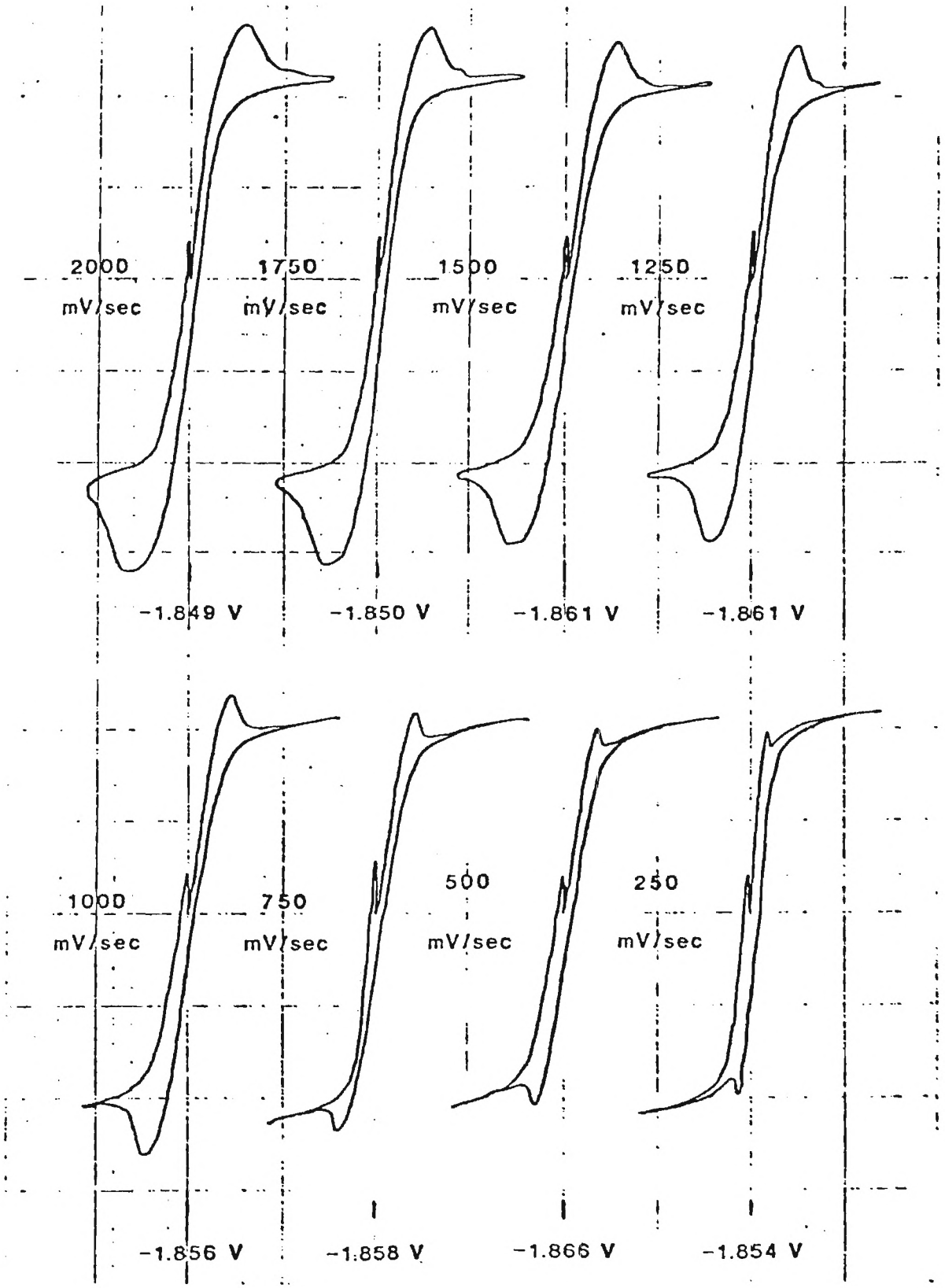


Figure 9. Cyclic Voltammograms for Process Gas Containing 1.5% $H_2S$

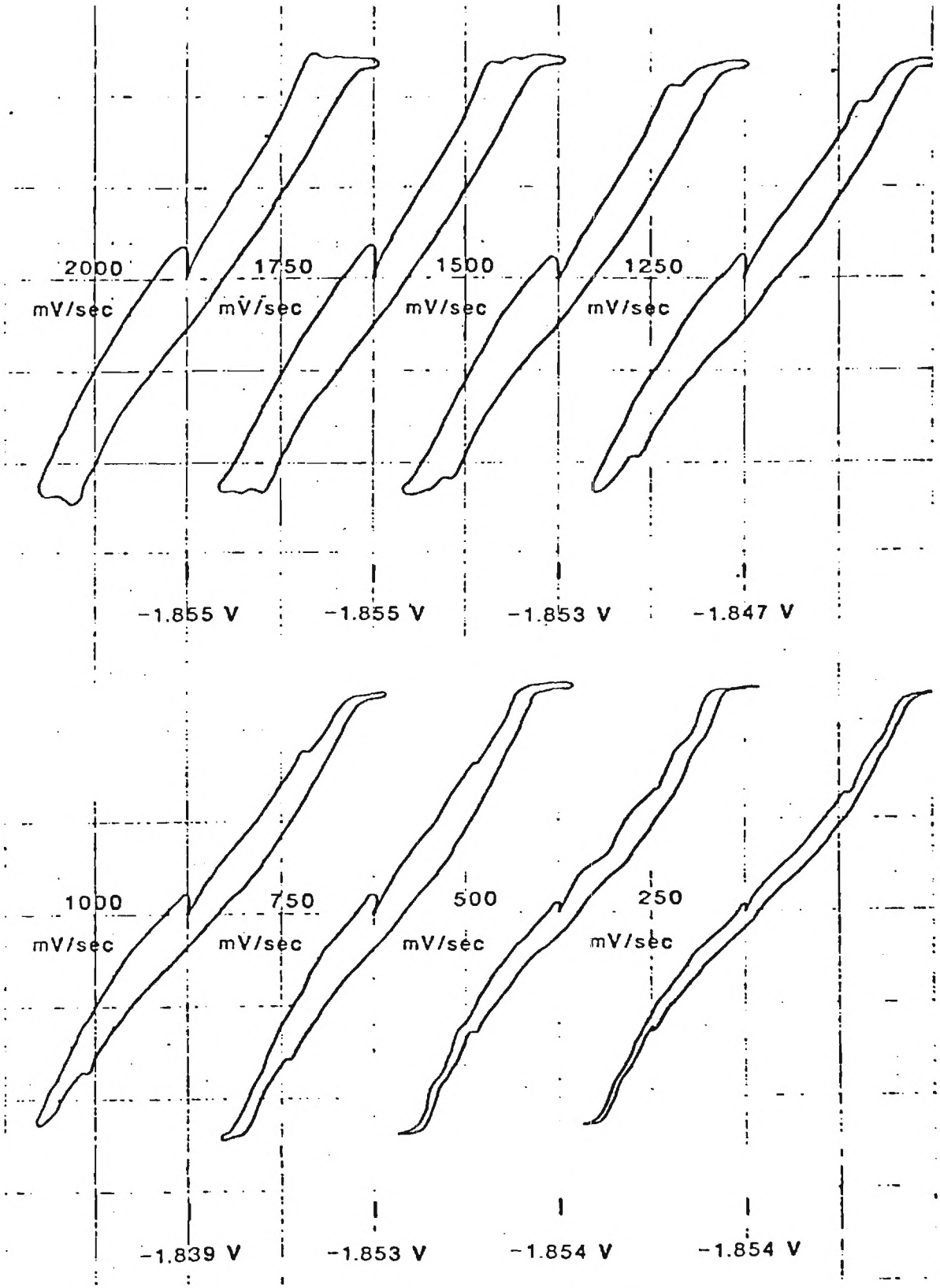


Figure 10. Cyclic Voltammograms for Process Gas Containing 0.65% $H_2S$ and 5.8% $CO_2$

Table 3. Peak Data for 0.30% $H_2S$ Gas .

| Sweeprate (mV/sec) | $i_{P_c}$ (A) | $i_{P_a}$ (A) | $E_{P_c}$ (V) | $E_{P_c}$ (V) |
|---|---|---|---|---|
| 250 | 0.0150 | 0.0165 | -2.210 | -1.578 |
| 500 | 0.0195 | 0.0200 | -2.266 | -1.476 |
| 750 | 0.0220 | 0.230 | -2.398 | -1.423 |
| 1000 | 0.0260 | 0.295 | -2.318 | -1.562 |
| 1250 | 0.0265 | 0.0300 | -2.358 | -1.452 |
| 1500 | 0.0270 | 0.0310 | -2.449 | -1.361 |
| 1750 | 0.0275 | 0.0320 | -2.500 | -1.310 |
| 2000 | 0.0278 | 0.0325 | -2.568 | -1.208 |

Table 4. Peak Data for 1.5% $H_2S$ Gas

| Sweeprate (mV/sec) | $i_{P_c}$ (A) | $i_{P_a}$ (A) | $E_{P_c}$ (V) | $E_{P_a}$ (V) |
|---|---|---|---|---|
| 250 | 0.0197 | 0.0197 | -2.074 | -1.684 |
| 500 | 0.0200 | 0.0210 | -2.236 | -1.546 |
| 750 | 0.0217 | 0.0235 | -2.310 | -1.436 |
| 1000 | 0.0235 | 0.0260 | -2.330 | -1.333 |
| 1250 | 0.0257 | 0.0285 | -2.387 | -1.385 |
| 1500 | 0.0260 | 0.0290 | -2.437 | -1.285 |
| 1750 | 0.0275 | 0.0315 | -2.458 | -1.273 |
| 2000 | 0.0280 | 0.0320 | -2.477 | -1.171 |

Table 5. Peak Data for 0.65% $H_2S$ Gas with 5.8% $CO_2$

| Sweeprate (mV/sec) | $i_{p_c}$ (A) | $i_{p_a}$ (A) | $E_{p_c}$ (V) | $E_{p_a}$ (V) |
|---|---|---|---|---|
| 250 | 0.0125 | 0.0125 | -2.916 | -0.842 |
| 500 | 0.0130 | 0.0130 | -2.867 | -0.941 |
| 750 | 0.0160 | 0.0160 | -2.919 | -0.887 |
| 1000 | 0.0170 | 0.0170 | -3.056 | -0.722 |
| 1250 | 0.0190 | 0.0190 | -3.066 | -0.678 |
| 1500 | 0.0210 | 0.0218 | -3.074 | -0.681 |
| 1750 | 0.0235 | 0.0235 | -3.128 | -0.632 |
| 2000 | 0.0245 | 0.0250 | -3.180 | -0.580 |

In equation (21) F represents the gas flowrate to the working electrode in cc of gas/minute. The value of $C_s$ denotes the average of the inlet/outlet mole fraction of the electroactive species as obtained from the FPD samples taken at open circuit, while $C_r$ represents the difference between the mole fraction of the electroactive species present at the outlet of the working electrode during open circuit and the mole fraction of the outlet stream when a certain current is applied. Table 6 tabulates the average currents measured or calculated under the specified conditions.

Table 6. Summarized Currents

| Working Electrode Gas | Actual $CO_2$ (%) | $i_{APPLIED}$ (mA) | $i_l$ (mA) | $i_s$ (mA) | $i_r$ (mA) |
|---|---|---|---|---|---|
| 0.26% $H_2S$ | 0 | -100 | 25.13 | 17.34 | 2.368 |
| 0.26% $H_2S$ | 0 | -50 | 25.13 | 17.49 | 2.176 |
| 0.42% $H_2S$ | 0 | -25 | 40.59 | 30.48 | 4.932 |
| 0.42% $H_2S$ | 0 | -10 | 40.59 | 30.54 | 4.416 |
| 0.42% $H_2S$ | 0 | -100 | 40.59 | 23.88 | 7.664 |
| 0.47% $H_2S$ | 5.8 | -100 | 27.57 | 45.11 | 24.419 |

## Sulfide Conversion

A fresh charge of electrolyte initially contains approximately 1.7 moles of sulfide. For every mole of $CO_2$ that is absorbed through the passage of process gas at the working electrode, one mole of $H_2S$ is liberated as shown in the following equation:

$$CO_2 + H_2O + S^{-2} \rightarrow CO_3^{-2} + H_2S \qquad (22)$$

A constant flowrate of 42 cc/min was maintained during the 49 hours that the process gas containing 5.8% $CO_2$ was actually absorbed into the electrolyte at a rate of 0.00609 moles $CO_2$/hr. This corresponds to a theoretical stoichiometric value of 0.2984 moles of $CO_2$ absorbed or 17.5 mole % of the sulfide converted to carbonate. The experimental conversion of sulfide to carbonate, as calculated from the FPD peaks during the same time period, was 4.16 mole % conversion while a lab analysis (Atlantic Microlab) showed that 3.3 mole % of the sulfide was converted to carbonate. It is most likely that the conversion is less than 4 mole %.

## Water-Gas Shift Effect

The process gas used to indicate the consequences of bubbling $CO_2$ into the cell had a composition of 0.65% $H_2S$,

8% $CO_2$, 25% CO, 20% $H_2$ and a balance of $N_2$ at room temperature. The actual composition varies at the operating temperature of 1000 K because of the water-gas shift equilibrium:

$$H_2 + CO_2 \rightleftharpoons H_2O + CO \qquad (23)$$

The kinetics of this reaction are no doubt rapid at the cell operating temperature. Table 7 compares the theoretical process gas composition calculated at 1000 K versus the composition of the gas determined by a TCD analysis of the gas after being heated to 1000 K in a Thermolyne Furnace.

Table 7. Process Gas Composition at 1000 K

| Component | Theoretical % | Experimental % |
|---|---|---|
| $CO_2$ | 5.7 | 5.8 |
| CO | 27.3 | 27.2 |
| $H_2$ | 17.7 | 17.8 |
| $H_2O$ | 2.3 | 2.2 |
| $H_2S$ | 0.65 | 0.65 |
| $N_2$ | BALANCE | BALANCE |

# CHAPTER VI

## DISCUSSION OF RESULTS

### Open-Circuit Voltages

The variation of the open-circuit voltage with gas composition given in Table 1 shows general qualitative agreement with theoretical expectations. It is expected that increasing the $H_2S$ concentration present at the working electrode will raise the potential of that electrode due to the tendency of $H_2S$ to be reduced:

$$H_2S + 2e^- \rightarrow H_2 + S^{2-} \qquad (24)$$

Similarly, the presence of $CO_2$ should raise the potential:

$$CO_2 + H_2O + 2e^- \rightarrow CO_3^{2-} + H_2 \qquad (25)$$

The presence of $H_2$ at an electrode should lower its potential:

$$H_2 \rightarrow 2H^+ + 2e^- \qquad (26)$$

The effect of these three gases can readily be seen as $H_2S$ and $CO_2$ bubble through the electrolyte; changes of several hundred millivolts would typically follow large changes in gas concentrations of $H_2S$ or $CO_2$.

## Cyclic Voltammetry

### Reversibility

The use of cyclic voltammetry is very popular for initial electrochemical studies of new systems and has proven very useful in obtaining information about fairly complicated electrode reactions. While this $Na_2S/K_2S$ system is too complex to derive quantitative kinetic data from cyclic voltammetry, sound qualitative assumptions can be made. These assumptions will be based on information such as the shape and size of the cathodic/anodic waves, the presence/absence of certain waves, and the variation of the peak with respect to different sweep rates. Process gases with and without $CO_2$ were tested in this investigation.

The first evaluation was to determine whether the data showed either totally reversible or totally irreversible tendencies. The peak potential, $E_p$, the $I_p$, and the sweep rate, $\nu$, were used for this analysis. From Bard [19], for a reversible wave, $E_p$ and the current function, $I_p/\nu^{1/2}$, are independent of sweep rate, which indicates that the reaction is diffusion controlled. For a Nernstian wave with stable products, the ratio of the anodic peak current, $I_{p_a}$, to the cathodic peak current, $I_{p_c}$, is equal to one at all sweep rates. The following equations also hold for a totally reversible system:

$$(E_{P_c} - E_{P_a}) = 2.3\ RT/nF \qquad (27)$$

$$|E_P - E_{P/2}| = 2.2\ RT/nF \qquad (28)$$

In the above equations, $E_{P_a}$ represents the anodic peak potential, $E_{P_c}$ represents the cathodic peak potential, while $E_{P/2}$ is the peak potential at the point where the current equals $(1/2)I_P$. As expected, when the data from the cyclic voltammograms was evaluated using the criteria outlined above, neither the process gas with or without $CO_2$ exhibited signs of reversibility. Therefore, the following equations were used which assume that the waves are irreversible to a certain extent:

$$\Delta E_P = |E_{P_1} - E_{P_2}| = 1.04\ RT/(\alpha n_a)\ F \qquad (29)$$

$$|E_P - E_{P/2}| = 1.857\ RT/(\alpha n_a)\ F \qquad (30)$$

Equation (29) assumes that $E_{P_1}$ is evaluated at a sweep rate of 2000 mV/sec, while $E_{P_2}$ is evaluated at 250 mV/sec. The transfer coefficient is represented by $\alpha$ and $n_a$ is the number of electrons involved in the rate-determining step. Table 8 was tabulated using equation (29) but similar values were obtained by using equation (30).. It is noted that $n_a$ is usually equal to one.

Table 8. Transfer Function

| Working Electrode Gas | Actual $CO_2$ (%) | $(\alpha n_a)_{CATHODIC}$ | $(\alpha n_a)_{ANODIC}$ |
|---|---|---|---|
| 0.3% $H_2S$ | 0 | 0.250 | 0.242 |
| 1.5% $H_2S$ | 0 | 0.222 | 0.175 |
| 0.47% $H_2S$ | 5.8 | 0.339 | 0.342 |

Coupled Chemical Reactions

If a homogeneous chemical reaction is coupled to the charge transfer reaction, cyclic voltammetry provides an extremely powerful method of investigating the kinetic parameters. The ECE* mechanism and the catalytic reaction have both been studied under this investigation so that a proposed reaction path could be postulated. The ECE mechanism represents the case in which a chemical reaction is coupled between two charge transfers.

$$O_1 + n_1 e \rightarrow R_1 \qquad E_1^{\circ} \tag{31}$$

$$R_1 + Z \rightarrow O_2 \tag{32}$$

*ECE is the common abbreviation for a reaction sequence of a chemical reaction preceded and followed by electrochemical reactions.

$$O_2 + n_2e - R_2 \qquad E_2^{o} \qquad (33)$$

The catalytic reaction scheme almost always involves a nonelectroactive species (Z) in the following chemical reaction which regenerates starting material.

$$O + ne - R \qquad (34)$$

$$R + Z \rightarrow O + Y \qquad (35)$$

In most treatments, it can be assumed that Z is present in large excess.

From the 1965 article by Nicholson and Shain [12], it is proposed that the ECE mechanism, Case I-R, could characterize the reaction when $CO_2$ containing process gas is bubbled through the electrolyte. In this case, the first charge transfer is irreversible and the second is reversible. The cyclic voltammograms fit the diagnostic criteria for Case I-R very well. The current function is independent of sweep rate, while the peak potential shifts in accordance with equation (29) for an 8-fold increase in the rate of the voltage sweep. As affirmed by the Case I-R criteria, the anodic wave of the cyclic voltammogram is present at slow sweep rates but is lost at much higher sweep rates. A final point of agreement with the Case I-R

assumption is that the shape and the size of the cathodic and anodic peaks are similar at particular sweep rates.

A proposed mechanism when $CO_2$-free process gas is bubbled through the electrolyte is not clearly distinguishable. The cyclic voltammograms resemble a Case VII catalytic reaction with a reversible charge transfer, as specified in the 1964 article by Nicholson and Shain [11]. This assumption is applied with great caution but the similarities do merit discussion. As suggested by the diagnostic criteria, the experimental anodic curves are the same shape as the cathodic curves. The next similarity is that the ratio of the cathodic peak currents to the anodic peak currents are approximately unity, regardless of sweep rate. The peak current functions also decreases with increasing sweep rate in a manner similar to Case VII. These diagnostic relations can at best only give a qualitative characterization of the unknown systems since only trends in the experimental behavior were used. To make a stronger justification for the catalytic reaction, an irreversible charge transfer could possibly follow the chemical reaction. This addition would answer some questions about the reversibility of the system as a whole.

Polysulfide as the Active Species

The third and most probable mechanism for this $Na_2S/K_2S$ system ~~system~~ assumes that the active species is polysulfide dissolved in sulfide. This hypothesis parallels the work done by Birk and Steunenberg [20], Tischer and Ludwig [21], and Selis [22] in similar melts. The prime difficulty for this basic work is posed by the variety of polysulfide ions present, which are hard to identify. Tischer and Ludwig suggested that the electroactive species was $S_2^{2-}$ in polysulfide melts and they experienced very high exchange current densities. At faster sweep rates, they saw that the slower chemical reactions could not remove the sulfur and therefore the current function, $I_p/v^{1/2}$, decreased with sweep rate. Thus, they concluded that the peak current does not represent a diffusion-controlled process but rather a process of a chemical reaction removing a blocking layer.

A point to be noted at this time is that the exchange currents reported by Tischer and Ludwig are two orders of magnitude higher than those reported by White [17]. Therefore, exchange current can be assumed to be dependent upon the polysulfide level in the electrolyte since Tischer and Ludwig's work was done with pure polysulfide at 350°C, while White's work was done with polysulfide dissolved in sulfide. The polysulfide concentration of this present

experiment is very low because of the high temperature and is assumed to be similar to the results of White. From viewing the work of Birk and Steunenberg, it is proposed that there are two one electron transfers occurring within one cyclic voltammogram peak. These reactions are happening at voltages very close together and cannot be distinguished.

$$2S + 2e^- - S_2^{2-} \qquad (36)$$

$$S_2^{2-} + 2e^- - 2S^{2-} \qquad (37)$$

This assumption was made based on the similarity of the experiment and cyclic voltammograms with those of Birk and Steunenberg and are in accordance with the work of Selis.

To add further justification to naming dissolved polysulfide as the active species, the concentration of the active species was calculated from the experimentally obtained peak currents and compared with the theoretical calculation of the polysulfide concentration from thermodynamics. By plotting the various peak currents versus the square root of their associated sweep rate from the cyclic voltammograms, the resulting slope can be used in conjunction with the following equation to calculate the concentration of the active species:

$$i_p = 0.4958\ nFAC_o^{*} D_o^{1/2} \nu^{1/2} \left(\frac{\alpha n_a F}{RT}\right)^{1/2} \qquad (38)$$

If an area of 2.5 $cm^2$ and a diffusivity of $10^{-6}$ $cm^2/sec$ is assumed, then the concentration of the active species is calculated to be $10^{-5}$ mole/cc.

An equilibrium constant can be calculated from the following equation by using the corresponding free energies at 1000 K:

$$(Na/K)_2\ S + H_2S \rightleftharpoons (Na/K)_2\ S_2 + H_2 \qquad (39)$$

From the equilibrium constant and by assuming that the system reacts as an ideal solution, the concentration of the polysulfide, $S_2^{2-}$, can be calculated to be $10^{-5}$ mole/cc. The fact that the experimentally derived concentration of the active species is of the same order of magnitude as the theoretically calculated concentration of the polysulfide adds much strength to the assumption that dissolved polysulfide is the active species for this $Na_2S/K_2S$ system.

## Removal Experiments

The removal current, $i_r$, gives an indication of how much sulfide is being removed from the electrolyte. It is influenced by the amount of current applied but its maximum value is dependent upon the limiting current. This system could not be operated at 100% efficiency because of the mass

transfer resistance between the film of the electrode and the bulk electrolyte, the convective effect of mixing around the electrode, and because of the residual current effect.

During the removal experiments, the process gas was bubbled to the electrode at the same time that current was applied. The desired overall reactions are as follows:

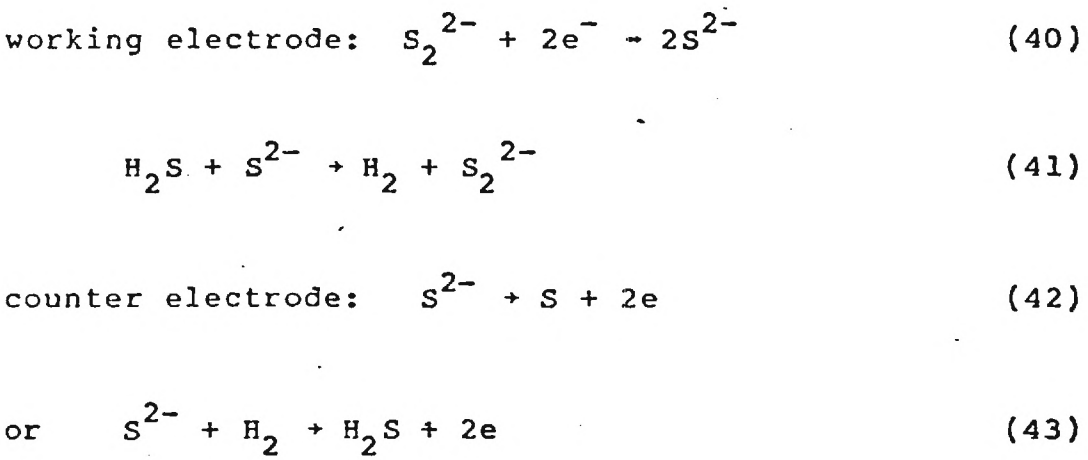

working electrode: $S_2^{2-} + 2e^- \rightarrow 2S^{2-}$ (40)

$H_2S + S^{2-} \rightarrow H_2 + S_2^{2-}$ (41)

counter electrode: $S^{2-} \rightarrow S + 2e$ (42)

or $S^{2-} + H_2 \rightarrow H_2S + 2e$ (43)

Bubbling process gas causes the electrolyte to become well mixed and a constant sulfide-polysulfide concentration gradient cannot be maintained. Fresh polysulfide rich electrolyte becomes mixed with the sulfide removed electrolyte around the electrode and polysulfide is reformed at the counter electrode by the following reaction:

$2S^{2-} \rightarrow S_2^{2-} + 2e$ (44)

This material gets recirculated to the working electrode thus causing little or no removal by equation (40). It is to be noted that in a commercial cell, the electrolyte would be fixed in a matrix and that this convective effect of mixing would not be experienced.

The electrolyte is initially full of polysulfides. These impurities are eventually driven off because of the effect of a reaction with $H_2$ at high operating temperatures. Part of the applied current during a removal experiment, acts to reduce the bulk polysulfide impurities to sulfides. This residual current effect lowers the removal current seen during the experiment and acts to reduce the electrolyte in the vicinity of the working electrode long after the applied current is turned off.

## Sulfide Conversion

Two separate analyses experimentally indicated that the conversion of sulfide to carbonate with the passage of $CO_2$ contained process gas through the electrolyte was approximately 3 mole %. The theoretical conversion was calculated by using thermodynamic free energies at 1000 K to determine an equilibrium constant from the following equation:

$$(Na/K)_2\ S + CO_2 + H_2O \rightarrow (Na/K)_2\ CO_3 + H_2S \qquad (45)$$

The free energy of reaction of the sodium compounds at 1000 K is 1290 cal/mol while that of the potassium is 6075. Assuming ideal mixing of the 40% sodium sulfide (and carbonate) and 60% potassium compounds, the mixture free energy of reaction is 4161 cal. This yields an equilibrium constant, $K_{eq}$ of 0.12.

$$\Delta G_R = -RT \ln K_{eq} \qquad (46)$$

The equilibrium constant is related to the activities of the various species in equilibrium:

$$K_{eq} = \frac{[CO_3^{2-}]\,[H_2S]}{[CO_2]\,[H_2O]\,[S^{2-}]}$$

where [ ] denotes activity

If we ignore any difference between sodium and potassium, presume the vapor phase is ideal and assume ideality as well in the electrolyte, we can estimate a 'measured' equilibrium constant:

$$K_{eq} = \frac{0.03 \times 0.0047}{0.058 \times 0.023 \times 0.97} = 0.11$$

This is in quite good agreement with the thermodynamic calculation; it permits us to make reasonable estimates of the degree of carbonation at lower temperatures and with other cation combinations.

# CHAPTER VII

## CONCLUSIONS

The electrochemistry in an electrochemical cell removing $H_2S$ from hot coal gas was explored. The behavior of the cell during cyclic voltammetric experiments and sulfide removal studies can readily be explained by accepted electrochemical theory. Most notably the cyclic voltammograms of Selis [22] greatly resemble the voltammograms obtained during this research. This adds further justification to the assumptions made in Chapter VI, naming dissolved polysulfide as the active species. The proposed ECE mechanism and the catalytic reaction mechanism are not as well documented in the literature but they provide a viable alternate method for viewing the electrode reactions.

The ratio of the removal current to the limiting current was 88% for the process gas containing $CO_2$ at the point of maximum sulfide removal. It must be understood that this electrochemical cell was designed to observe certain kinetic and removal principles rather than to operate at 100% efficiency. Mass transfer resistance, the convective effect of mixing in the vicinity of the electrode and residual current effects all took away from the efficiency of the cell. An actual commercial cell would hold the electrolyte in an inert matrix such as $LiAlO_2$ and would experience a much higher reliable efficiency.

An electrolyte of 60 mole % $K_2S$ and 40 mole % $Na_2S$ was used during this investigation. Lim [8] suggested that an electrolyte containing potassium as the cation would be most resistant to the conversion of sulfide to carbonate with the passage of $CO_2$ contained process gas. This study proves the validity of that assumption in that a lab analysis of the spent electrolyte showed that less than 4 mole % of the original sulfide was converted to carbonate.

A partially carbonated electrolyte, as would be encountered in treating actual coal gas, gave markedly improved performance. The $H_2S$ removal increased to a point limited only by mass transfer.

# BIBLIOGRAPHY


1. Schmitt, R. W.; J. of the Institute of Energy, 54, (419), p. 63, 1981.

2. Dawes, M. H. and Peterson, J. R.; in Proceedings of the 16th Intersociety Energy Conversion Engineering Conference, Vol. 1, p. 703, 1981.

3. Houghtby, W. E., et. al.; Electric Power Research Institute (EPRI) EM-956, 1978.

4. Apte, A. J. and Fein, H. L.; in Proceedings of the 16th Intersociety Energy Conversion Engineering conference, Vol. 2, p. 1047, 1981.

5. Cornilis, B., et. al.; in Proceedings of the 16th Intersociety Energy Conversion Engineering Conference, Vol. 2, p. 1050, 1981.

6. Langhoff, J., et. al.; in Proceedings of the Second World Congress of Chemical Engineering, Vol. 2, p. 47, 1981.

7. Cheng, A. Y.; "The Claus Process for Sulfur Recovery", (unpublished literature review), 1982.

8. Lim, H. S.; Doctoral Dissertation, School of Chemical Engineering; Georgia Institute of Technology, September 1982.

9. Bockris, J. O'M. and Reddy, A. K. N.; Modern Electrochemistry, Plenum/Rosetta, 1973.

10. Guggenheim, E. A.; Thermodynamics, Wiley-Interscience, Chapter 10, 1950.

11. Nicholson, R. S. and Shain, I.; Anal. Chem., 36, p. 706, 1964.

12. Nicholson, R. S. and Shain, I.; and Chem., 37, p. 178, 1965.

13. Nicholson, R. S. and Shain, I.; and Chem., 37, p. 190, 1965.

14. Piekarski, S. and Adams, R. N.; Voltammetry with Stationary and Rotated Electrodes, Wiley-Interscience, p. 531, 1971.

15. Shores, D. A. and Fang, W. C.; J. Electrochem. Soc., 128, (2), p. 346, 1981.

16. Watt, G. W., et. al.; Proceedings of the Second International Symposium on Molten Salts, p. 81, 1981.

17. White, K. A.; Master's Thesis, School of Chemical Engineering, Georgia Institute of Technology, January 1984.

18. Vetter, K. J.; Electrochemical Kinetics, Academic Press, 1967.

19. Bard, A. J. and Faulkner, L. R.; Electrochemical Methods, Wiley, 1980.

20. Birk, J. R. and Steunenberg, R. K.; Advances in Chemistry, American Chemical Society, 140, 1974.

21. Tischer, R. P. and Ludwig, F. A.; Advances in Electrochemistry and Electrochemical Engineering, Wiley-Interscience, 10, 1977.

22. Selis, S. M.; Electrochimica Acta, 15, p. 1285, 1970.

GRI-84/0201

# HYDROGEN SULFIDE REMOVAL FROM HOT GAS AND CONCENTRATION OF SULFUR USING ELECTROCHEMISTRY

FINAL REPORT
(August 1, 1982 - December 31, 1984)

**Gas Research Institute**
**8600 West Bryn Mawr Avenue**
**Chicago, Illinois 60631**

# HYDROGEN SULFIDE REMOVAL FROM HOT GAS AND CONCENTRATION TO SULFUR USING ELECTROCHEMISTRY

FINAL REPORT
(August 1, 1982 - December 31, 1984)

Gas Research Institute
8600 West Bryn Mawr Avenue
Chicago, Illinois 60631

## GRI DISCLAIMER

LEGAL NOTICE This report was prepared by Georgia Institute of Technology as an account of work sponsored by the Gas Research Institute (GRI). Neither GRI, members of GRI, nor any person acting on behalf of either:

a. Makes any warranty or representation, express or implied, with respect to the accuracy, completeness, or usefullness of the information contained in this report, or that the use of any apparatus, method, or process disclosed in this report may not infringe privately owned rights; or

b. Assumes any liability with respect to the use of, or for damages resulting from the use of, any information, apparatus, method, or process disclosed in this report.

| | |
|---|---|
| Title | Hydrogen Sulfide Removal From Hot Gas and Concentration to Sulfur Using Electrochemistry |
| Contractor | Georgia Institute of Technology |
| Principal Investigator | J. Winnick |
| Time Span | August 1983 - July 1985<br>Final Report |
| Major Achievements | The technical feasibility of the electrochemical removal of $H_2S$ from gaseous fuels at high temperatures (650-900$^0$C) has been demonstrated by laboratory scale tests for a limited range of process parameters. It was found that the intrinsic chemical kinetics exceed the rate controlling, mass transfer, processes. The mechanism for the electrochemical reduction of $H_2S$ and oxidation of $S^{-2}$ was found to be the same as that observed at lower temperatures in sulfur batteries. The effect of $CO_2$ and $H_2O$ in the gaseous mixture was to convert part of the electrolyte ($K_2S$-$Na_2S$) to carbonate. A high level of electrolyte carbonation can be tolerated since only a small concentration of $S^{-2}$ is required to transfer the electrolysis current. Furthermore, the presence of carbonate in the electrolyte enhanced the $H_2S$ removal efficiency. |
| Description of Work Completed | A high temperature (650-700$^o$C) electrochemical cell was constructed and used to study the removal of $H_2S$ from gaseous fuel streams by electrolysis. The $H_2S$ removal entails the reduction of $H_2S$ in the gaseous mixture at the cathode, transport of sulfide ions across the electrolyte to the anode where they are oxidized to elemental sulfur and released by vaporization. Electronanalytical techniques were employed to investigate the chemical and electrochemical steps involved in the process over a limited range of gas compositions and experimental parameters. |
| Recommendations | The technical feasibility should be studied of operating an electrolysis cell for the removal of $H_2S$ at lower temperatures (300-500$^o$C). This should entail the search for suitable electrolytes and electrode materials, a study of their compatibility with the electrolysis concept, and removal efficiencies (voltage, rate, current efficiency) as a function of temperature, gas composition and pressure. |

Project Implications

Acid gas ($H_2S$ and $CO_2$) removal from natural and substitute natural gas is generally required to produce a fuel gas suitable for commercial use. The cost and efficiency of existing processes for acid gas removal, which can be considerable, translates into higher costs of methane to consumers. Acid gas removal can constitute as much as 10-15% of the cost of substitute natural gas.

An efficient, cost effective process for the high temperature (300-700°C) removal of acid gases would fit particularly well into coal gasification processes where the gas issuing from the gasifier can be processed to remove the $H_2S$ without having to first cool it to the low temperature required for conventional $H_2S$ removal technology. This investigation is developing fundamental information on an electrochemical technique that appears to have the potential of providing such an option. The effort is directed toward providing fundamental information on the electrochemical $H_2S$ removal that is needed to assess its technical and economic viability. While results to date are encouraging, a broader data base is required to make a technical and economic study of its viability. Further studies will be undertaken with specific focus on identifying the lower temperature limits for electrochemical removal of $H_2S$.

John L. Cox, Manager
Organic Chemistry
Basic Research

Attachment D

# HYDROGEN SULFIDE REMOVAL FROM HOT GAS AND CONCENTRATION TO SULFUR USING ELECTROCHEMISTRY

FINAL REPORT
(August 1, 1982 - December 31, 1984)

Prepared by

Jack Winnick

Georgia Institute of Technology
School of Chemical Engineering
Atlanta, Georgia 30332-0100

For
GAS RESEARCH INSTITUTE
Grant 5082-260-0652

GRI Project Manager
John L. Cox
Organic Chemistry

July 1985

Attachment E

REPORT DOCUMENTATION PAGE

Recipient's Accession No.
GRI-84/0201

Title
Hydrogen Sulfide Removal From Hot Gas And Concentration to Sulfur Using Electrochemistry

Report Date
July 1985

Author
Jack Winnick

Performing Organization
Georgia Institute of Technology
Department of Chemical Engineering
Atlanta, Georgia 30332-0100

Grant Number
5082-260-0652

Sponsoring Organization
Gas Research Institute
8600 West Bryn Mawr Avenue
Chicago, Illinois 60631

Rprt Type & Prd. Cov.
Final Report
July 1985

The virtual omnipresence of sulfur in fossil fuels raises concern regarding the increased use of coal for high temperature fuel utilization and conversion processes. A typical raw gas composition from burning Illinois #6 coal (3.9% sulfur) in an air-blown gasifier is 19.6% CO, 8.1% $CO_2$, 10% $H_2$, 3.4% $H_2O$, 3% $CH_4$, 0.6% $H_2S$ with the balance being inerts. This gas has several potential uses. Of most interest is its conversion to high-BTU SNG which requires passage over a methanation catalyst at 300-400°C. The methanation catalysts, however, are sensitive to even small (5ppm) concentrations of $H_2S$. Thus, in the absence of a very effective high-temperature sulfur clean-up process, the gas must be cooled to the temperatures of operation of commercially available processes (e.g., Selexol or Rectisol). The use of high-temperature clean-up is estimated to allow savings of up to 7% of the energy value of the gas[1].

Since a high-temperature sulfur removal process is desirable several have undergone examination. Most are based on reaction of a metal oxide with the $H_2S$, with subsequent regeneration to the fresh sorbent and a concentrated stream of $H_2S$. This $H_2S$ is then sent to a Claus Plant to be oxidized to elemental sulfur (and water). Difficulties of various kinds have not permitted any of these processes from as yet reaching commercialization.

[1]Grainger, L. and J. Gibson, "Coal Utilization," New York: Wiley, 1981 Wen, C. Y. and E. S. Yee, "Coal Conversion Technology," London: Addison-Wesley, 1979.

# NOMENCLATURE

| | |
|---|---|
| $a$ | Activity of a phase |
| $A$ | Active electrode area ($cm^2$) |
| $C_o$ | Concentration of the active species (mole/cc) |
| $C_{dl}$ | Double-layer capacitance (mF) |
| C/R | Potential from counter to reference electrode (V) |
| $D_o$ | Diffusivity of the active species ($cm^2$/sec) |
| $e^-$ | An electron |
| $E$ | Potential (V) |
| $E_p$ | Peak potential (V) |
| $F$ | Gas flow rate (cc/min) |
| $F$ | Faraday's constant (96500 coul/eq) |
| GC | Gas chromatograph |
| $\Delta G^o$ | Standard state free energy |
| $i_l$ | Limiting current (mA) |
| $i_p$ | Peak current (mA) |
| $i_r$ | Removal current (mA) |
| $i_s$ | Stoichiometric current (mA) |
| $I_{APP}$ | Applied current (mA) |
| $j$ | Current density |
| $k_g$ | Mass transfer coefficient |
| $n$ | Number of electrons exchanged |
| $n_a$ | Number of electrons involved in rate determining step |
| $N_{max}$ | Maximum flux |
| OX | Oxidized species |
| OD | Outside diameter (inches) |

| | |
|---|---|
| P | Pressure (PSIA) |
| Q | Number of coulombs passed |
| R | Universal gas constant (1.987 cal/mol K) |
| RED | Reduced species |
| $R_e$ | Reynolds number |
| $R_s$ | Solution resistance (Ω) |
| Sc | Schmidt number |
| t | Time (sec) |
| T | Temperature (K) |
| w/C | Potential from working to counter electrode (V) |
| w/R | Potential from working to reference electrode (V) |

Subscripts

| | |
|---|---|
| a | Anodic |
| c | Cathodic |

Superscripts

| | |
|---|---|
| s | At the electrode surface |
| * | In the bulk phase |

## Greek Letters

| | |
|---|---|
| $\alpha$ | Transfer coefficient |
| $\Delta$ | Denotes a change of any variable |
| $\eta$ | Overpotential |
| $\nu$ | Cyclic voltammetric sweep rate (mV/sec) |
| $\phi$ | Inner potential |
| $\Psi$ | Surface potential |
| $\psi$ | Outer potential |

## SUMMARY

The virtual omnipresence of sulfur in fossil fuels raises concern regarding the increased use of coal for high temperature fuel utilization and conversion processes. A typical raw gas composition from burning Illinois #6 coal (3.9% sulfur) in an air-blown gasifier is 19.6% CO, 8.1% $CO_2$, 10% $H_2$, 3.4% $H_2O$, 3% $CH_4$, 0.6% $H_2S$ with the balance being inerts. This gas has several potential uses. Of most interest is its conversion to high-BTU SNG which requires passage over a methanation catalyst at 300-400°C. The methanation catalysts, however, are sensitive to even small (5ppm) concentrations of $H_2S$. Thus, in the absence of a very effective high-temperature sulfur clean-up process, the gas must be cooled to the temperatures of operation of commercially available processes (e.g., Selexol or Rectisol). The use of high-temperature clean-up is estimated to allow savings of up to 7% of the energy value of the gas[1].

Since a high-temperature sulfur removal process is desirable several have undergone examination. Most are based on reaction of a metal oxide with the $H_2S$, with subsequent regeneration to the fresh sorbent and a concentrated stream of $H_2S$. This $H_2S$ is then sent to a Claus Plant to be oxidized to elemental sulfur (and water). Difficulties of various kinds have not permitted any of these processes from as yet reaching commercialization.

(1) Grainger, L. and J. Gibson, "Coal Utilization," New York: Wiley, 1981 Wen, C. Y. and E. S. Yee, "Coal Conversion Technology," London: Addison-Wesley, 1979.

Recently, an electrochemical membrane cell was shown to have a distinct promise[2]. In addition to providing high-temperature $H_2S$ removal, the sulfide is oxidized directly to elemental sulfur. Further, the hydrogen (in the $H_2S$) is added to the coal gas. Thus, to the advantage in energy savings of high-temperature clean-up is added the elimination of the need for a Claus plant.

This feasibility study left many questions of fundamental nature unanswered. To understand more fully the chemistry and electrochemistry involved, an experiment using free-electrolyte (no ceramic membrane) was devised. The electrolyte consisted of a binary mixture of $Na_2S$ and $K_2S$. An operating temperature of 1000 K was used for all runs. Cyclic voltammetric experiments were conducted to examine the effect of variable gas composition on the electrochemical electrode reactions. In addition, gas chromatography was used to monitor the effect of applied current on $H_2S$ removal.

The qualitative cyclic voltammetric experiments corresponded well with the accepted literature results. The most probable mechanism for this system assumes that the active species is a low concentration of polysulfide disolved in sulfide. It is proposed that there are two reactions each transferring one electron at volatages very close together occurring within one cyclic voltammogram peak. The exchange current is also assumed to be dependent upon the polysulfide level in the electrolyte.

(2)Lim, H. S. and J. Winnick, J. Electrochem. Soc., 131, 562 (1984).

The removal experiments proved that electrochemistry is a viable desulfurization method. For an applied current of 100 mA, the ratio of the removal current to the limiting current was approximately 10% with a process gas containing 0.26% $H_2S$ and approximately 20% for a process gas containing 0.42% $H_2S$. It must be understood that this electrochemical cell was designed to observe certain kinetic and removal principles rather than to operate at 100% efficiency. An actual commercial cell would hold the electrolyte in an inert matrix and would experience a much higher reliable efficiency.

The effect of the presence of $CO_2$ upon the removal of $H_2S$ from a process gas stream is very important because this experiment better represents the industrial case. The ratio of the removal current to the limiting current was 88% for the process gas containing $CO_2$ at the point of maximum sulfide removal. As expected with the $Na_2S/K_2S$ electrolyte, less than 4 mole % of the original sulfide was converted to carbonate with the passage of process gas which contained $CO_2$.

Detailed Report

# "Hydrogen Sulfide Removal From Hot Gas and Concentration to Sulfur Using Electrochemistry"

Aug. 1, 1982 - Dec. 31, 1984

A part of the final report by the

Georgia Institute of Technology

Prepared for the

Gas Research Institute

under Grant No. 5082-260-0652

July 1985

## TABLE OF CONTENTS

# INTRODUCTION

Today's society is placing ever-increasing demands on the fuel industry. Market projections predict that very soon existing energy sources will no longer be able to supply our needs. Environmentalists are concerned that it is our sources of relatively clean fuels which are being dissipated rapidly. We are being forced to turn to less conventional methods of energy production. These methods must involve either the application of new technology or the introduction of new fuels.

As the nation's energy requirements increase, it is believed that the United States will turn to coal to supply a greater portion of the national energy requirements [1]. One of the problems delaying the greater use of coal now is the sulfur content of the coal. When the coal is burned in a conventional manner, the sulfur is converted to sulfur dioxide. Removal of the sulfur dioxide from the combustion gases is costly and often produces a large volume of waste material that must be disposed of.

An alternate to direct combustion of the coal is coal gasification. It is likely that coal gasification will be a major factor in the increased use of high-sulfur coals [2, 3]. Instead of the sulfur in the coal forming sulfur dioxide, in coal gasification the sulfur is found in the gas as hydrogen sulfide.

The removal of hydrogen sulfide from a gas is easier than the removal of sulfur dioxide. However, commercial hydrogen

sulfide removal technology requires that the gas stream be at or near the ambient temperature. In addition, removal of hydrogen sulfide accounts for a significant percentage of the cost of a coal gasification plant. The overall coal gasification process would become more competitive if the cost of cleaning the hot $H_2S$ process gas could be lowered.

## Hydrogen Sulfide Removal Process

Wet scrubbing processes are presently used to remove the $H_2S$ from coal gasification product streams. These processes require energy-wasting cooling of the syngas and normally suffer economically because of the use of a Claus plant (see Figure 1). Two such processes are the Selexol and Rectisol processes. Both require the bubbling of a syngas stream through a scrubbing liquid with resultant pressure drops on the order of 10-20 inches of $H_2O$.

The Selexol process, licensed by Allied Chemical, is the most widely used and employs a high molecular weight polymer (dimethyl ether of polyethylene glycol) to wash the syngas of $H_2S$, COS, $CO_2$ and various mercaptans. This enriched solvent is flashed to a lower pressure, after which the flash gas containing $CO_2$, CO, and $H_2$ goes to a boiler. The solvent stream leaving the flash drum goes to a stripping column, where the $H_2S$, COS, and remaining $CO_2$ are removed and sent to a Claus plant [4]. The Selexol process is often used with the Texaco gasification process which has been proven successful with any type of coal except semi-anthracite [5].

The Rectisol process is similar to the Selexol process. It generally is used with a Lurgi gasifier [6] and refrigeration is required since the Rectisol solvent (methanol) is much more volatile than the Selexol solvent.

Aside from the fact that both the Selexol and Rectisol processes are low-temperature processes, another disadvantage is that the product gas enriched in $H_2S$ must be further treated in a Claus plant. Developed in the 1880's, the Claus process consists of oxidizing the $H_2S$, either catalytically or thermally, to form elemental sulfur. Over 50% of the sulfur produced in 1970 was produced by the Claus process [7]. However, the process is designed to treat gases containing 20% or more $H_2S$, and is therefore only a sulfur recovery process.

Figure 1 shows that a high-temperature desulfurization process would be advantageous. Such technology would eliminate the need for cooling of the syngas which is associated with irreversible heat exchange and energy loss.

## Electrochemical Desulfurization

Lim [8] demonstrated on a laboratory scale that a scheme for electrochemically removing $H_2S$ at high temperatures performs quite well. Figure 2 conceptually shows the cell used. Process gas containing $H_2S$ leaves a coal gasifier and flows past the working electrode of an electrochemical cell, where it is reduced:

$$H_2S + 2e^- \rightarrow H_2 + S^{2-} \qquad (1)$$

The $S^{2-}$ ions produced migrated through the electrolyte to the counter electrode. If a $N_2$ stream flows past the counter, sulfide ions are oxidized according to the reaction:

$$S^{2-} \rightarrow 1/2\ S_2 + 2e^- \qquad (2)$$

Alternately, a $H_2$ stream may flow past the counter in which case the following reaction occurs:

$$H_2 + S^{2-} \rightarrow H_2S + 2e^- \qquad (3)$$

The current required is calculated directly from the rate of $H_2S$ to be removed, at two Faradays per mole. The power demand follows from knowledge of the potential needed to drive the separation.

The equilibrium potential can be calculated from the Gibbs free energy of the overall reactions and the activities of the gas components in the electrochemical anodic and cathodic reactions through the Nernst equation. If $N_2$ is supplied to the counter electrode, the potential, E, refers to the combined cathode and anode reaction:

$$H_2S \rightarrow H_2 + 1/2\ S_2 \qquad (4)$$

The equilibrium potential becomes

$$E = E_o - \frac{RT}{nF} \ln \left[ \frac{(a_{H_2})_{CA} \; (a_{S_2})^{1/2}_{AN}}{(a_{H_2S})_{CA}} \right] \qquad (5)$$

where:

$$-nFE_o = \Delta G^o_{H_2S}$$

$$(a_{H_2})_{CA} = P \bullet (C_{H_2})_{CA}$$

$$(a_{H_2S})_{CA} = P \bullet (C_{H_2S})_{CA}$$

$$(a_{S_2})_{AN} = P \bullet (C_{S_2})_{AN}$$

Equation (5) shows the small equilibrium potential required for this separation. For example, with a gasifier operating at 20 atmospheres at 1000 K this potential is only 0.67 volts for an exit stream of 10 ppm $H_2S$ in a fuel gas of 10% $H_2$, with an anode product of pure sulfur vapor (at 20 atm):

$$E = E_o - \frac{RT}{2F} \ln \frac{(0.1 \times 20) \; (20)^{1/2}}{(10 \times 10^{-6} \times 20)}$$

with $E_o = -0.21$ v

Reduction of the exit $H_2S$ to 1 ppm requires only an additional 0.1 v. Lower temperature or pressure operation lowers the equilibrium voltage.

This is an extreme example. In practice, the sulfur vapor would be purged from the anode chamber, lowering its activity markedly. Further, an operational device would be constructed in stages so that only the final stage would encounter this low $H_2S$ partial pressure. At this final stage very little $H_2S$ is transferred, thus the current required at the higher voltages is very low. The main current demand will be at the most upstream stage where the $H_2S$ pressure is about 1% of the total pressure. Here the equilibrium potential will be less than 0.2 v.

The actual potential required depends on kinetic considerations. Thus, it is important to find the parameters which are influential in determining these driving forces.

# THEORY

## Basic Electrochemistry

In the chemical reactions known as redox, the fundamental step is the exchange of one or more electrons between two species, 1 and 2:

$$OX_1 + ne^- \rightarrow RED_1 \qquad (6)$$

$$RED_2 \rightarrow OX_2 + ne^- \qquad (7)$$

$$OX_1 + RED_2 \rightarrow OX_2 + RED_1 \qquad (8)$$

where OX and RED represent the oxidized and reduced forms, respectively. Frequently, this fundamental process is complicated by other chemical changes, but the basic process is simply the transfer of electrons from species 1 to 2.

The importance of a redox reaction lies in the fact that the transfer of electrons from reductant to oxidant can be made to take place at a pair of electrodes connected through external circuitry. The reductant transfers one or more electrons to the counter electrode. To maintain overall electrical balance, an equal number of electrons must leave the counter electrode and pass through the external wiring. Simultaneously, the working electrode yields a like number of electrons to the oxidant. This constitutes a complete electrical circuit, and the extent of the redox process can be monitored or controlled by electronic operations on the external portion of the circuit. It is this

ability to control the extent and direction of a reaction by electrical means that constitutes the unique importance of electrochemistry.

Analytical electrochemistry is concerned with small currents (seldom greater than a few milliamperes) at low voltages (up to perhaps 2 volts). This is precisely the magnitude easily handled by modern integrated-circuit electronics, allowing the vast body of electronic techniques of measurement and control to be utilized directly. In electrochemical experiments, most of the change in potential occurs within several angstroms of the electrode-electrolyte interface [9]. The consequence of this occurrence is that tremendous electric fields exist in the vicinity of the electrode. Such high electric fields enable electrochemical reactions to occur at a much faster rate than corresponding chemical reactions since the activation energy barrier can be easily crossed.

If the cell is left without an external controlling instrument, it will exhibit a difference of potential, E, between its electrodes, indicating the tendency of the electrons to circulate outside the cell. This potential, in turn, is a measure of the free energy, $\Delta G$, of the reaction:

$$E = - \Delta G/nF \qquad (9)$$

where the negative sign indicates that $\Delta G$ is negative for a spontaneous reaction. In equation (9), the factor n is the number of electrons exchanged, and F is the Faraday constant.

Equation (9) is strictly valid only if there is no current passing through the cell. This is because the passage of current causes not only changes of concentration, but also voltage drops and heat effects. Fortunately, with the very small currents needed by modern measuring devices, the error is usually negligible, and one can measure E, and thus $\Delta G$, with great accuracy.

For electric current to pass through the cell, redox processes must occur at both electrodes, to the extent of one mole for each nF coulombs. It can thus be written:

$$\text{Number of moles reacted} = Q/nF = (1/nF) \int I \, dt \qquad (10)$$

where Q is the number of coulombs passed, which in turn, is equal to the time-integral of the current, I.

## Galvanostatic Measurements

If the current passing through an electrochemical cell is specified, the extent of the total redox process is completely determined at each moment. The only condition required of the chemical species is that there is enough of it present at the electrode to be oxidized or reduced at the rate required by the current. In order to obtain meaningful analytical measurements, one of the electrodes should be of constant potential without changing from experiment to experiment. This electrode is called the reference electrode and because of its invariance, any change in the cell potential must be due to the condition of the working

electrode. For these measurements, it is desirable to utilize a cell containing three electrodes, so connected that the reference electrode cannot pass any appreciable current. The remaining electrode is designated as the counter electrode, and the reactions taking place in its vicinity are generally of little interest.

## Open-Circuit Voltage Measurements

One always measures differences of potentials rather than the separate values for the two electrodes. The existence of such absolute potentials has preoccupied chemists for a long time, and it appears that it is not possible to measure the potential of a single electrode [10]. Moreover, one cannoteven measure the difference of potential between two dissimilar chemical phases. The only measurable quantity is the difference of potential between two portions of chemically identical material.

The electrical potential of a phase can be defined as the work necessary to bring a unit charge from a great distance to the interior of the phase. The charge must not alter the potential of the phase by its presence and must not enter into any chemical interaction. The potential so defined is called the inner, or Galvani, potential, $\phi$, and is not a measurable quantity.

It is possible to define a very similar quantity, the outer, or Volta, potential, $\psi$, which is accessible to measurement. This concept can be derived from the model of the Galvani potential by

removing the condition that the charge must actually penetrate the phase [9]. It is now only required to approach it very closely. The difference between $\phi$ and $\Psi$ is known as the surface potential, $\chi$. Of the three, only the outer potential $\psi$ is measurable, although the inner potential $\phi$ has a clearer thermodynamic significance. Even though inner potentials cannot be measured directly, some combinations of them are accessible through experimentation.

## Voltage Measurements with Finite Current

In the previous discussion, the current passing through the cell was considered to be very small. In contrast, if appreciable current is allowed to pass, the following types of alterations in the voltage may occur:

1. An ohmic drop, usually referred to as an IR-drop caused by the transport of electricity through the solution and various conductors.
2. Concentration overpotential, $\eta_c$, a shift in potential caused by changes in the concentrations of OX and RED in the immediate vicinity of the electrodes. The redox process causes an increase in the concentration of one species and a corresponding decrease of the other. This change is partially offset by diffusion or stirring but the concentrations at the electrode surface $C^s_{ox}$ and $C^s_{RED}$, will still be different from those in the bulk of the solution, $C^*_{OX}$ and $C^*_{RED}$. This causes a shift in the potential as calculated by the Nernst equation to the new potential, Es:

$$E^s = E^* + \eta_c = E^* + \frac{0.0592}{n} \log \left(\frac{C_{OX}^s \cdot C_{RED}^*}{C_{RED}^* \cdot C_{OX}^*}\right) \qquad (11)$$

where $E^*$ is the potential exhibited when the surface concentrations are equal to the bulk values. Note that $E^S$ is an equilibrium quantity in a sense.

3. Charge-transfer overpotential, $\eta_T$, which is the excess voltage necessary to accelerate the redox reaction to the desired rate. It is a kinetic rather than a thermodynamic quantity.

In light of the above, the total voltage, E, of a cell that uses a reference electrode can be written as follows:

$$E_{CELL} = E_{WORKING} - E_{REF} = \left(E^o + \frac{0.0592}{n} \log \frac{C_{OX}^*}{C_{RED}^*} + \eta_c + \eta_T + IR\right) - E_{REF} \qquad (12)$$

at 298K

## Electrochemical Kinetics

Electrode kinetics is part of that branch of kinetics in which chemical reactions are stoichiometrically linked to electrons through Faraday's laws, and thus the rates of these processes are directly linked to the passage of current. When the electrode kinetics being referred to include only those of the actual electrode process in which the form of charge movement changes between ionic conduction and electronic conduction, they are called charge-transfer kinetics.

## Polarization

It is an experimental fact that when a net current flows through the interphase region around an electrode, the potential of that electrode will be changed. If the potential of an electrode through which zero net current if flowing is written as E(O), the difference between the actual potential of the electrode, E, and E(O) is called the polarization of the electrode:

$$\eta = E - E(O) \tag{13}$$

Polarization is a function of the current density, j, and generally increases with increasing current density.

## Transfer Coefficient

The effect of overpotential on the two reactions directions is a complicating factor that has not yet been considered. If the overpotential is positive, it would accelerate the movement of charge in the direction so as to increase anodic current. It would also decelerate the movement of charge in the direction of the cathodic current. Thus, the effects are twofold: an increase in anodic current and a decrease in cathodic current. These two effects need not be equal. Their difference will depend on the symmetry of the electrochemical activation energy barrier that exists in the electrode interphase region (the compact double layer). The possibility of asymmetry is taken into consideration by

introduction of the transfer coefficient $\alpha$. The transfer coefficient is that fraction of the overpotential that goes to increase the anodic current. Since $0 < \alpha < 1$, the fraction $(1 - \alpha)$ must therefore be the fraction of the overpotential that goes to decrease the cathodic current. The transfer coefficient $\alpha$ normally does not change significantly with potential over small potential ranges, and is frequently taken equal to 0.5. The assumption is then that the activation energy surface is symmetric.

Measured values of transfer coefficients in aqueous solution generally range from 0.2 to 0.8.

## Reversible and Irreversible Reactions

The terms reversible and irreversible are commonly used in kinetics. The acceptable meaning of an irreversible reaction is that the rate of the forward reaction is so much greater than that of the backward reaction that the backward reaction can be neglected. If the rate of the forward reaction is equal to or less than the rate of the backward reaction, then the reaction is reversible. Unfortunately, the rates of charge-transfer reactions are potential dependent. Thus, the meaning of reversible and irreversible depends upon the current demanded and the overpotential thereby produced. Great care must be used when applying these terms to a system.

## Chronoamperometry

The transient-potential-step technique of chronoamperometry can be used to obtain i - $\eta_{ac}$ data. For the application of a potential step to a poised electrochemical system, the chronoamperometric response is ideally given by

$$i(t) = i(0)\ \exp(\lambda^2\ t)\ \mathrm{erfc}(\lambda\sqrt{t}) \quad (14)$$

where i(0) is the true faradic current at time zero. The diffusion parameter, $\lambda$, depends on the intrinsic rate constant, the diffusivities of the reacting species, and the absolute temperature. It is practically constant at a given temperature.

The ideal chronoamperometric response given by (14) is generally applicable, but its derivation depends on assumptions which are not always valid. Przasnyski [15] and Nagy [16] have given a more general solution for the chronoamperometric response to a potential step

$$i = \frac{i(0)}{t_2\lambda^2}\ \{\exp(\lambda^2 t)\mathrm{erfc}(\lambda\sqrt{t}) + 2\lambda\sqrt{t/\pi} - \exp[\lambda^2(t-t_2)]\mathrm{erfc}[\lambda\sqrt{t-t_2}] - 2\lambda\sqrt{\frac{t-t_2}{\pi}}\} \quad (15)$$

Here, $t_2$ is the double-layer charging time. The Nagy equation is more applicable for molten salt systems, where values of $C_{dl}$ are considerably larger than in aqueous systems.

## Cyclic Voltammetry

Rapid voltage scan techniques in which the direction of voltage scan is reversed are called cyclic techniques. In these techniques, a ramp is applied over the full voltage scan range and then reversed so that a descending range returns, almost invariably to the original potential. The scan rate in the forward and reverse direction is normally the same, so that the excitation waveform is actually an isosceles triangle. Cyclic voltammetry is that voltammetric technique in which the current that flows in a system is measured as a function of time and in which the excitation signal is a triangular potential (see Figure 3). Cyclic voltammetry can be used in single-cycle or multicycle modes, depending upon the electrode, the reaction in question, and the information sought. Multicycle techniques have not been used for quantitative measurements because the theory is not that far developed. They are, however, useful diagnostic tools when complex mechanisms are involved. The theoretical equations for cyclic voltammetry have been developed by Nicholson and Shain [11,12,13], and by Piekarski and Adams [14].

It is usual to plot the cyclic voltammogram on an X-Y potentiometric recorder. The measured parameters in cyclic voltammetry are the anodic and cathodic peak potentials $E_{p,c}$ and $E_{p,a}$; the anodic and cathodic peak currents $I_{p,c}$ and $I_{p,a}$; and the half-peak potentials, which are the potentials $E_{p/2,c}$ and $E_{p/2,a}$ at which the cathodic and anodic currents reach half of their peak values. The independent variables are the

voltage scan rate and the range of potential over which the scan is made.

## INSTRUMENTATION AND EQUIPMENT

### Furnace

The electrochemical reaction occurs in a 12.5 inch high furnace which is constructed of 4 inch schedule 80 #310 SS P size and is located in a fume hood (see Figure 4). The upper 4 inches of the furnace is cooled by a baffled water jacket. A 1 liter alumina crucible (Coors CN-1000) fits inside the furnace to protect the #310 SS from any spilled electrolyte. Several layers of refractory brick and of a kaolin-based wool insulate the furnace to assure an accurately controlled operating temperature.

The top of the furnace is sealed by a 5 inch diameter Pyrex disc. Four holes are drilled in the disc through which a 1/4 inch OD $Al_2O_3$ tube, a 5/16 inch OD mullite tube, and two 3/4 inch OD $Al_2O_3$ tubes are passed. The 1/4 inch OD $Al_2O_3$ tube is closed at the bottom and serves as a thermocouple protection tube. The mullite tube is also closed at the bottom and houses the reference electrode. Each 3/4 inch OD outer $Al_2O_3$ tube encases a 3/8 inch OD inner $Al_2O_3$ tube which contains a 1/8 inch thick grade HLM graphite electrode (Great Lakes Carbon Coporation). This configuration is more fully explained in the next section.

The 99.8% $AL_2O_3$ tubes (Coors grade AD-998) are immersed in a 100 ml conical $Al_2O_3$ crucible which serves as the reaction vessel containing the electrolyte. A strip of Grafoil (Union Carbide) is wrapped around the reaction vessel to detect the unwanted presence of air in the furnace. One hundred percent silicon sealant is used at the top of the furnace to create an air-tight seal between the tubes and the Pyrex disc.

A #316 SS gas inlet tube is located 5 inches from the top of the furnace. A #316 SS gas outlet tube is at the same height on the opposite side of the furnace. The inlet tube delivers a constant purge stream of $H_2$ to the furnace while the outlet tube directs the gas flow to the fume hood. Airtight operation was assured by the use of O-ring seals above and below the Pyrex plate.

Tygon tubing is used for all gas connections outside the furnace. The tubing is not affected by any gas except COS which is present in trace amounts:

$$H_2S + CO_2 \rightarrow COS + H_2O \qquad (16)$$

When COS flows through Tygon, the tubing turns amber but is not otherwise altered. Rotameters (Airco 752) used to measure the gas flow were fabricated from stainless steel to prevent corrosion.

## Reference, Working and Counter Electrodes

The reference electrolyte is a mixture of 10 wt. % $Ag_2SO_4$ in a ternary alkali-sulfate eutectic (79 m % $Li_2SO_4$, 12 m % $K_2SO_4$, 9 m % $Na_2SO_4$). The electrolyte and a silver wire is added to the $Na^+$ conducting mullite tube to complete the electrode. The top of the mullite tube was sealed around the Ag lead with silicone sealant.

The working/counter electrode configuration consists of a 1/8 inch diameter graphite rod encased in a 3/8 inch OD $Al_2O_3$ gas inlet tube which is mounted in a 3/4 inch OD $Al_2O_3$ gas outlet tube. The graphite rod is positioned such that the rod terminates flush with the bottom of the inner $Al_2O_3$ tube. This assured that the electrode gas which flowed downward through the annular region between the $Al_2O_3$ tube and the graphite rod makes good contact with the electrode-electrolyte interface. The smaller inner $Al_2O_3$ tube is terminated 7/8 inches from the bottom of the larger outer $Al_2O_3$ tube. The entering gas will react and then exit up through the outlet tube rather than bubble through the electrolyte into the reaction crucible (see Figure 5). This follows the principle that a gas will always take the path of least resistance or lowest pressure drop.

The graphite rods are 12 inches long and it was necessary to use gold wire leads from the rods to the outside of the furnace. The gold lead was threaded through the Tygon connection and sealed with silicone on one end. At the other

end, it was threaded through a 0.5 mm diameter hole in the electrode.

A hole was drilled through the 1 inch OD section of Tygon, which was connected to the outlet $Al_2O_3$ tube, so that the inlet $Al_2O_3$ tube could be installed at its proper position. Rubber septum stoppers were installed into the side arm of plastic tees to create sampling ports for gas syringe samples. These sampling ports were placed into the Tygon tubing at convenient locations so that the inlet/outlet streams could be analyzed (see Figure 6). All connections were made airtight with silicone sealant.

## Electrical Instrumentation

Two Hewlett-Packard 5840A gas chromatographs (GC) were used to analyze the composition of the various gas streams. The GC is a digital processor-based instrument operated from a terminal. The terminal is connected to the main-frame module which houses the injection port, column oven, detectors, gas flow systems and the electronics. One GC is fitted with a Thermal Conductivity Detector (TCD) to analyze for $CO_2$ composition, while the other is equipped with a Flame Photometric Detector (FPD) to examine for sulfur levels.

A 30 amp variable auto transformer (Standard Electrical Products Company) was used to power two semi-cylindrical heating elements (Lindberg) capable of 1473 K operation. The

thermocouple protection tube houses a Type K (Chromel-Alumel) thermocouple which was connected to a voltmeter (Simpson 460 Series 5) so that the furnace temperature could be constantly monitored. A 3050 RMP fan (Redmond) was used to assist the baffled water jacket in keeping the top of the furnace cool.

A potentiostat-galvanostat (Princeton Applied Research Model 371) powered the electrochemical experiments. Current and voltage monitors integral to the Model 371 allowed observation of these parameters by a storage oscilloscope (Tektronix 5111A with 5A19N Differential Amplifier and 5B10N Time Base/Amplifier). A function generator (Hewlett-Packard 3310B) provided sinusoidal inputs or step inputs as needed, while an X-Y recorder (Hewlett-Packard 7015B) documented certain cell responses.

# EXPERIMENTAL PROCEDURE

## Melting Points

Commercially available samples of $K_2S$, $Na_2S$, and $Li_2S$ were obtained (Alfa Chemical). The $K_2S$ was only of 44% nominal purity, the principal impurities being $K_2S_2$, $K_2S_3$, $K_2S_4$, $K_2S_5$, $K_2S_6$, as well as various hydrates of these polysulfides. The method of purification involved heating this mixture to temperatures as high as 1270 K, either under vacuum or in a $N_2$ atmosphere. The hydrates are easily removed by this procedure, since the water of hydration is driven off at higher temperatures. Removal of the excess sulfur from the polysulfides, according to reaction (8), proved considerably more difficult. Other methods of purification were considered but the above method was deemed most satisfactory for this work. The purity of the $K_2S$ was verified by observing the melting point of 1110 K. Purified samples of $Na_2S$ and $Li_2S$ were similarly obtained.

Once sufficient quantities of $Na_2S$, $Li_2S$, and $K_2S$ were purified, a melting point study was commenced. Only those binary mixtures containing $K_2S$ were considered. For each mixture to be tested, weighed quantities were placed in a 2 or 5 mL, 99.8% $Al_2O_3$ crucible, which was then placed in the vacuum furnace. As many as five mixtures at a time could be tested in the furnace. After heating rapidly under $N_2$ to about 820 K,

the furnace was then heated slowly. The mixtures were observed visually through the Pyrex disc. When all the mixtures were molten, the furnace was then cooled slowly back through the freezing points of all the mixtures. The accuracy to which the melting points could be determined was ± 10 K, taking into account the accuracy in reading the temperature from the dial face of the temperature recorder.

For each electrolyte chosen, a sufficient quantity of the binary mixture was prepared. Weighed quantities of $K_2S$ and $Na_2S$ were placed in a 100mL $Al_2O_3$ crucible, and the resulting mixture was heated beyond its melting point and left at an elevated temperature for sufficient time to insure a homogeneous mixture. After cooling to room temperature, the resulting mixture was crushed into tiny chunks with a clean hammer. The mixture was then stored in a container, flushed with $N_2$, and placed in a dessicator for further use. The same sample was used for all experimental runs; aliquots of this sample were removed from the dessicator for use as needed.

To start an experimental run, the cell was first prepared outside the furnace. The crucible was filled with electrolyte and the entire assembly was lowered in the furnace, which was then sealed. After displacing the air in the furnace with $H_2$, the cell was heated through the melting point of the electrolyte. During the heating period, $H_2$ was bubbled to both electrodes and to the furnace purge. After observing the

melting point of the electrolyte visually and on an AC-impedence bridge, gas flow to the electrodes was observed. If bubbling of gas through the electrolyte was not seen, the cell was cooled to room temperature, more electrolyte was added, and then the cell was reheated.

After the gas flows to the electrodes were steady, and the cell was at a constant temperature of 1105 K, $R_s$ and $C_{dl}$ could be measured. The current interruption technique [18] was used to measure $R_s$. To determine $C_{dl}$, a current step, $I_{app}$, was applied to the cell, and the voltage response recorded on an oscilloscope. The value of the double-layer capacitance is calculated as

$$C_{dl} = \frac{I_{app}}{(dE/dt)_{t=0}} \tag{17}$$

The slope was measured from a Polaroid picture of the oscilloscopic trace.

The determination of transfer coefficients, reaction orders, and exchange current densities was next accomplished through application of potential steps. After the flow rates of the gases bubbled to the electrodes had stabilized, the anode to cathode (A/C) and reference to cathode (R/C) voltages were observed. An equilibrium state was assumed when these voltages showed no change over a three to four minute period. Fluctuations of less than 2 mV in these values were ignored.

When the cell reached equilibrium, the gas flows to the electrodes were interrupted, values of A/C and R/C were again noted, a potential step was applied, the values of A/C and R/C were again noted, and the circuit was opened. The chronoamperometric response was recorded on a storage oscilloscope, and a Polaroid picture was taken of the oscillographic trace. The potential step to the working electrode was typically applied for 5-15 seconds.

For each set of gas-flow conditions, potential steps were made at 50mV (nominal) intervals, up to a magnitude of 500 mV. Both anodic and cathodic polarizations were performed. After each chronoamperometric experiment, it was necessary to wait for 5 minutes (for high $H_2S$ concentrations) to 1.5 hours (for low $H_2S$ concentrations) for the cell to return to an equilibrium state. When a complete set of chronoamperometric experiments for a particular set of gas-flow conditions was completed, the gas compositions were changed and the cell was given at least two hours to return to a new equilibrium condition (as evidenced by steady A/C and R/C values).

Table 1 shows the test parameters for all experiment runs reported. In all cases, the temperature is 1105 K. Gas compositions reported in Table 1 are those existing at room temperature, and are not those at the cell operating temperature. The compositions vary because of the water-gas shift equilibrium:

$$H_2 + CO_2 \rightleftharpoons H_2O + CO \qquad (18)$$

The kinetics of reaction (18) are assumed to be rapid at the cell operating temperature, although equilibrium is not attained. Hence for the process gases containing 8% $CO_2$, 20% $H_2$, and 25% CO at room temperature, the equilibrium composition at the cell operating temperature of 1110 K is 4.9% $CO_2$, 16.9% $H_2$, 28.1% CO, and 3.1% $H_2O$. In all cases, $N_2$ makes up the balance fo the simulated process gas. The small amount of COS formed is not reported in Table 1.

Table 1. Test Parameters For Experimental Runs

| Data Series | Working Gas Composition | Counter Gas |
|---|---|---|
| 1 | 6500 ppm $H_2S$, 50% $H_2$ | $H_2$ |
| 2 | 6500 ppm $H_2S$, 50% $H_2$ | He |
| 3 | 6500 ppm $H_2S$, 8% $CO_2$, 20% $H_2$, 25% CO | He |
| 4 | 3000 ppm $H_2S$, 50% $H_2$ | $H_2$ |
| 5 | 1062 ppm $H_2$, 82% $H_2$ | $H_2$ |
| 6 | 336 ppm $H_2S$, 94% $H_2$ | $H_2$ |
| 7 | 1.5% $H_2S$, 50% $H_2$ | $H_2$ |
| 8 | 6500 ppm $H_2S$, 8% $CO_2$, 20% $H_2$, 25% CO | $H_2$ |

## Voltammetry and Gas Analysis

To determine the effects of various gas compositions on the kinetics of the $H_2S$ removal process, the exchange current density, $i_o$, was measured for eight different combinations of gas flow conditions. For a particular test, gases were observed (either visually or electronically) to be bubbling past the working and counter electrodes. These gases were then shut off, and the pressure in the system was equilibrated. The potential of the working electrode relative to the reference

electrode was instantaneously changed using the potentiostat/galvanostat, and the current between the working and counter electrodes was recorded as a function of time by a storage oscilloscope. After 10-15 seconds of current flow, the potentiostat was switched off, and bubbling was re-started. A picture of the trace on the oscilloscope screen was taken to insure a permanent record of the experiment.

GC Preparation

The GC requires a minimum amount of routine maintenance to guarantee reproducible results. The initial maintenance procedure was followed as specified by the operations manual. To check the accuracy of the two detectors, several gases with varying compositions of $H_2S$, $CO_2$, CO, $H_2$ and $N_2$ were sampled until reproducible peaks were obtained. So as to operate within the dynamic range of the detectors, a 50 µl syringe was always used for FPD analyses while a 500 µl syringe was constantly used when sampling with the TCD. A FPD calibration curve was constructed by sampling the standardized 1.5% $H_2S$ gas bottle with different µl syringes and recording the resulting peaks. Then, the peak area was plotted versus the amount injected to obtain a curve which blanketed the range within which sample results were expected (see Figure 7).

Cell Preparation

To begin an experimental run, the Pyrex plate, with its associated four tubes sealed into place, was positioned on a stand outside the furnace. The 100 ml $Al_2O_3$ reaction crucible was placed at an appropriate height below the plate and the electrolyte powder was firmly packed into the crucible between the inner walls and tubes. The whole assembly was carefully lowered into the furnace and the furnace was sealed. After the proper gas connections were made, the furnace was purged with $H_2$ and the furnace was slowly heated.

During the heating process, the melting point of the electrolyte was observed visually and by an AC-impedance method. The AC-impedance method involved application of a sinusoidal voltage across the series combination of the cell and a resistor of known value. AC voltages across the cell and across the resistor were measured. As the melting point of the electrolyte was approached, the voltage across the cell decreased rapidly and suddenly, indicating that the electrolyte was becoming ionically conductive.

After the melting point was noted, the cell was heated to an operating temperature of 1000 K. Gas flow to the electrodes was checked visually by observing the reaction crucible for bubbling. If vigorous bubbling was not evident, the furnace was cooled to room temperature and more electrolyte was added. In general, a sufficient quantity of electrolyte was

added by the second or third attempt to insure proper cell performance.

Solution Resistance and Double-layer Capacitance

The solution resistance, $R_s$, and the double-layer capacitance, $C_{dl}$, are important parameters of the electrolyte. After the particular gas flow to the electrodes had stabilized and the system had reached thermal equilibrium, $R_s$ and $C_{dl}$ could be determined. The current interruption technique [18] is the standard measurement technique for solution resistance. After a steady-state current was established in the cell, the current was shut off, and the voltage response was recorded on an oscilloscope. The instantaneous voltage drop is equal to the IR drop and the value of $R_s$ could be calculated. To determine $C_{dl}$, a current step, $I_{APP}$, was applied to the cell using the galvanostat and the voltage response was recorded as an oscilloscope trace. The value of the double-layer capacitance was calculated from the following equation:

$$C_{dl} = \frac{I_{APP}}{(dE/dt)_{t=0}} \qquad (19)$$

As an aid to accurately determine the slope, a Polaroid picture of the oscilloscopic trace was taken using an Oscilloscope Camera (Tektronix C-5C).

Cyclic Voltammetry Experiments

Cyclic voltammetry made it possible to investigate the electrode reaction kinetics of the cell. The flow rate of the gas bubbled to the working electrode was allowed to stabilize. Voltages between the working/counter electrodes, the working/reference electrodes and the counter/reference electrodes were observed. These values were recorded as W/C, W/R, and C/R respectively. An equilibrium state was assumed when W/C, W/R, and C/R showed no trend to change over a five minute period. As the electrolyte became saturated with the particular process gas, the electrical instrumentation was prepared for the cyclic voltammetry experiment.

The potentiostat/galvanostat was set to the potentiostatic mode and the appropriate connections were made to the cell. A multimeter was then placed into the system to read W/R. The potentiostat was set to the applied voltage which made W/R = 0. This was done so that all voltage sweeps would begin at the equilibrium potential of the cell and then exhibit the cathodic/anodic overpotentials.

The function generator was connected to the potentiostat so that the voltage would sweep in the negative direction first and then sweep in the positive direction. A multimeter was connected to the function generator to read the voltage output level. The phase button on the function generator was adjusted

until the voltages swept negatively and positively by the same amount after the manual trigger button was depressed. The X-Y recorder was placed into the system to document the resulting current response when the voltage was swept. By trial and error, the output level of the function generator was manipulated until both the cathodic and anodic peaks could be clearly distinguished on the X-Y recorder. So that each sweep would start at a current of i = 0, the DC offset of the function generator was adjusted until the current monitor on the potentiostat read zero. With the help of a stopwatch, the sweeprate of the function generator was determined in mV/sec when the range bottom was set at its slowest value of 0.0001.

The following process gases* were used in the cyclic voltammetry experiments on different days:

1) 1.5% $H_2S$ ---50% $H_2$----BALANCE $N_2$

2) 0.3% $H_2S$----50% $H_2$----BALANCE $N_2$

3) 0.65% $H_2S$---8% $CO_2$----25% $CO_2$---20% $H_2$----BALANCE $N_2$

Sweep rates of 250, 500, 750, 1000, 1250, 1500, 1750 and 2000 mV/sec were used for each of the three gases so that the effect of different compositions could be studied. The range and fine tuning range buttons of the function generator were adjusted to achieve the desired sweeprates. Once it was certain that the

* Water-gas-shift equilibrium brought gas no. 3 to simulated coal-gas composition. This is detailed later.

electrolyte was saturated with the particular process gas, the gas to the electrode was shut off and the excess pressure between the gas lines and the electrolyte (due to a pressure drop associated with gas bubbling through the electrolyte) was released. The power was applied to the cell and a cyclic voltammogram was run at the given sweeprate. After the sweep, the power was turned off and the gas was turned back on to the electrode. The system was allowed to return to equilibrium (approximately 30 minutes) before the next sweeprate was run. When all the sweeprates had been run with the particular gas of the day, the function generator was reconnected to the potentiostat so that it would sweep in the positive direction first before sweeping negatively. The above procedure was also used for this set of runs.

Removal Experiments

In several of the experimental runs, it was necessary to dilute a standardized $H_2S$ containing gas with $H_2$ to produce a gas stream of a lower $H_2S$ concentration. Measurement of concentration of this diluted stream was accomplished by an accurate measurement of the flow rates of the two unmixed streams. For this a bubblemeter was employed. A bubblemeter is a volumetric device which allows one to measure the time for a given volume of gas to be displaced. All rotameters were calibrated by setting the needle valves over a wide range of

scale readings and then directing the gas flows through the bubblemeter to determine the flowrate at each particular rotameter scale reading. Excellent reproducibility was achieved, and the desired $H_2S$ concentration could be obtained in the diluted stream.

The valves on the working/counter electrode outlet sampling lines were closed during initial heat-up to keep the purge gas from exiting through the sample lines. A small $H_2$ stream was passed through both electrode inlet tubes to keep the electrolyte from blocking the inlet tubes as it became molten. To assure that the outlet sampling lines were working properly, the inlet flow to each electrode was individually interrupted and the flow through the respective sampling line was observed.

All removal experiments were run with diluted $H_2S$ gas stream bubbling through the working electrode with no gas flow at the counter electrode. Both the inlet and outlet streams of the working electrode were daily sampled at open circuit with a 50 µl syringe. This was done to get a clear understanding of the background sulfur emitted from the electrolyte when no current was applied. The W/C, W/R and C/R open circuit voltages were daily and continuously recorded to observe the equilibrium potential of the cell.

To test for the removal of the sulfur species from the outlet gas stream, currents of ±10, ±25, ±50 and ±100 mA were

applied to the cell. The inlet and outlet streams of the working electrode were sampled on the FPD so that the effect of removal could be noted by comparing the open circuit outlet samples versus the applied current outlet samples. After sufficient data had been collected with the diluted $H_2S$ gas, a new process gas was introduced to the working electrode which contained 0.65% $H_2S$, 8% $CO_2$, 25% CO, 20% $H_2$ and a balance of $N_2$. To examine the combined effects of $CO_2$ and $H_2S$ on the cell, open circuit samples were taken of the inlet/outlet working electrode streams on both the TCD and FPD, respectively. Again, open circuit voltages were recorded and then inlet/outlet samples were taken on both the TCD and FPD when currents of ±10, ±25,±50, and ±100 mA were applied.

## EXPERIMENTAL RESULTS

### Melting Points

Table 2 shows the binary compositions which have been tested and the approximate melting point of the mixture.

TABLE 2.

Melting Points of Alkal Sulfide Mixtures

| Mole % | | | |
|---|---|---|---|
| $K_2S$ | $Na_2S$ | $Li_2S$ | Melting Point ($^oC$) |
| 80 | | 20 | 870 |
| 61 | | 39 | 810 |
| 50 | | 50 | 780 |
| 43 | | 57 | 750 |
| 20 | | 80 | 820 |
| 30 | 70 | | 850 |
| 50 | 50 | | 820 |
| 60 | 40 | | 740 |
| 70 | 30 | | 780 |
| 80 | 20 | | 780 |

## Chronoamperometry

A typical oscillographic trace is presented in Figure 8 for a cathodic polarization. These data were then plotted as total current (capacitive plus faradaic) versus time. Fig. 9 shows such a plot of the chronoamperometric response of Fig. 8. Using the lowest estimate of the double-layer capacitance, $c_{min}$, associated with a particular data series, the double-layer charging time was calculated as

$$t_2 = 4\ R_s c\ min$$

For all times greater than $t_2$, the current is thus assumed to be exclusively faradaic current. Once $t_2$ was estimated, equation (15) was applied to determine $i_o$ and $\lambda$ through non-linear regression of the data. The quality of fit of equation (15) to a representative potential-step experiment is illustrated in Fig 9. $R_s$ represents the solution resistance for the chronoamperometric experiment in question, and is determined from the total initial current, $I_*$:

$$R_s = \frac{\Delta E}{I_*}\sqrt{A} \qquad (\text{ohm} - \text{cm}^2)$$

Values of $R_s$ were within 2 or 3% of values determined from the current interruption technique.

Table 3 lists the results of the data fitting for $i_o$ using equation (15). The excellence of the fit shown in Fig. 9 is mirrored in the reproducibility of the value of $i_o$ for a broad range of potential steps with a given gas. Values for $\lambda$, the mass-transfer parameter, ranged from 0.3 to 0.5 $sec^{-1/2}$ with no apparent dependence upon step size or gas composition. These values of $i_o$ and $\lambda$ indicate that, while mass-transfer is dominant (50-80% of the overpotential), the process is under mixed-control [11].

## Reaction Orders

The electrochemical reaction orders $P_k$, for reactions (1) through (3) can be calculated once the relationship between the exchange current density and gas concentration is known;

$$P_k = \left(\frac{\partial \ln i_o}{\partial \ln C_k}\right)_{n,\, C_j} \pm \frac{\alpha}{n} \qquad (20)$$

Note this form of the reaction order equation is at constant overpotential [13].

In order to assess the reaction orders with equation (20), the exchange currents were plotted against $H_2S$ pressure, Figures 10 and 11. The slopes, on a logarithmic basis, are 0.12 and 0.27 for cathodic and anodic polarizations respectively. The transfer coefficients, $\alpha$, were estimated from cyclic voltammetry in this melt [28]. These showed irreversible peaks with $\alpha n_a \approx 0.6$ in

Table 3

Experimental Exchange Current Densities

| | $i_o$, ma/cm$^2$ | | Potential Steps, V, mv | | Number of Runs | |
|---|---|---|---|---|---|---|
| Data Set* | Cathodic | Anodic | Cathodic | Anodic | Cathodic | Anodic |
| 1 | 43. ± 1. | 64. ± 2. | 30. - 150. | 20. - 80. | 8 | 4 |
| 2 | 39. ± 2. | 137. ± 3. | 30. - 160. | 6. - 54. | 8 | 7 |
| 3 | 89. ± 4. | 133. ± 3. | 10. - 90. | 6. - 54. | 9 | 7 |
| 4 | 38. ± 3. | 50. ± 2. | 15. - 165. | 10. - 110. | 10 | 8 |
| 5 | 32. ± 3. | 38. ± 2. | 15. - 175. | 15. - 130. | 8 | 8 |
| 6 | 29. ± 4. | 27. ± 3. | 20. - 180. | 20. - 120. | 6 | 8 |
| 7 | 45. ± 2. | 75. ± 3. | 15. - 150. | 60. - 100. | 5 | 5 |
| 8 | 98. ± 5. | 64. ± 2. | 5. - 75. | 10. - 95. | 8 | 7 |

* See Table 2 for gas compositions.

either direction. If we presume the number of electrons in the irreversible step, $n_a = 1$, $\alpha_{a,c} \approx 0.6$. Note the sum of $\alpha_a + \alpha_c$ does not add to n/ $\nu$ (presumably 2), indicating the cathodic and anodic processes are not the reverse of each other.

The reaction order in $H_2S$ is thus calculated to be about 0.4 cathodic and zero anodic. The possible mechanisms are discussed below.

## Open-Circuit Voltages

A multimeter was employed to measure the open circuit voltages (OCV) of the cell. These voltages were recorded while no current was flowing through the electrolyte and they do not include any type of overpotential or IR drop. Therefore, the open-circuit voltage should only include Nernstian effects. Table 4 reports values of the working to counter, working to reference and counter to reference voltages for the four different gas flow conditions reported in this work. Each gas containing $H_2S$ was run for approximately a week and the reported values are an average of the voltages observed during that time period.

Table 4. Open-Circuit Voltages

| Process Gas | Electrode Gas | Counter Electrode Gas | Working $CO_2$(%) | Actual W/C (mV) | W/R (V) | C/R (V) |
|---|---|---|---|---|---|---|
| 1 | None | $H_2$ | 0 | -10.8 | -1.898 | -1.888 |
| 2 | None | 0.26% $H_2S$ | 0 | -17.0 | -1.911 | -1.895 |
| 3 | None | 0.42% $H_2S$ | 0 | +25.0 | -1.830 | -1.857 |
| 4 | None | 0.47% $H_2S$ | 5.8 | +68.8 | -1.928 | -1.991 |

## Resistance, Capacitance, Electrode Area and Limiting Currents

Values of the solution resistance, $R_s$, were constant for different applied currents during a particular day. The average value of $R_s$ was 1.0 Ω. Determination of the double-layer capacitance $C_D$, was dependent upon taking the slope of a tangent to a curve and was therefore somewhat subject to interpretation. An average value of $C_D$ was 750 mF. Of more interest is the apparent double-layer capacitance per unit electrode area. Using a value for the electrode area of 2.5 $cm^2$, as observed by White [17], an average value for this parameter was 296 $mF/cm^2$.

When the limiting current flows, $i_l$, the electrode process is occurring at the maximum rate possible for the given set of mass transfer conditions. The $i_l$ is dependent upon parameters which can be calculated for this experiment such as Reynolds number, Schmidt number, mass-transfer coefficient and the maximum flux. The calculated limiting currents for this experiment are listed in Table 5.

$$k_g L/D_o = (0.65)\ Re^{1/2}\ Sc^{1/3} \tag{21}$$

$$N_{max} = k_g A\ (C_{inlet} - C_{surface}) \tag{22}$$

$$i_l\ (coul/sec) = (N_{max}\ mole/sec)\ (96500\ coul/eq)\ (2\ eq/mole) \tag{23}$$

Table 5. Limiting Currents

| Process Gas | Working Electrode Gas | Actual $CO_2$(%) | $i_l$ (mA) |
|---|---|---|---|
| 2 | 0.26% $H_2S$ | 0 | 25.13 |
| 3 | 0.42% $H_2S$ | 0 | 42.59 |
| 4 | 0.47% $H_2S$ | 5.8 | 27.57 |

## Cyclic Voltammetry

Figures 12 through 14 show the current-potential profiles obtained for this system. All profiles begin from the equilibrium rest potential and then sweep the voltage in the cathodic direction before reversing and sweeping the voltage in the anodic direction. The peak currents, $i_p$, and the actual peak voltages, $E_p$, obtained at their respective sweeprates are recorded in Tables 6 through 8 for different gases. Note that the actual peak voltages have been corrected by the following equation:

$$E_p \text{ (actual)} = E_p \text{ (from scan)} + i_p R_s \qquad (24)$$

## Stoichiometric Current and Removal Current

The current is a basic measure of the rate of an electrochemical reaction. The stoichiometric current, $i_s$, and the removal current, $i_r$, were calculated for this experiment by using the following equations:

$$\begin{aligned} i \text{ (mA)} = \; & \text{(96500 coul/eq) (2 eq/mole)} \\ & \text{(F cc gas/min) (C cc } H_2S\text{/100 cc gas)} \\ & \text{(mole } H_2S\text{/24000 cc } H_2S\text{) (min/60 sec)} \\ & \text{(Amp/(coul/sec)) (1000 mA/amp)} \end{aligned} \qquad (25)$$

Table 6. Peak Data for 0.30% $H_2S$ Gas

| Sweeprate (mV/sec) | $i_{p_c}$ (A) | $i_{p_a}$ (A) | $E_{p_c}$ (V) | $E_{p_c}$ (V) |
|---|---|---|---|---|
| 250 | 0.0150 | 0.0165 | -2.210 | -1.578 |
| 500 | 0.0195 | 0.0200 | -2.266 | -1.476 |
| 750 | 0.0220 | 0.230 | -2.398 | -1.423 |
| 1000 | 0.0260 | 0.295 | -2.318 | -1.562 |
| 1250 | 0.0265 | 0.0300 | -2.358 | -1.452 |
| 1500 | 0.0270 | 0.0310 | -2.449 | -1.361 |
| 1750 | 0.0275 | 0.0320 | -2.500 | -1.310 |
| 2000 | 0.0278 | 0.0325 | -2.568 | -1.208 |

Table 7. Peak Data for 1.5% $H_2S$ Gas

| Sweeprate (mV/sec) | $i_{p_c}$ (A) | $i_{p_a}$ (A) | $E_{p_c}$ (V) | $E_{p_a}$ (V) |
|---|---|---|---|---|
| 250 | 0.0197 | 0.0197 | -2.074 | -1.684 |
| 500 | 0.0200 | 0.0210 | -2.236 | -1.546 |
| 750 | 0.0217 | 0.0235 | -2.310 | -1.436 |
| 1000 | 0.0235 | 0.0260 | -2.330 | -1.333 |
| 1250 | 0.0257 | 0.0285 | -2.387 | -1.385 |
| 1500 | 0.0260 | 0.0290 | -2.437 | -1.285 |
| 1750 | 0.0275 | 0.0315 | -2.458 | -1.273 |
| 2000 | 0.0280 | 0.0320 | -2.477 | -1.171 |

Table 8. Peak Data for 0.65% $H_2S$ Gas with 5.8% $CO_2$

| Sweeprate (mV/sec) | $i_{p_c}$ (A) | $i_{p_a}$ (A) | $E_{p_c}$ (V) | $E_{p_a}$ (V) |
|---|---|---|---|---|
| 250 | 0.0125 | 0.0125 | -2.916 | -0.842 |
| 500 | 0.0130 | 0.0130 | -2.867 | -0.941 |
| 750 | 0.0160 | 0.0160 | -2.919 | -0.887 |
| 1000 | 0.0170 | 0.0170 | -3.056 | -0.722 |
| 1250 | 0.0190 | 0.0190 | -3.066 | -0.678 |
| 1500 | 0.0210 | 0.0218 | -3.074 | -0.681 |
| 1750 | 0.0235 | 0.0235 | -3.128 | -0.632 |
| 2000 | 0.0245 | 0.0250 | -3.180 | -0.580 |

$$i_s \text{ (mA)} = 1.34 \, FC_s \qquad (26)$$

$$i_r \text{ (mA)} = 1.34 \, FC_r$$

In equation (26) F represents the gas flowrate to the working electrode in cc of gas/minute. The value of $C_s$ denotes the average of the inlet/outlet mole fraction of the electroactive species as obtained from the FPD samples taken at open circuit, while $C_r$ represents the difference between

the mole fraction of the electroactive species present at the outlet of the working electrode during open circuit and the mole fraction of the outlet stream when a certain current is applied. Table 8 tabulates the average currents measured or calculated under the specified conditions.

Table 9. Summarized Currents

| Working Electrode Gas | Actual $CO_2$ (%) | $i_{APPLIED}$ (mA) | $i_l$ (mA) | $i_s$ (mA) | $i_r$ (mA) |
|---|---|---|---|---|---|
| 0.26% $H_2S$ | 0 | -100 | 25.13 | 17.34 | 2.368 |
| 0.26% $H_2S$ | 0 | -50 | 25.13 | 17.49 | 2.176 |
| 0.42% $H_2S$ | 0 | -25 | 40.59 | 30.48 | 4.932 |
| 0.42% $H_2S$ | 0 | -10 | 40.59 | 30.54 | 4.416 |
| 0.42% $H_2S$ | 0 | -100 | 40.59 | 23.88 | 7.664 |
| 0.47% $H_2S$ | 5.8 | -100 | 27.57 | 45.11 | 24.419 |

## Sulfide Conversion

A fresh charge of electrolyte initially contains approximately 1.7 moles of sulfide. For every mole of $CO_2$ that is absorbed through the passage of process gas at the

working electrode, one mole of $H_2S$ is liberated as shown in the following equation:

$$CO_2 + H_2O + S^{-2} \rightarrow CO_3^{-2} + H_2S \qquad (27)$$

A constant flowrate of 42 cc/min was maintained during the 49 hours that the process gas containing 5.8% $CO_2$ was actually absorbed into the electrolyte at a rate of 0.006 moles $CO_2$/hr. This corresponds to a theoretical stoichiometric value of 0.30 moles of $CO_2$ absorbed or 17.5 mole % of the sulfide converted to carbonate. The experimental conversion of sulfide to carbonate, as calculated from the FPD peaks during the same time period, was 4.16 mole % conversion while a lab analysis (Atlantic Microlab) showed that 3.3 mole % of the sulfide was converted to carbonate. It is most likely that the conversion is less than 4 mole %.

## Water-Gas Shift Effect

The process gas used to indicate the consequences of bubbling $CO_2$ into the cell had a composition of 0.65% $H_2S$, 8% $CO_2$, 25% CO, 20% $H_2$ and a balance of $N_2$ at room temperature. The actual composition varies at the operating temperature of 1000 K because of the water-gas shift equilibrium:

$$H_2 + CO_2 \rightarrow H_2O + CO \qquad (28)$$

The kinetics of this reaction are assumed to be rapid at the cell operating temperature. Table 10 compares the theoretical process gas composition calculated at 1000 K versus the composition of the gas determined by a TCD analysis of the gas after being heated to 1000 K in a Thermolyne Furnace.

Table 10. Process Gas Composition at 1000 K

| Component | Theoretical % | Experimental % |
|---|---|---|
| $CO_2$ | 5.7 | 5.8 |
| CO | 27.3 | 27.2 |
| $H_2$ | 17.7 | 17.8 |
| $H_2O$ | 2.3 | 2.2 |
| $H_2S$ | 0.65 | 0.65 |
| $N_2$ | BALANCE | BALANCE |

# DISCUSSION OF RESULTS

## Electrode Kinetics

The results given above show that the proposed process will perform to expectations. In an actual cell, diffusion of gas through the electrolyte to the electrode may well be the limiting step of the process. The high exchange current densities reported rule out the possibility of sluggish kinetics limiting the process. Additionally, it appears that formation of sulfur is the preferred anodic reaction, which would allow the byproduct to be sold, and, more importantly, would allow the process to function without need for a Claus plant.

The higher exchange currents found with $CO_2$ present in the gas verify that $CO_2$ would react if $H_2S$-limiting currents are exceeded. Design and operation must therefore be based upon such limits, as expected. Since the kinetics are so rapid, the limiting currents will be those based upon gas diffusion of the dilute $H_2S$.

## Open-Circuit Voltages

The magnitude of the observed open-circuit W/R voltage, as well as changes in this voltage with gas composition, show good agreement with theoretical prediction.

$$Ag|Ag^+,\ Na^+,\ SO_4^{2-}||Na^+,S^{2-}|H_2,\ H_2S|C(graphite). \qquad (29)$$

The Nernst equation can be used to predict the W/R volatage at 1100 K:

$$Na_2SO_4 = 2Na^+ + SO_4^{2-}, \qquad (30)$$

$$2Ag^o + SO_4^{2-} = Ag_2SO_4 + 2e, \qquad (31)$$

$$2Na^+ + H_2S + 2e^- = Na_2S + H_2. \qquad (32)$$

Reactions (30) and (31) occur within the mullite tube, and reaction (32) occurs at the working electrode. The circuit is completed by $Na^+$ conduction through mullite along the grain boundaries. Denoting concentrations in the bulk electrolyte by b, and those within the mullite by m, the Nernst relation can be written:

$$E_{eq} = E^o - \frac{RT}{2F} \ln \left[\frac{(Na_2S)_b(H_2)_b\ (Ag_2SO_4)_m(Na^+)^2_m}{(Na^+)^2_b\ \ (H_2S)_b\ (Ag^o)^2_m(Na_2SO_4)_m}\right]. \qquad (33)$$

If the activities of $H_2$ and $H_2S$ can be assumed proportional to theri concentrations in the entering gas, the open circuit W/R voltage with a gas containing 6500 ppm $H_2S$ and 50% $H_2$ is predicted as:

$$E_{eq} = -1.741 + 0.020 = -1.721 \text{ V.} \quad (34)$$

The observed W/R voltage at the start of an experimental run was typically -1.890 ± 0.890 V. This is acceptable agreement with the calculated value considering the probable inaccuracies of published high-temperature free energy values. The W/R voltage at open circuit remained constant for all chronoamperometric experiments, but was typically observed to shift to more negative values over a month-long period. The shift in W/R voltage is due to several factors. Silver is transported to some extent through the mullite tube, as evidenced by a darkening of the mullite. The sulfates of the reference electrolyte also decompose.

$$M_2SO_4 = M_2O + SO_3. \quad (35)$$

Although the mullite tube was sealed, reaction (29) will always occur to a greater extent when more reference electrolyte is added to the mullite tube. The passage of current (100 pA - 2nA) through the electrolyte causes reactions (30) and (31) to occur to an extremely small extent.

Changes in open-circuit W/R voltage with gas composition also agreed well with those calculated from the Nernst equation (33), as seen in Table 3. Minor differences

are attributed to different Henry's law constants for $H_2$ and $H_2S$. The presence of $CO_2$ should raise the potential:

$$CO_2 + H_2O + 2e^- \rightarrow CO_3^{2-} + H_2 \quad (36)$$

and the presence of $H_2$ at an electrode should lower its potential:

$$H_2 \rightarrow 2H^+ + 2e^- \quad (37)$$

The effect of these three gases can readily be seen as $H_2S$ and $CO_2$ bubble through the electrolyte; changes of several hundred millivolts would typically follow large changes in gas concentrations of $H_2S$ or $CO_2$.

## Cyclic Voltammetry

### Reversibility

The use of cyclic voltammetry is very popular for initial electrochemical studies of new systems and has proven very useful in obtaining information about fairly complicated electrode reactions. While this $Na_2S/K_2S$ system is too complex to derive quantitative kinetic data from cyclic voltammetry, sound qualitative assumptions can be made. These assumptions will be based on information such as the shape and size of the cathodic/anodic waves, the presence/absence of certain waves, and the variation of the

peak with respect to different sweep rates. Process gases with and without $CO_2$ were tested in this investigation.

The first evaluation was to determine whether the data showed either totally reversible or totally irreversible tendencies. The peak potential, $E_p$, the $I_p$, and the sweep rate, $\nu$, were used for this analysis. From Bard [19], for a reversible wave, $E_p$ and the current function, $I_p/\nu^{1/2}$, are independent of sweep rate, which indicates that the reaction is diffusion controlled. For a Nernstian wave with stable products, the ratio of the anodic peak current, $I_{p_a}$, to the cathodic peak current, $I_{p_c}$, is equal to one at all sweep rates. The following equations also hold for a totally reversible system:

$$(E_{p_c} - E_{p_a}) = 2.3\ RT/nF \tag{38}$$

$$|E_p - E_{p/2}| = 2.2\ RT/nF \tag{39}$$

In the above equations, $E_{p_a}$ represents the anodic peak potential, $E_{p_c}$ represents the cathodic peak potential, while $E_{p/2}$ is the peak potential at the point where the current equals $(1/2)I_p$. As expected, when the data from the cyclic voltammograms was evaluated using the criteria outlined above, neither the process gas with or without $CO_2$ exhibited signs of reversibility. Therefore, the following

equations were used which assume that the waves are irreversible to a certain extent:

$$\Delta E_p = |E_{p_1} - E_{p_2}| = 1.04\ RT/(\alpha n_a)\ F \qquad (40)$$

$$|E_p - E_{p/2}| = 1.857\ RT/(\alpha n_a)\ F \qquad (41)$$

Equation (40) assumes that $E_{p_1}$ is evaluated at a sweep rate of 2000 mV/sec, while $E_{p_2}$ is evaluated at 250 mV/sec. The transfer coefficient is represented by $\alpha$ and $n_a$ is the number of electrons involved in the rate-determining step. Table 11 was tabulated using equation (40) but similar values were obtained by using equation (41). It is noted that $n_a$ is usually equal to one.

Table 11. Transfer Function

| Working Electrode Gas | Actual $CO_2$ (%) | $(\alpha n_a)_{CATHODIC}$ | $(\alpha n_a)_{ANODIC}$ |
|---|---|---|---|
| 0.3% $H_2S$ | 0 | 0.250 | 0.242 |
| 1.5% $H_2S$ | 0 | 0.222 | 0.175 |
| 0.47% $H_2S$ | 5.8 | 0.339 | 0.342 |

Coupled Chemical Reactions

If a homogeneous chemical reaction is coupled to the charge transfer reaction, cyclic voltammetry provides an

extremely powerful method of investigating the kinetic parameters. The ECE* mechanism and the catalytic reaction have both been studied under this investigation so that a proposed reaction path could be postulated. The ECE mechanism represents the case in which a chemical reaction is coupled between two charge transfers.

$$O_1 + n_1e \rightleftharpoons R_1 \qquad E_1^{o} \tag{42}$$

$$R_1 + Z \rightarrow O_2 \tag{43}$$

$$O_2 + n_2e \rightleftharpoons R_2 \qquad E_2^{o} \tag{44}$$

The catalytic reaction scheme almost always involves a nonelectroactive species (Z) in the following chemical reaction which regenerates starting material.

$$O + ne \rightleftharpoons R \tag{45}$$

$$R + Z \rightarrow O + Y \tag{46}$$

In most treatments, it can be assumed that Z is present in large excess.

* ECE is the common abbreviation for a reaction sequnce of a chemical reaction preceded and followed by electrochemical reactions.

From the 1965 article by Nicholson and Shain [12], it is proposed that the ECE mechanism, Case I-R, could characterize the reaction when $CO_2$-containing process gas is bubbled through the electrolyte. In this case, the first charge transfer is irreversible and the second is reversible. The cyclic voltammograms fit the diagnostic criteria for Case I-R very well. The current function is independent of sweep rate, while the peak potential shifts in accordance with equation (33) for an 8-fold increase in the rate of the voltage sweep. As affirmed by the Case I-R criteria, the anodic wave of the cyclic voltammogram is present at slow sweep rates but is lost at much higher sweep rates. A final point of agreement with the Case I-R assumption is that the shape and the size of the cathodic and anodic peaks are similar at particular sweep rates.

A proposed mechanism when $CO_2$-free process gas is bubbled through the electrolyte is not clearly distinguishable. The cyclic voltammograms resemble a Case VII catalytic reaction with a reversible charge transfer, as specified in the 1964 article by Nicholson and Shain [11]. This assumption is applied with great caution but the similarities do merit discussion. As suggested by the diagnostic criteria, the experimental anodic curves are the same shape as the cathodic curves. The next similarity is that the ratio of the cathodic peak currents to the anodic peak currents are approximately unity, regardless of sweep

rate. The peak-current functions also decrease with increasing sweep rate in a manner similar to Case VII. These diagnostic relations can at best only give a qualitative characterization of the unknown systems since only trends in the experimental behavior were used. To make a stronger justification for the catalytic reaction, an irreversible charge transfer could possibly follow the chemical reaction. This addition would answer some questions about the reversibility of the system as a whole.

Polysulfide as the Active Species

The third and most probable mechanism for this $Na_2S/K_2S$ system system assumes that the active species is polysulfide dissolved in sulfide. This hypothesis parallels the work done by Birk and Steunenberg [20], Tischer and Ludwig [21], and Selis [22] in similar melts. The prime difficulty for this basic work is posed by the variety of polysulfide ions present, which are hard to identify. Tischer and Ludwig suggested that the electroactive species was $S_2^{2-}$ in polysulfide melts and they experienced very high exchange current densities. At faster sweep rates, they saw that the slower chemical reactions could not remove the sulfur and therefore the current function, $I_p/\nu^{1/2}$, decreased with sweep rate. Thus, they concluded that the peak current does not represent a diffusion-controlled process but rather a process of a chemical reaction removing a blocking layer.

A point to be noted at this time is that the exchange currents reported by Tischer and Ludwig are two orders of magnitude higher than those reported by White [17]. Therefore, exchange current can be assumed to be dependent upon the polysulfide level in the electrolyte since Tischer and Ludwig's work was done with pure polysulfide at 350°C, while White's work was done with polysulfide dissolved in sulfide. From viewing the work of Birk and Steunenberg, it is proposed that there are two one-electron transfers occurring within one cyclic voltammogram peak. These reactions are happening at voltages very close together and cannot be distinguished.

$$2S + 2e^- \rightleftharpoons S_2^{2-} \qquad (47)$$

$$S_2^{2-} + 2e^- \rightleftharpoons 2S^{2-} \qquad (48)$$

This assumption was made based on the similarity of the experiment and cyclic voltammograms with those of Birk and Steunenberg and are in accordance with the work of Selis.

To add further justification to naming dissolved polysulfide as the active species, the concentration of the active species was calculated from the experimentally obtained peak currents and compared with the theoretical calculation of the polysulfide concentration from thermodynamics. By plotting the various peak currents

versus the square root of their associated sweep rate from the cyclic voltammograms, the resulting slope can be used in conjunction with the following equation to calculate the concentration of the active species [19];

$$i_p = 0.4958\ nFAC_o^* D_o^{1/2} \nu^{1/2} \left(\frac{\alpha n_a F}{RT}\right)^{1/2} \qquad (49)$$

If an area of 2.5 $cm^2$ and a diffusivity of $10^{-6}$ $cm^2/sec$ is assumed, then the concentration of the active species is calculated to be $10^{-5}$ mole/cc.

An equilibrium constant can be calculated from the following equation by using the corresponding free energies at 1000 K:

$$(Na/K)_2\ S + H_2S \rightarrow (Na/K)_2\ S_2 + H_2 \qquad (50)$$

From the equilibrium constant and by assuming that the system reacts as an ideal solution, the concentration of the polysulfide, $S_2^{2-}$, can be calculated to be $10^{-5}$ mole/cc. The fact that the experimentally derived concentration of the active species is of the same order of magnitude as the theoretically calculated concentration of the polysulfide adds much strength to the assumption that dissolved polysulfide is the active species for this $Na_2S/K_2S$ system.

## Removal Experiments

The removal current, $i_r$, gives an indication of how much sulfide is being removed from the electrolyte. It is influenced by the amount of current applied but its maximum value is dependent upon the limiting current. This system could not be operated at 100% efficiency because of the mass transfer resistance between the film of the electrode and the bulk electrolyte, the convective effect of mixing around the electrode, and because of the residual current effect.

During the removal experiments, the process gas was bubbled to the electrode at the same time that current was applied. The desired overall reactions are as follows:

working electrode: $S_2^{2-} + 2e^- \rightarrow 2S^{2-}$ (51)

$$H_2S + S^{2-} \rightarrow H_2 + S_2^{2-} \quad (52)$$

counter electrode: $S^{2-} \rightarrow S + 2e$ (53)

or $S^{2-} + H_2 \rightarrow H_2S + 2e$ (54)

Bubbling process gas causes the electrolyte to become well mixed and a constant sulfide-polysulfide concentration gradient cannot be maintained. Fresh polysulfide-rich electrolyte becomes mixed with the sulfide removed

electrolyte around the electrode and polysulfide is reformed at the counter electrode by the following reaction:

$$2S^{2-} + S_2^{2-} + 2e \qquad (55)$$

This material gets recirculated to the working electrode thus causing little or no removal by equation (52). It is to be noted that in a commercial cell, the electrolyte would be fixed in a matrix and that this convective effect of mixing would not be experienced.

The electrolyte is initially full of polysulfides. These impurities are eventually driven off because of the effect of a reaction with $H_2$ at high operating temperatures. Part of the applied current during a removal experiment acts to reduce the bulk polysulfide impurities to sulfides. This residual current effect lowers the removal current seen during the experiment and acts to reduce the electrolyte in the vicinity of the working electrode long after the current is discontinued.

## Sulfide Conversion

Two separate analyses experimentally indicated that the conversion of sulfide to carbonate with the passage of $CO_2$ contained process gas through the electrolyte was approximately 4 mole %. The theoretical conversion was calculated by using thermodynamic free energies at 1000 K to

determine an equilibrium constant from the following equation:

$$(Na/K)_2\ S + CO_2 + H_2O \rightarrow (Na/K)_2\ CO_3 + H_2S \qquad (56)$$

The free energy of reaction of the sodium compounds at 1000 K is 1290 cal/mol while that of the potassium is 6075. Assuming ideal mixing of the 40% sodium sulfide (and carbonate) and 60% potassium compounds, the mixture free energy of reaction is 4161 cal. This yields an equilibrium constant, $K_{eq}$ of 0.12.

$$\Delta G_R = -RT\ \ell n\ K_{eq} \qquad (57)$$

The equilibrium constant is related to the activities of the various species in equilibrium:

$$K_{eq} = \frac{[CO_3^{2-}]\ [H_2S]}{[CO_2]\ [H_2O]\ [S^{2-}]} \qquad (58)$$

where [ ] denotes activity

If we ignore any difference between sodium and potassium, presume the vapor phase is ideal and assume ideality as well in the electrolyte, we can estimate a 'measured' equilibrium constant:

$$K_{eq} = \frac{0.03\ x\ 0.0047}{0.058\ x\ 0.023\ x\ 0197} = 0.11 \qquad (59)$$

This is in quite good agreement with the thermodynamic calculation; it permits us to make reasonable estimates of the degree of carbonation at lower temperatures and with other cation combinations.

# CONCLUSIONS

The electrochemistry in an electrochemical cell removing $H_2S$ from hot coal gas was explored. The behavior of the cell during cyclic voltammetric experiments and sulfide removal studies can readily be explained by accepted electrochemical theory. Most notably the cyclic voltammograms of Selis [22] greatly resemble the voltammograms obtained during this research. This adds further credibility to the presumption that dissolved polysulfide is the active species. The proposed ECE mechanism and the catalytic reaction mechanism are not as well documented in the literature but they provide a viable alternate method for viewing the electrode reactions.

The ratio of the removal current to the limiting current was 88% for the process gas containing $CO_2$ at the point of maximum sulfide removal. It must be understood that this electrochemical cell was designed to observe certain kinetic and removal principles rather than to operate at 100% efficiency. Mass transfer resistance, the convective effect of mixing in the vicinity of the electrode and residual current effects all took away from the efficiency of the cell. An actual commercial cell would hold the electrolyte in an inert matrix such as $LiAlO_2$ and would experience a much higher reliable efficiency.

An electrolyte of 60 mole % $K_2S$ and 40 mole % $Na_2S$ was used during this investigation. Lim [8] suggested that an electrolyte containing potassium as the cation would be most resistant to the conversion of sulfide to carbonate with the passage of $CO_2$ contained process gas. This study proves the validity of that assumption; a lab analysis of the spent electrolyte showed that less than 4 mole % of the original sulfide was converted to carbonate.

A partially carbonated electrolyte, as would be encountered in treating actual coal gas, gave markedly improved performance. The $H_2S$ removal increased to a point limited only by mass transfer.

## BIBLIOGRAPHY


1. Schmitt, R. W.; J. of the Institute of Energy, 54, (419), p. 63, 1981.

2. Dawes, M. H. and Peterson, J. R.; in Proceedings of the 16th Intersociety Energy Conversion Engineering Conference, Vol. 1, p. 703, 1981.

3. Houghtby, W. E., et. al.; Electric Power Research Institute (EPRI) EM-956, 1978.

4. Apte, A. J. and Fein, H. L.; in Proceedings of the 16th Intersociety Energy Conversion Engineering conference, Vol. 2, p. 1047, 1981.

5. Cornilis, B., et. al.; in Proceedings of the 16th Intersociety Energy Conversion Engineering Conference, Vol. 2, p. 1050, 1981.

6. Langhoff, J., et. al.; in Proceedings of the Second World Congress of Chemical Engineering, Vol. 2, p. 47, 1981.

7. Cheng, A. Y.; "The Claus Process for Sulfur Recovery", (unpublished literature review), 1982.

8. Lim, H. S.; Doctoral Dissertation, School of Chemical Engineering; Georgia Institute of Technology, September 1982.

9. Bockris, J. O'M. and Reddy, A. K. N.; Modern Electrochemistry, Plenum/Rosetta, 1973.

10. Guggenheim, E. A.; Thermodynamics, Wiley-Interscience, Chapter 10, 1950.

11. Nicholson, R. S. and Shain, I.; Anal. Chem., 36, p. 706, 1964.

12. Nicholson, R. S. and Shain, I.; and Chem., 37, p. 178, 1965.

13. Nicholson, R. S. and Shain, I.; and Chem., 37, p. 190, 1965.

14. Piekarski, S. and Adams, R. N.; Voltammetry with Stationary and Rotated Electrodes, Wiley-Interscience, p. 531, 1971.

15. Shores, D. A. and Fang, W. C.; J. Electrochem. Soc., 128, (2), p. 346, 1981.

16. Watt, G. W., et. al.; Proceedings of the Second International Symposium on Molten Salts, p. 81, 1981.

17. White, K. A. and J. Winnick, Electrochimca Acta, Vol. 30, No. 4, pp. 511-519, 1985

18. Vetter, K. J.; Electrochemical Kinetics, Academic Press, 1967.

19. Bard, A. J. and Faulkner, L. R.; Electrochemical Methods, Wiley, 1980.

20. Birk, J. R. and Steunenberg, R. K.; Advances in Chemistry, American Chemical Society, 140, 1974.

21. Tischer, R. P. and Ludwig, F. A.; Advances in Electrochemistry and Electrochemical Engineering, Wiley-Interscience, 10, 1977.

22. Selis, S. M.; Electrochimica Acta, 15, p. 1285, 1970.

Progress Assessment

It is instructive, on completion of the contract, to compare our progress with that proposed at the onset:

1. Equilibrium Potentials

Using a thermodynamic reference electrode, the equilibrium potentials determined verify the proposed reactions with or without $CO_2$ and $H_2O$ in the process gas. The water-gas shift reaction:

$$CO + H_2O = H_2 + CO_2$$

was found to be very close to equilibrium at the cell temperature.

2. Electrode Kinetics, Reaction Order

Using accurate transient techniques, the true kinetic currents have been found, in both cathodic and anodic directions. The reaction orders in $H_2S$ in both directions, found from the variation in exchange currents with $H_2S$ concentration, are favorably low.

The addition of gas-return tubes has allowed the analysis of $H_2S$ removal in the free electrolyte as a function of current.

3. Melting Points

The melting points of ten binary mixtures of the Li, K and Na sulfides have been determined. One of these has been used exclusively to this point.

4. Electrode Materials

One electrode candidate material has been used successfully for all tests. Dense carbon has been found stable, conductive and fully wetted by the melt. Other candidates include $TiO_2$ (doped rutile) and metal sulfides. These might be necessary if carbon deposition or removal occurs due to the Boudouard reaction:

$$2CO = C + CO_2$$

5. Temperature Range

The studies have been confined to two single temperatures well within the range proposed (600-1000$^{o}$C). Due to experimental difficulties it was deemed advisable to generate a consistent set of data at these temperatures rather than an incomplete set over a range of temperatures.

6. Mechanism

Although not specifically proposed, much work has gone into elucidating the reaction paths. Cyclic

voltammetry, begun early in this year, was aided by comments at the February 1984 group session. Since then, combination of literature review and more complete voltage sweep analysis has provided reasonable reaction mechanisms.

## Proposed Future Work

The success of the first two years of the study, along with the requirements of the industry, sets a clear path for future study. Lower temperature operation is highly desirable. The process temperature is limited, on the low end, by the melting point of the electrolyte and the carbonation reaction:

$$CO_2 + H_2O + S^{2-} = CO_3^{2-} + H_2S$$

The electrode kinetics are so fast that it is unlikely that lower temperatures will cause any problem in this regard.

Since binary mixtures show melting points only as low as 700°C, ternary mixtures should be tested. At first, mixtures of Li, K and Na sulfides are indicated. Ideal solution thermodynamics predicts increased carbonation of Na-containing melts at lower temperatures; our results reported here confirm these predictions. Yet a partially-carbonated melt showed strikingly improved $H_2S$-removal performance, as compared with a pure sulfide melt.

Further, carbonate mixtures have lower melting points than do sulfide. For example, a ternary Li, K, Na carbonate melts at 392°C. A melt which equilibrates to primarily carbonate will likely have a low melting point. The transport will still be via sulfide since the oxidation of carbonate at the anode requires nearly a volt higher potential than does sulfide (at equivalent activities).

Thus, it is quite likely ternary melts of Li, K and Na (cations) will satisfy both constraints. If not, calcium sulfide is a candidate for addition. It will lower the melting point and has high stability against carbonation.

The same sequence of testing which has been used in the binary melt would be used in the ternary at lower temperatures:

a) A melting point study will find a ternary (or ternaries) of Li, K, Na sulfides which melt below 600°C (when $H_2S$-containing gas is equilibrated with these melts, the polysulfides formed lower the melting point further).

b) Cyclic voltammetry will be used to ascertain whether the same electrode reaction sequences occur.

c) Carbonation equilibrium will be determined by bubbling $CO_2$ and $H_2O$-containing gas through the melt at the lower temperatures.

d) Reaction kinetics and $H_2S$ removal will be assessed in both the pure sulfide and carbonated melt.

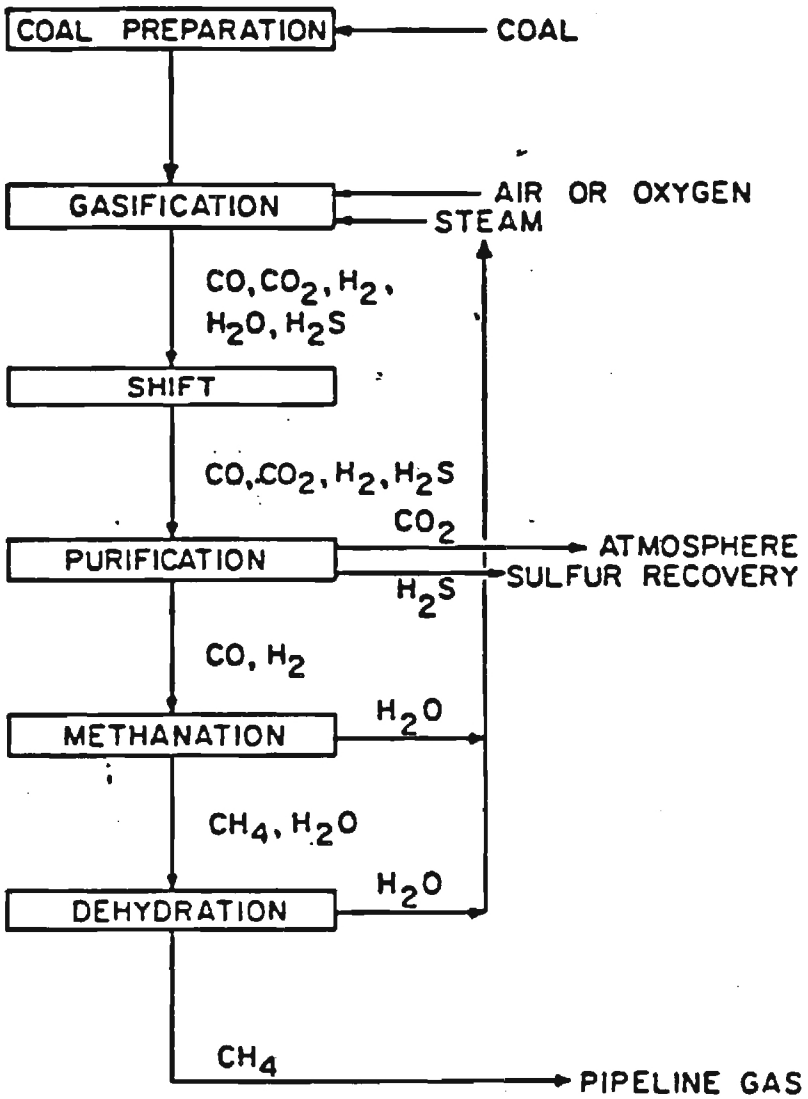


Figure 1. General high Btu gasification process scheme.

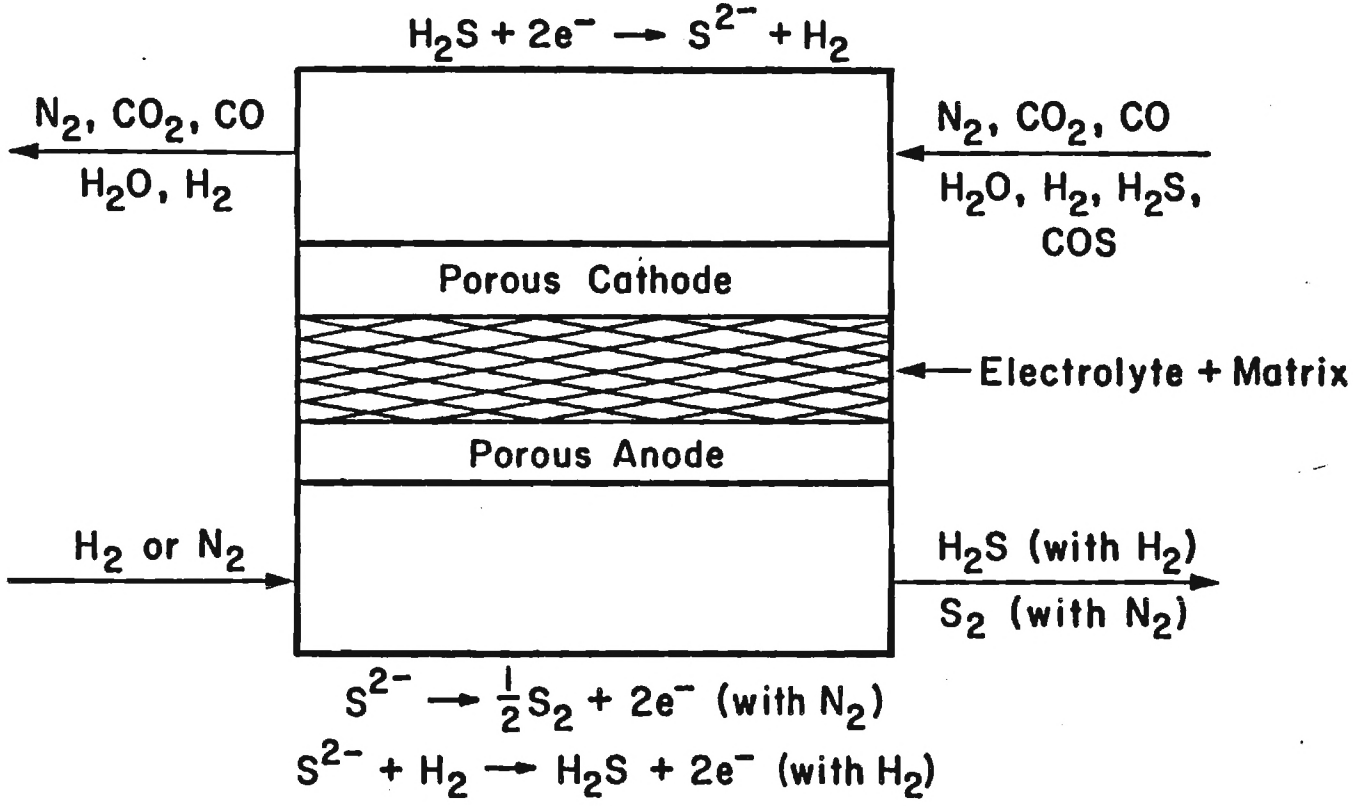


Electrochemical Desulfurization Cell

Figure 2. Gas Flow in an Electrochemical Desulfurization Cell

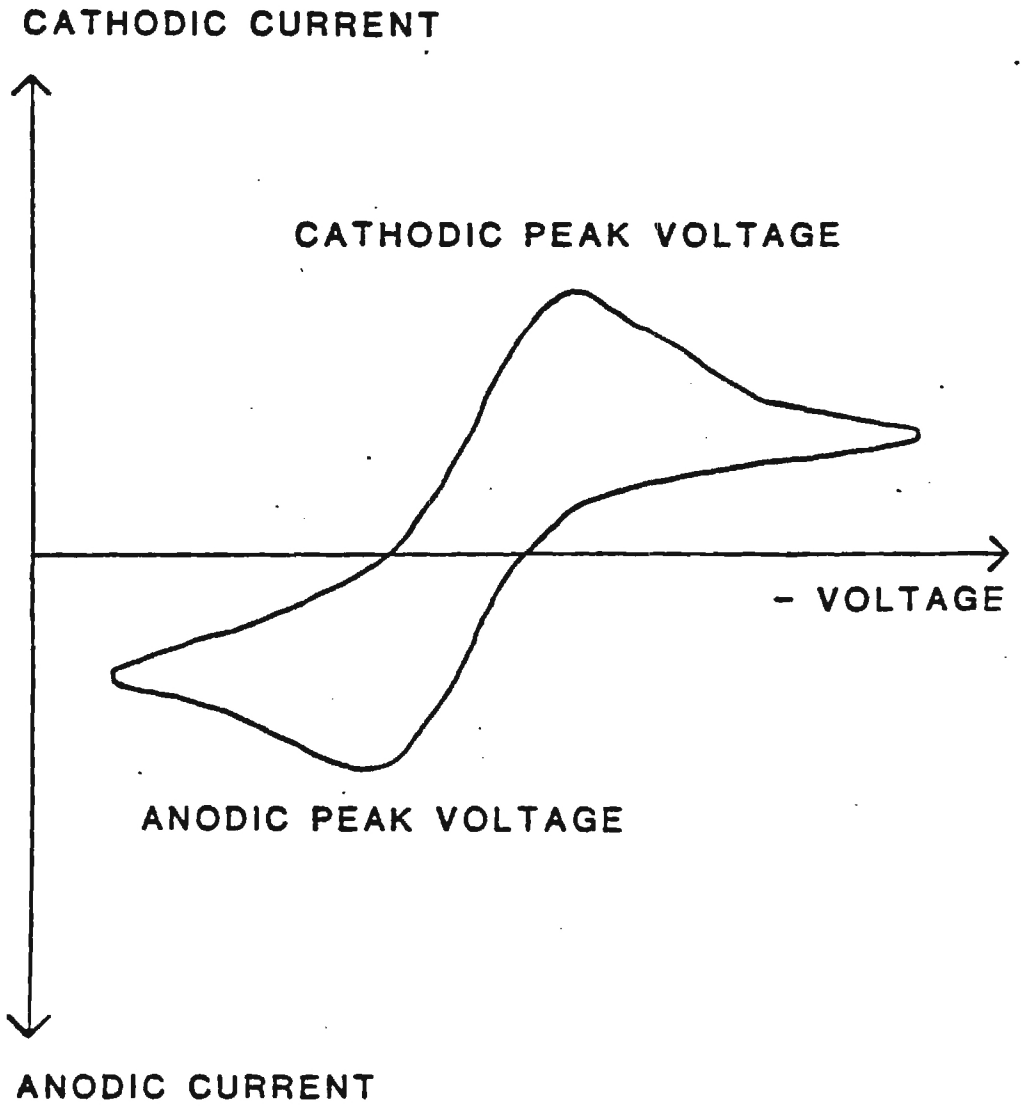


Figure 3. Cyclic Voltammogram

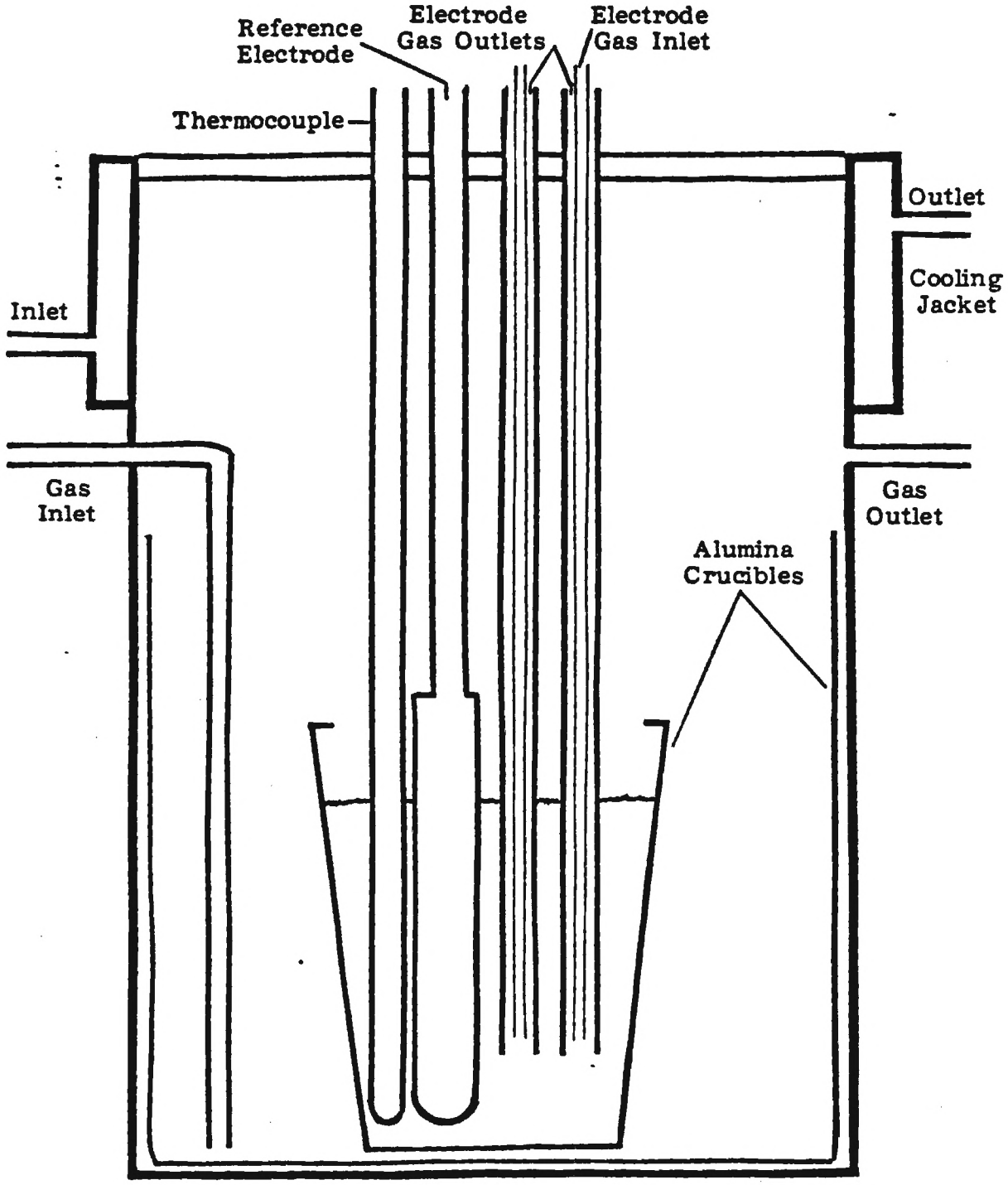


Figure 4. Reaction Furnace

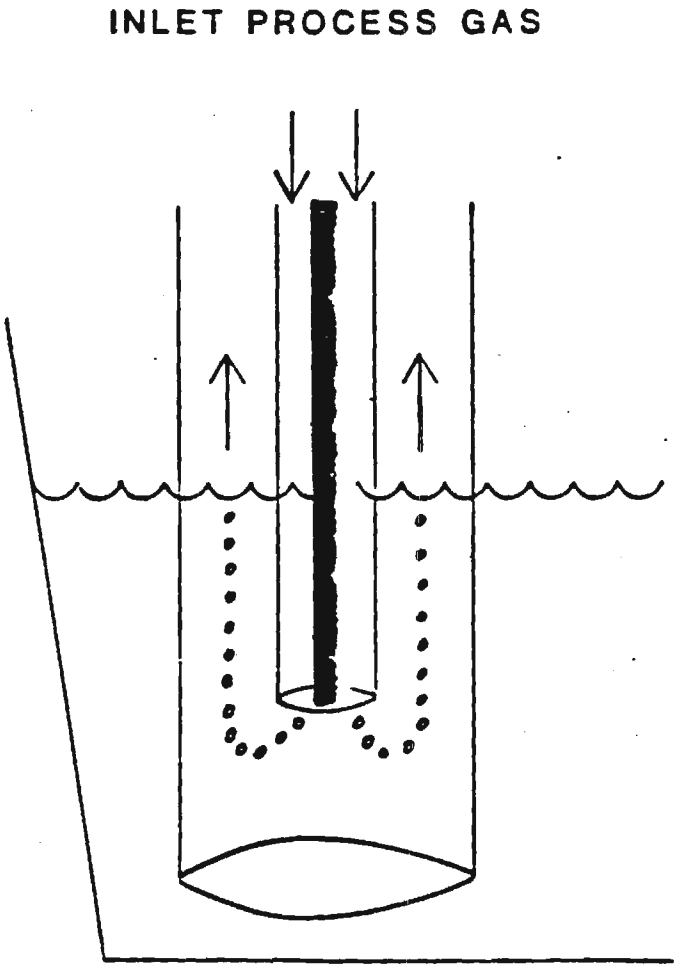


Figure 5. Gas Flow Inside the Furnace

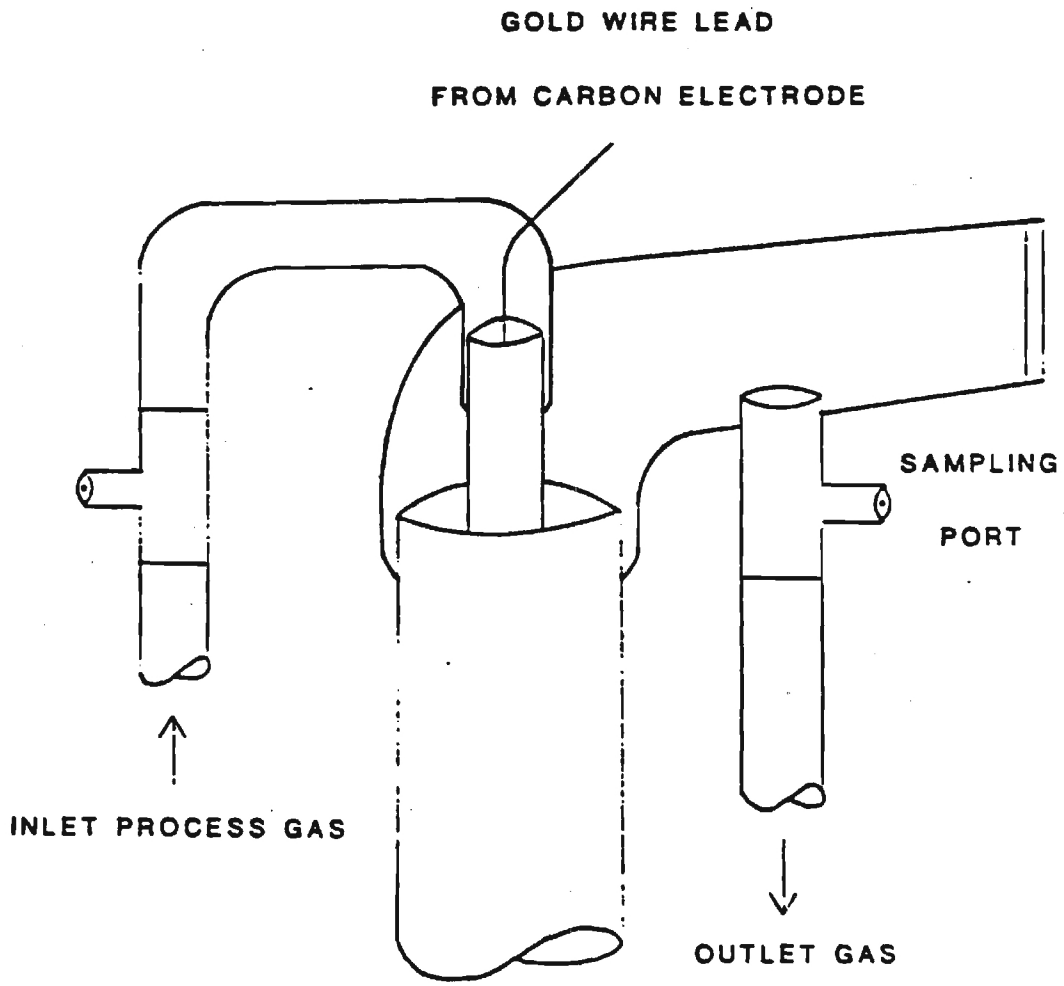


Figure 6. Gas Flow Into the Furnace

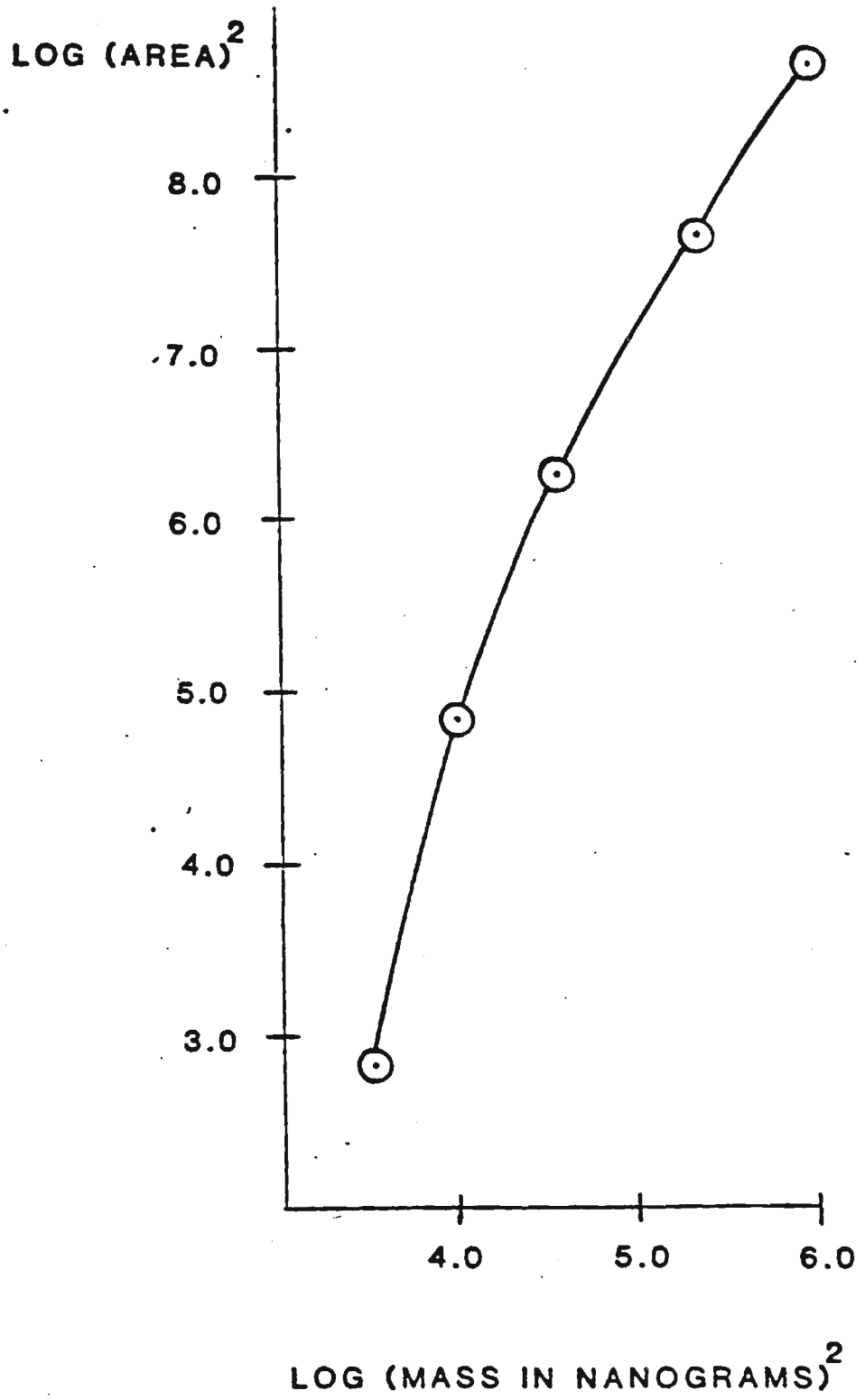


Figure 7. FPD Calibration Curve

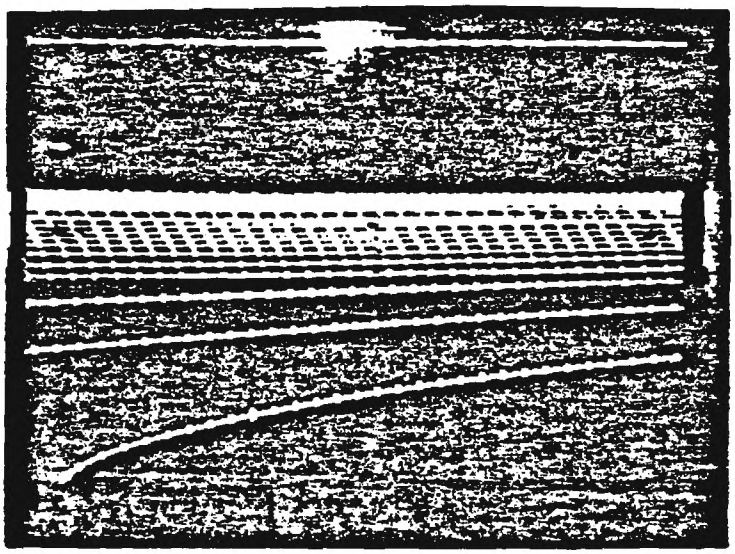

Sweep rate: 50 $\frac{ms}{div}$ -299 mV step

Vertical: 50 $\frac{mA}{div}$ $R_i$ = 0.841 Ω

Figure 8. Oscillographic Trace
For A Cathodic Polarization

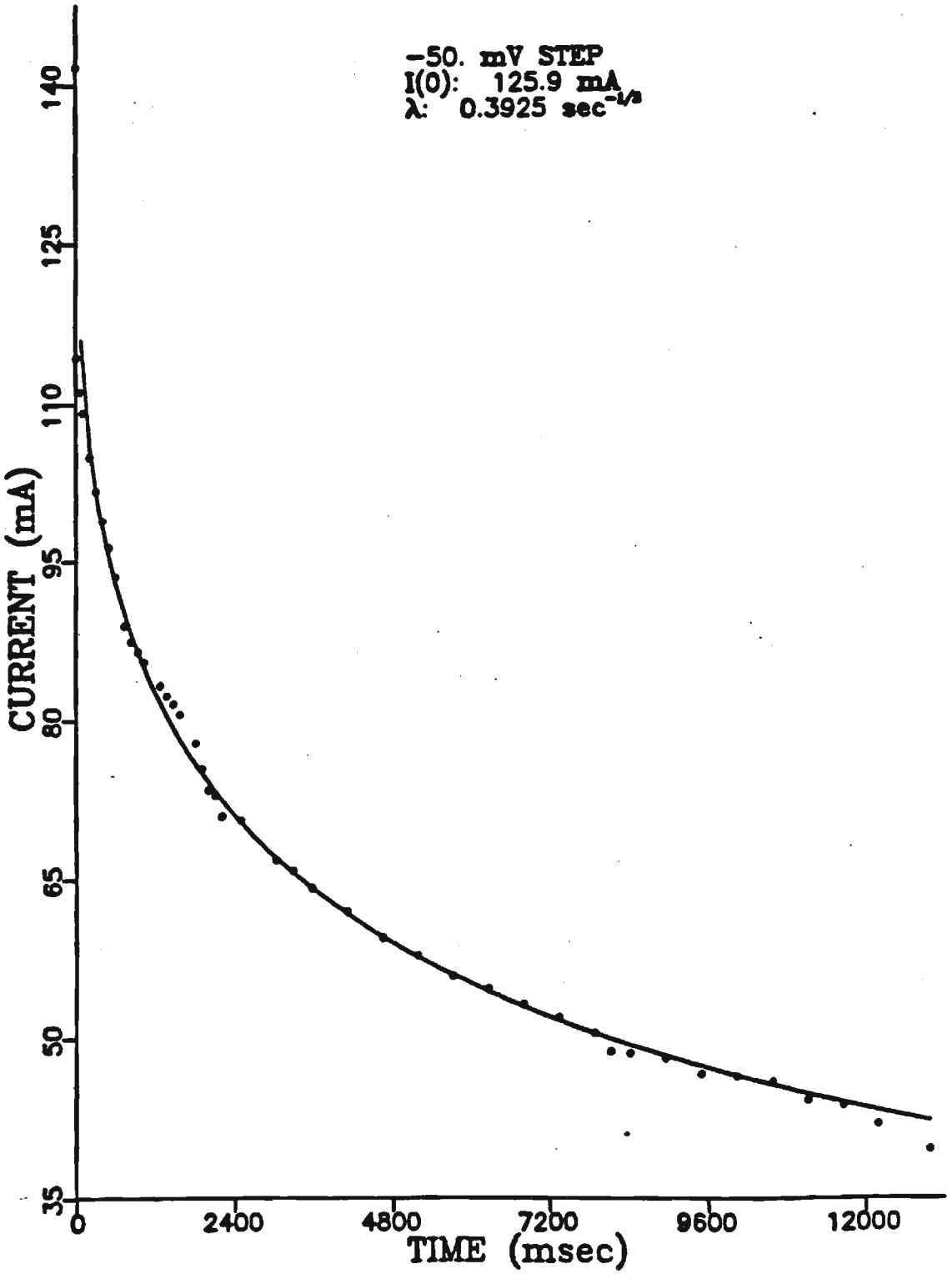


Figure 9. Comparison of Experimental Chronoamperometric Data With Equation (21)

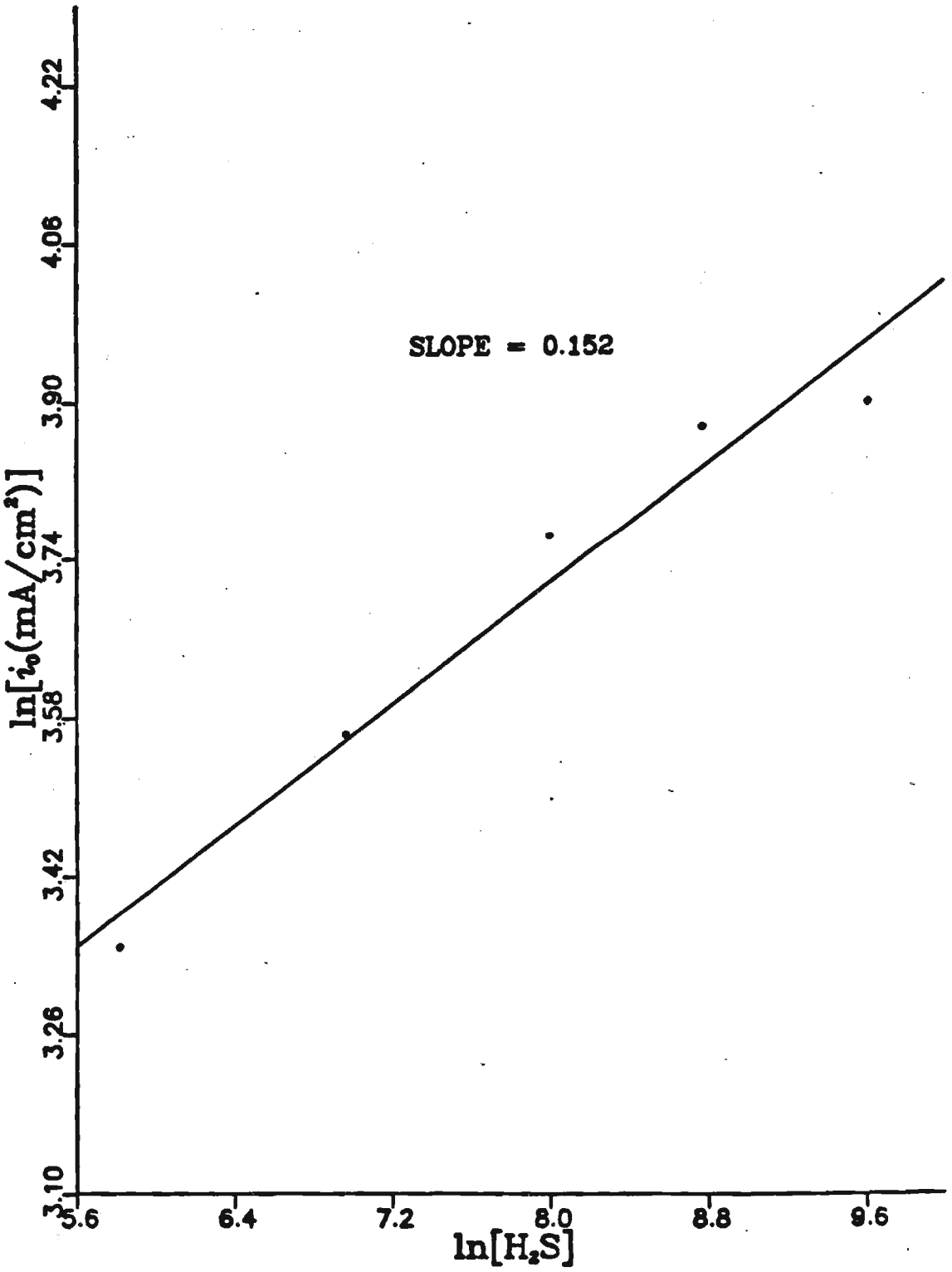


Figure 10. Dependence of $i_o$ on $H_2S$ Concentration in Gas: Cathodic Polarizations

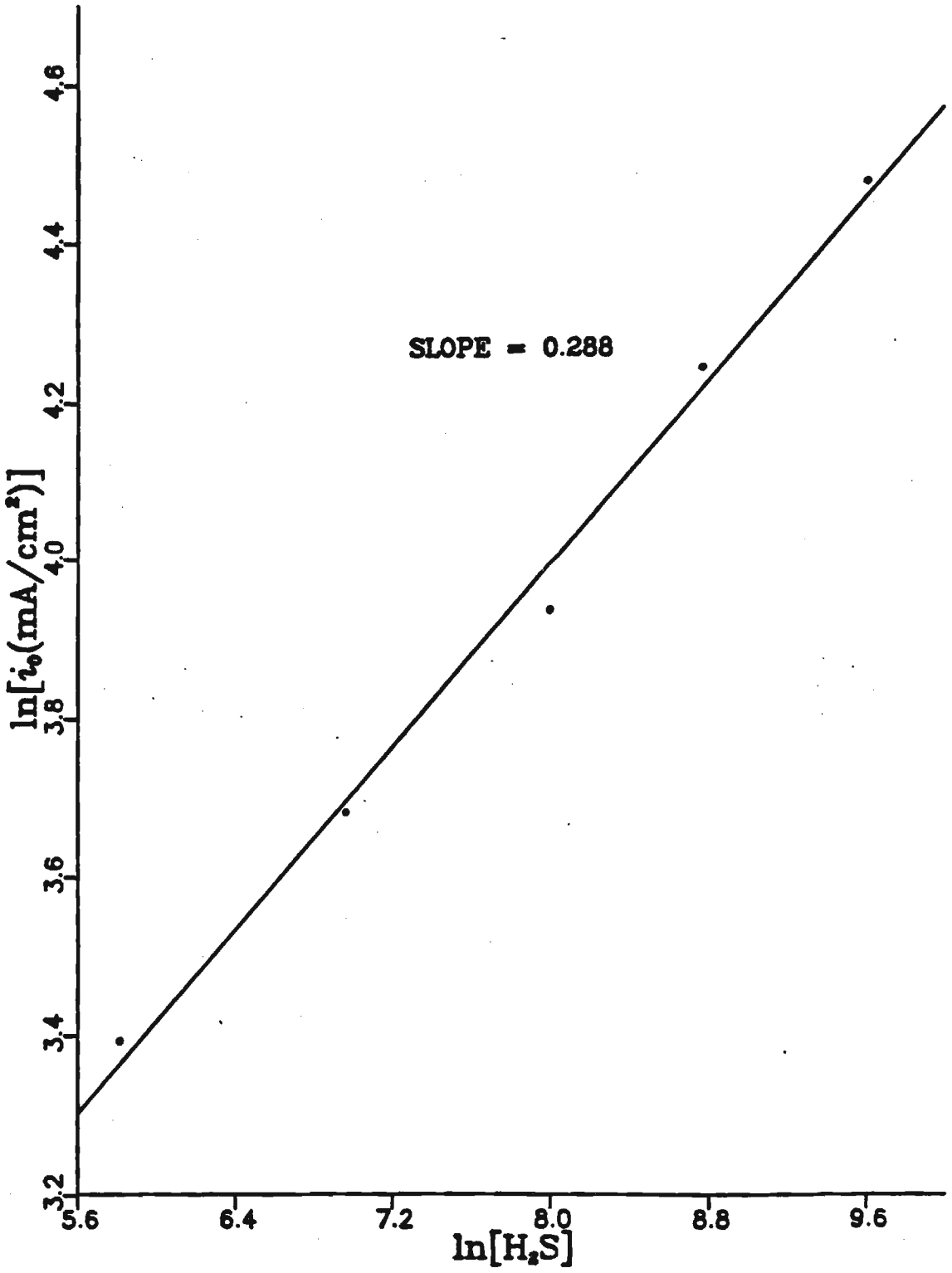


Figure 11. Dependence of $i_o$ on $H_2S$ Concentration in Gas: Anodic Polarizations

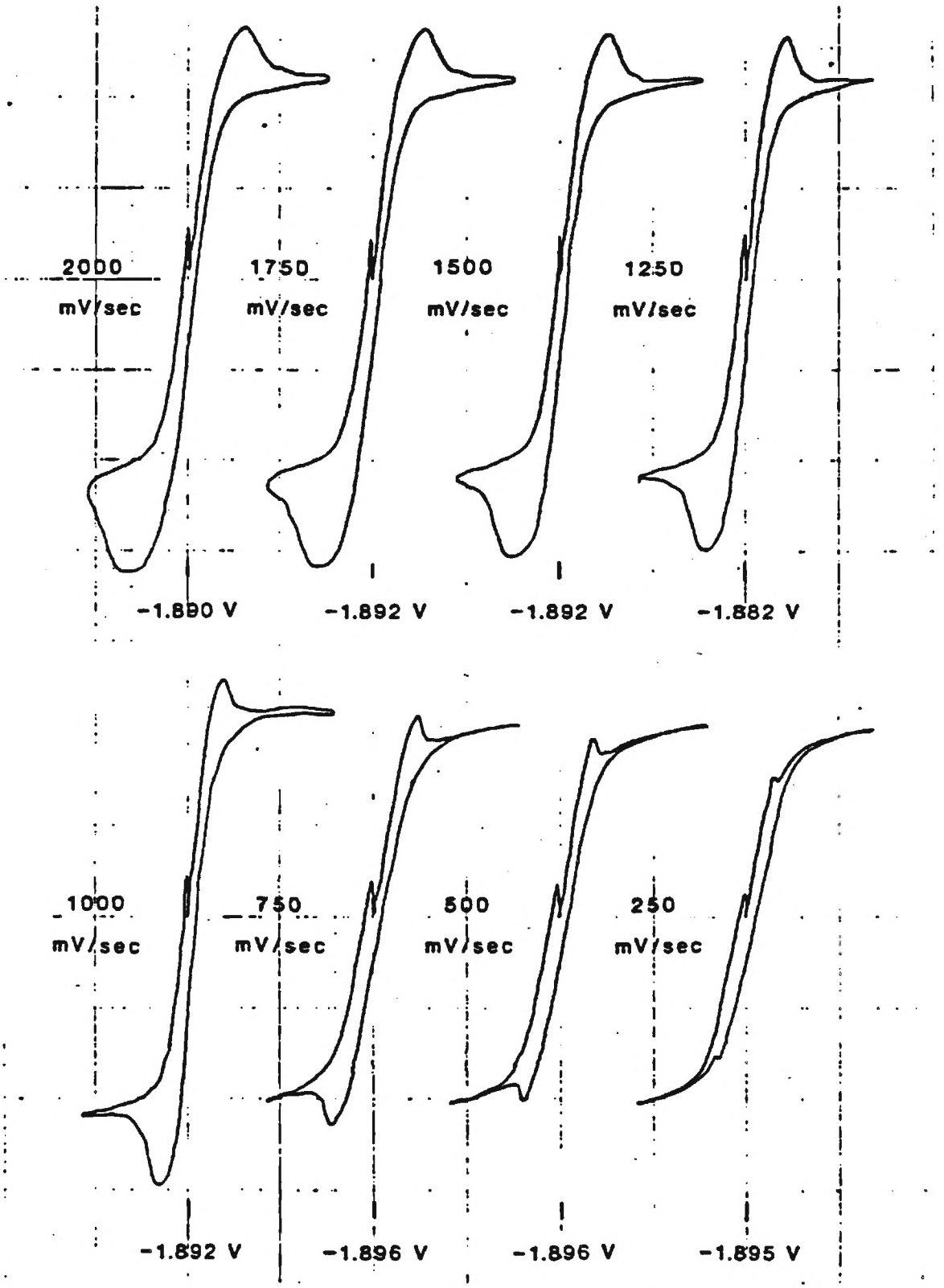


Figure 12. Cyclic Voltammograms for Process Gas Containing 0.3% $H_2S$

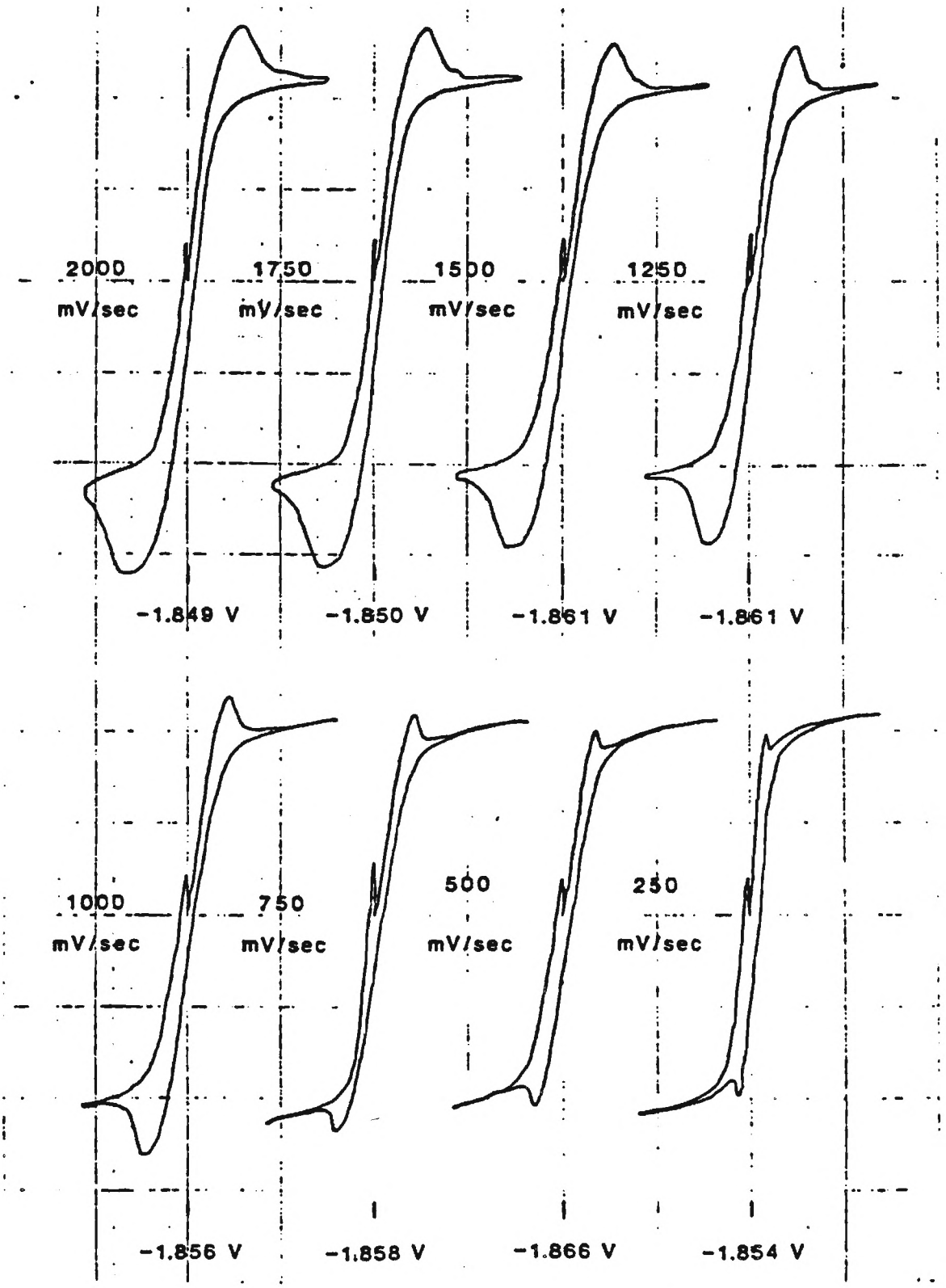


Figure 13. Cyclic Voltammograms for Process Gas Containing 1.5% $H_2S$

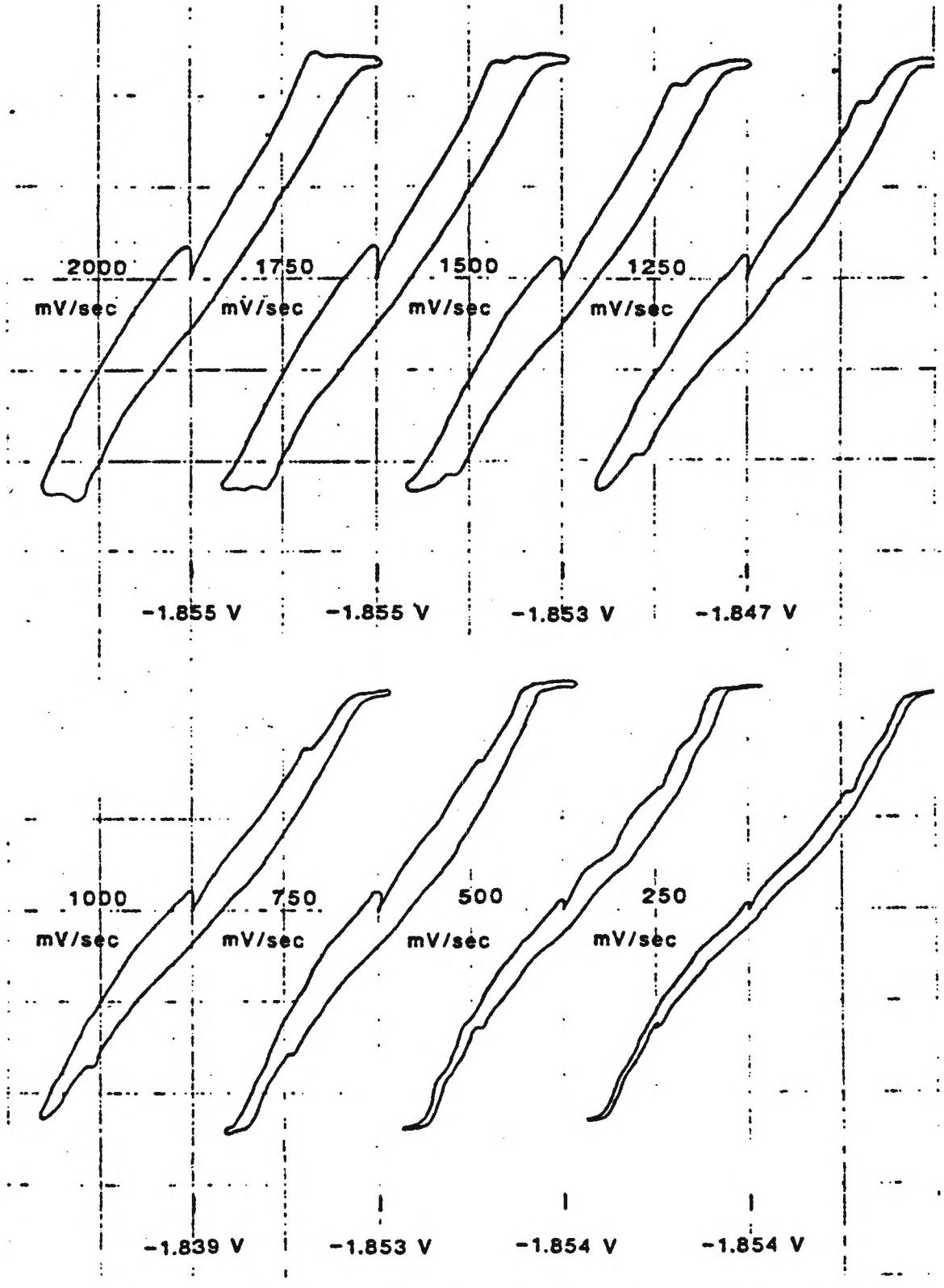


Figure 14. Cyclic Voltammograms for Process Gas Containing 0.65% $H_2S$ and 5.8% $CO_2$